11-8-2004

Isolation and Identification of O-linked-β-N-acetylglucosamine Modified Proteins (O-GlcNAc) in the Developing Xenopus laevis Oocyte

Sreelatha Paspuleti
University of South Florida

Isolation and Identification of *O*-linked-β-N-acetylglucosamine Modified Proteins

(*O*-GlcNAc) in the Developing *Xenopus laevis* Oocyte

by

Sreelatha Paspuleti

A thesis submitted in partial fulfillment
of the requirements for the degree of
Master of Science
Department of Chemistry
College of Arts and Sciences
University of South Florida

Major Professor: Dr. Robert Potter, Ph.D.
Committee Members: Dr. David Merkler, PhD
Dr. Larry Solomonson, PhD

Date of Approval:
November 8, 2004

Keywords:,Thesaurin a, Cytoplasmic mRNA binding protein p54, Vg1 RNA binding protein variant A, Zygote arrest 1,Two-dimensional gel electrophoresis.

Dedication

To those who have given me the confidence, ability, love and encouragement to complete this thesis; I dedicate this new scientific information to my late sister Sunitha, my parents (P. S. Pandu Ranga Rao and P.V. Roopavathi), my aunt (P. V. Vijayakumari), my brothers (Sreedhar and Shashidhar), my sisters (Swapna and Supriya) and my beloved husband (Ravi Jonna).

ACKNOWLEDGEMENTS

I wish to acknowledge and thank those who helped me throughout my study at the University of South Florida. I thank my major Professor Robert Potter for his guidance and support throughout the project. I thank my senior, Dr. Stephen A Whelan who is currently post-doctoral fellow in Dr. G. W. Hart laboratory at John Hopkins University for the protein sequencing and identification.

I am also indebted to all my friends in the laboratories and the department, who were plentiful source of encouragement. I thank my brother, Sreedhar Paspuleti for encouraging me to continue my studies in US. The selfless attitude of my husband, Ravi Jonna, has allowed me to pursue my goal of finishing this thesis, and I appreciate his patience, love and affection.

I thank all of the USF Professors who offered their time for discussions and their laboratories to me. These include Dr. Larry P Solomonson, Dr. Sidney Pierce, Dr. David Merkler, and Dr, Ted Gauthier. Additionally, I thank the chemistry department at USF for the financial support throughout my study.

Table of contents

List of Tables

List of Figures

Isolation and Identification of the *O*-linked-β-N-aetylglucosamine (*O*-GlcNAc) Modified Proteins in the Developing Oocytes of *Xenopus laevis*

Sreelatha Paspuleti

ABSTRACT

Oocyte development in *Xenopus laevis* spans six morphologically distinct stages (stage I-VI), and is associated with a decrease in protein *O*-GlcNAc levels. As a first step in elucidating the role of *O*-GlcNAc in developing oocytes, initial efforts were focused on isolation and identification of fifteen modified proteins that decrease during oocyte development. Stage I oocytes due to their high amounts of these proteins, were used as starting material for purification. Multiple affinity and specific antibody based purification technique were initially used in an attempt to enrich the *O*-GlcNAc proteins. Due to the unique properties of the proteins ultimately identified, these techniques were unable to provide sufficient material for sequencing. However, differential centrifugation coupled with 2D-gel electrophoresis was highly successful. The majority of isolated proteins were strongly basic in nature with pIs 8-10. Coomassie stained bands from 2D-analysis were trypsin digested, and peptides were sequenced by mass spectroscopy (Finnigan LCQ). Mass data were interpreted by Bioworks software, and protein sequences were compared to multiple protein databases. Initially, six proteins were identified as *Thesaurin a* (42Sp50), *cytoplasmic mRNA binding protein p54, y-box homolog, Xp 54 (ATP dependent RNA helicase p54), Vg1 RNA binding protein variant A,*

Zygote arrest 1(Zar1) and Poly (A) binding protein (PABP). Thesaurin a, the main component of 42S particle of previtellogenic oocytes (stages I-III) is involved in tRNA storage and possess low tRNA transfer activity; *y-box factor* homolog and *Xp54* are present in oocyte mRNA storage ribonucleoprotein particles; *Vg1 RBP variant A* associates mVg1 RNA to microtubules in order to translocate to the vegetal cortex; *Zar1* is involved in oocyte-to-embryo transition; and *PABP* initiates mRNA translation. This study is the first to characterize these oocyte specific proteins as *O*-GlcNAc modified proteins. Overall, the presence of several *O*-GlcNAc proteins in oocytes, the reduction in their levels/ *O*-GlcNAc levels, and the variation in maturation time in the presence of HBP-flux modulators in developing oocyte indicates *O*-GlcNAc may play important roles in metabolism, cell growth and cell division of *X. laevis* oocytes. Therefore, identifying the remainder of these proteins and elucidating the *O*-GlcNAc role in their function is a worthwhile pursuit.

Chapter 1

Introduction

1. The use of *Xenopus laevis* oocyte as a model system for the cell developmental studies involving *O*-GlcNAc modified proteins:

1.1 Statement of the Problem

O-linked-β-N-Acetylglucosamine (*O*-GlcNAc) modification characterized two decades ago [1] has been found to be ubiquitous in metazoans and is a dynamic post-translational modification of many nuclear and cytosolic proteins. Subsequent studies have found the modification on a wide variety of proteins suggesting the diversity in functions of this modification [2]. Importantly, the levels of *O*-GlcNAc in different types of cells changes in response to the external stimuli, such stress [3], insulin signaling [4], glucose metabolism [5-7], and cell cycle progression [7] suggesting a potential regulatory role for *O*-GlcNAc modified proteins in many cellular processes. Additionally, changes in *O*-GlcNAc have been linked to diseases such as Alzheimer's [5], diabetes [8], and cancer [9] highlighting its potential clinical importance.

As one approach to investigating the possible function of *O*-GlcNAc in cell growth and division, oocytes from the South African clawed frog, *Xenopus laevis* were selected as a model system. This oocyte system has long been used as a general model for the study of growth and differentiation as well as analysis of cell cycle processes in eukaryotes [10]. Interestingly, recent reports have demonstrated that changes of *O*-GlcNAc

levels in oocytes impact the oocyte growth and maturation [11-13], although the exact function of the modification and the role of modified proteins are still unclear.

For instance, the toxic effect of the galactosyl capping of *O*-GlcNAc residues observed in maturing *Xenopus laevis* oocyte has suggested the possible role of the *O*-GlcNAc in the aster formation during meiosis [12]. A delayed progesterone stimulated maturation of the fully grown oocytes when incubated with compounds which elevate *O*-GlcNAc levels, and a reduction in *O*-GlcNAc levels of developing oocyte during the stage progression (stage I-VI) have indicated that one or more *O*-GlcNAc modified proteins may be critical for oocyte maturation and development [11,13].

In addition, the decrease in *O*-GlcNAc levels during the stage progression [11] (stage I-VI) is in correlation to the increase in *O*-GlcNAc removal activity of *O*-GlcNAcase. The reduction in levels that occurs especially in high molecular weight protein (> 36 kDa) reflects the metabolic transition from glycolytic to gluconeogenic state [11]. A similar phenomenon of *O*-GlcNAc levels was observed during the transition of cell to malignancy, indicating the fully grown oocyte (stage VI) has at least some characteristics in common with a malignant cell where the regulation of the modification is also altered [11].

All these experimental findings suggest that the *O*-GlcNAc modification might play some important regulatory role in connecting cell growth, division and metabolism. As one step in elucidating these connections in a developmental system, it is important to first isolate and identify the modified oocyte proteins that change during oocyte development. Since a relatively large fraction of stage I oocyte proteins are *O*-GlcNAc modified, these oocytes were used as source for the studies described herein [11].

1.2 Introduction to *Xenopus laevis* oocyte

The oocyte of *Xenopus laevis*, the South African Clawed frog (Figure 1.2.1.1) is a good model system for biochemical studies for several reasons. First of these is the availability of abundant literature on its anatomy, morphology and metabolism [10]. Second, the frogs being highly adaptable and resistant to infection can be easily maintained at low cost in the laboratory. Third, because of continuous and asynchronous oogenesis, the oocytes in all stages of development can be obtained from the ovary of an adult female frog. The ovarian tissue regenerates in two to three months and oocyte can be harvested up to four times from each frog [13]. Finally, in particular, the stage VI oocyte due to its large sizes can be used with ease for semi-quantitative microinjection studies that have proven instrumental in understanding the control of cell proliferation and the regulation of cell cycle [15, 16].

1.2.1 Oogenesis

Oogenesis is defined as the process of formation of ova or unfertilized eggs from the oogonia. The process is comprised of two phases, the first phase is a growth phase and second phase is a maturation phase. The oogonia enter meiosis I and become arrested at prophase I, where they are termed oocytes. At the prophase I arrest, the oocytes begins accumulating a large store of mRNA, mitochondrial DNA, and proteins required for the initial rapid cell divisions, along with a large amounts of yolk proteins and glycogen also required for post-fertilization. This first phase is further sub-divided into six major stages based on the morphology and anatomy of the growing oocyte [17] (Figure I.2.2.1). During this stage progression, the oocyte transforms from a small and transparent stage I to large and banded stage VI oocyte that are described stage-wise in

Figure 1.2.1- Female *Xenopus laevis* (South African Clawed Frog) Female frogs larger than males. An average frog weighs approximately 130-150 g and capable regenerating the ovarian tissue in three-four weeks. They are maintained in tanks containing room temperature dechlorinated water and approximately 1 liter of water per frog). They are fed twice to thrice a week with the nutrient rich frog brittle. (Nasco)

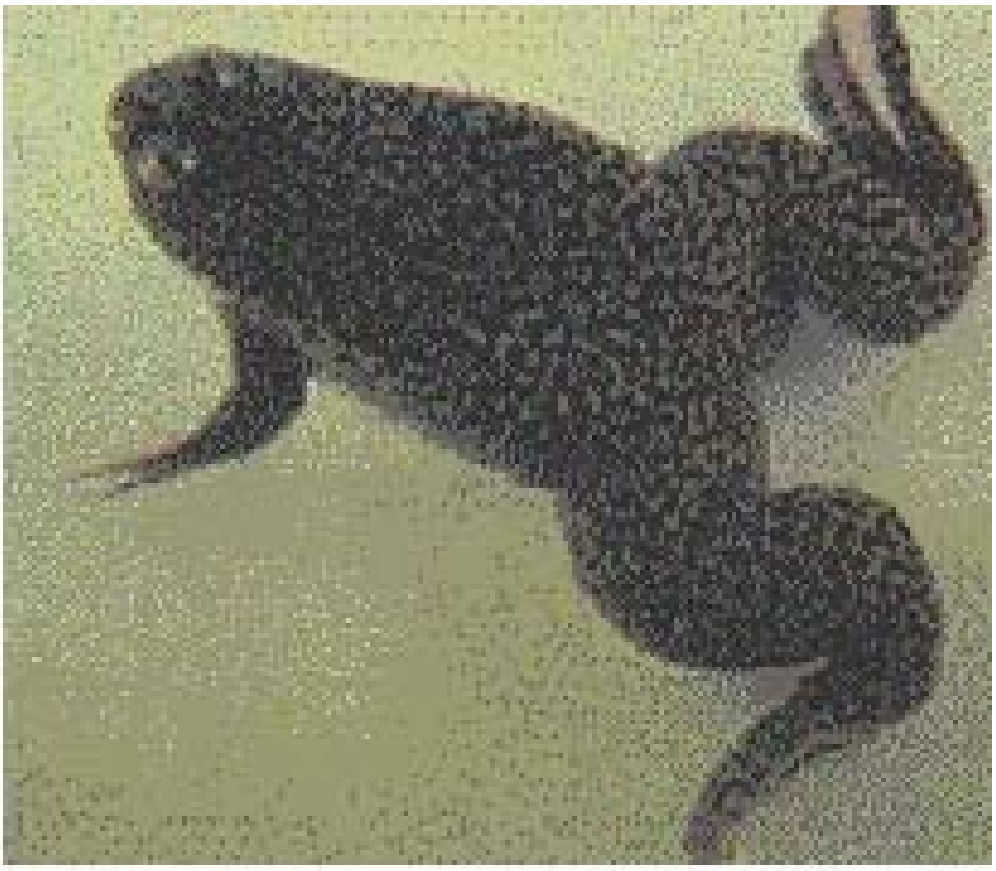

Figure 1.2.2.1- The different stages of *Xenopus laevis* oocytes during oogenesis. Two phases of the oogenesis (formation of egg for fertilization) are displayed. The first phase constitutes the oocyte growth, and further sub-divided into six major stages (I-VI) based on the features such as, diameter, pigmentation color and the amount of yolk protein in the cytoplasm. The second phase is maturation of fully grown oocyte (stage VI) where the oocyte undergoes germinal vesicle breakdown (GVBD) on progesterone stimulation. Figure from the website: http://www.luc.edu/depts/biology/dev/xenoogen.htm.

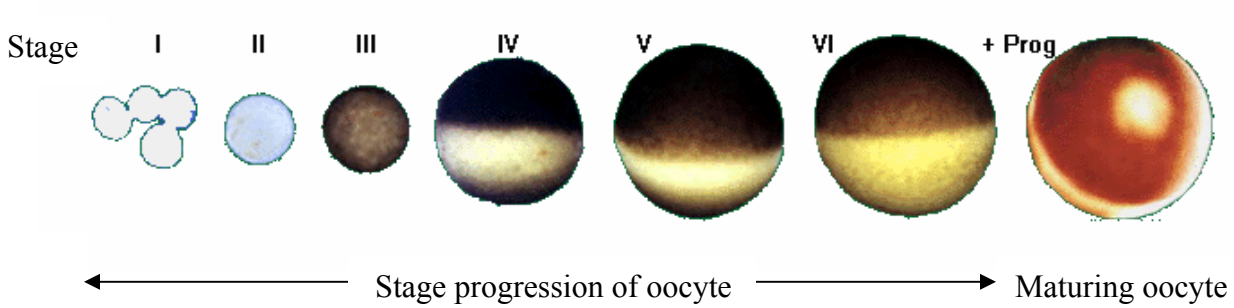

Stage I oocytes- clear and transparent (50-300 µm)
Stage II oocytes- white and opaque (300-450 µm)
Stage III oocytes- lightly pigmented all over (450-600 µm)
Stage IV oocytes- yolk protein deposition at the upper animal hemisphere (600-1000 µm)
Stage V oocytes- accumulating yolk and have darker pigmented color (1000-1100 µm)
Stage VI oocytes- fully grown and have progesterone receptors on their plasma membrane (1100-1300 µm)
Stage VI oocytes undergo meiosis when exposed to the steroid progesterone producing a white spot at the animal pole.

detail in the following section 1.2.3.

In the maturation phase, the fully grown oocyte (stage VI) forms an unfertilized egg upon stimulation with the steroid hormone, progesterone [18]. The stimulated oocyte arrested at the G_2/M border resumes meiosis I, and progresses through meiosis II to become once again arrested at metaphase II. A white spot, the attachment of meiotic spindle to plasma membrane was formed on the animal hemisphere of stage VI oocyte indicating the breakdown of the oocyte nucleus or germinal vesicle (GVBD) [19]. The formation of white spot on the animal hemisphere is the most obvious external indication of oocyte maturation (Figure 1.2.1.1). Thus the stimulated oocyte undergoes a number of morphological and biochemical changes prior to arrest at the metaphase II. The result of maturation process is a matured oocyte or unfertilized egg that is now ready for fertilization.

1.2.2 Oocyte Development

As found in the frog ovary, oocytes are arrested at prophase I between the second growth phase (G2) and the mitotic phases (M). They undergo a significant change from a small transparent oocyte at stage I to a large banded oocyte by stage VI with a distinct brown hemisphere or so called animal pole and green vegetal hemisphere or vegetal pole [17]. The nucleus and majority of the metabolic functional organelles are found in approximately 0.5 µl of the animal hemisphere while the equal sized vetegal hemisphere contains mainly yolk protein and glycogen in stages IV-VI (Figure 1.2.2.1). The small stage I oocytes range from 50 to 300 µm in diameter with a transparent cytoplasm and visible germinal vesicle (nucleus). The clear cytoplasm contains a microscopic yellowish mitochondrial mass and stains intensely for RNA and lightly for polysaccharides. These oocytes are previtellogenic, which means they are not involved in active accumulation of

the yolk proteins. In the ovary, the interspersed oocytes from all stages of development are surrounded by three layers; the innermost follicular epithelium, the middle theca made up of connective tissue containing blood vessels and fibroblasts, and the outermost surface epithelium [17].

The white and opaque stage II oocytes are 300-450 μm in diameter, and comprises of 45% of the Stage II to VI oocyte population. At this stage, the acellular vitelline envelope begins to develop. At Stage III, the visible pigmentation and the vitellogenesis (the process of active accumulation of the yolk proteins) are initiated. These oocytes are tan or light brown in color but with no visible differentiation of the animal and vegetal poles. They range from 450-600 μm in diameter and RNA synthesis peaks at this stage. The stage IV oocytes range in size from 600-1000 μm. They show the clear differentiation of the animal and vegetal poles. The animal pole is dark brown in color containing the nucleus. Stage V grow from 1000-1200 μm in diameter and develops a distinct boundary between the dark brown animal and the greenish yellow vegetal hemispheres [17].

Stage VI oocytes are post vitellogenic. The two distinct brown animal and light greenish yellow vegetal hemispheres separated by an unpigmented 0.2 mm wide equatorial band. The nucleus is eccentrically situated near the animal pole, and a clear polarization of nuclear envelope becomes visible [17]. The fully grown oocyte is 1,000,000 times the volume of typical somatic cell [10]. Half of the volume consists of the yolk proteins while the nucleus is now 300-400 nm in diameter [10]. These oocytes at the G2/M border arrest are responsive to the hormone, progesterone and upon stimulation undergo germinal vesicle breakdown (GVBD) into an unfertilized egg.

1.2.3 Protein synthesis during oogenesis

The *Xenopus* oocytes arrested at prophase I have accumulated massive amounts of yolk proteins, lipids and maternal mRNA required for the series of cell divisions that take place during maturation, fertilization and embryogenesis. Therefore a fully grown oocyte (stage VI) as described above is an abnormally large cell with a bloated nucleus referred to as the germinal vesicle. The contents of this unusual cell are summarized in the table 1.5.1 [20]. Table 1.5.1 shows that the oocyte at stage VI consists of largest amounts of yolk protein, ribosomal protein mRNA, mitochondrial DNA and rGTP (precursors). Whereas non-yolk proteins, heat shock 70 mRNA, oocyte chromosomal DNA, and dTTP (precursors) were present in lowest amounts. The accumulation of mRNA is completed by the end of stage II of oogenesis. However, the lampbrush chromosomes that exhibit transcription rates higher than those typical for somatic cells remains active during the entire period of oogenesis [21-23]. The estimated rate of poly (A) mRNA entry into cytoplasm in stage III and VI oocytes is approximately 1.4 ng per day. Even though, this is a small percentage of the total maternal mRNA, the actual amount of message that enters the cytoplasm is quite high due to the enormous rate of nuclear RNA synthesis [23]. The DNA microinjection experiments show that maternal transcripts are responsible for most of the protein synthesis during oogenesis, not the DNA injected into the oocyte nucleus [24].

The non-yolk proteins are accumulated in the oocytes by endogenous protein synthesis and yolk deposition by micropinocytosis of vitellogenin synthesized by the adult frog in the liver [25, 26]. The rate of protein synthesis increases over 100-fold during the stage progression from stage I-VI. A similar increasing trend was observed in the

Table 1.2.3.1- Composition of a *Xenopus* oocyte, full grown and without follicles cells.

(Total Volume, 1 µl; yolk-free volume 0.5 µl; GV volume 40 nl)

Component	Weight	Number of components	% of total in cytoplasm
DNA			
Oocyte chromosomal	12 pg	-	None
Nucleolar (rDNA)	25 pg	2 x 10^6 rDNA repeats	None
Mitochondrial	4000 pg	~10^8 gemones	100%
RNA			99%
Ribosomal protein m-RNA	5 µg	10^{12} ribosomes	99%
5S	60 ng	10^{12}	99%
tRNA	60 ng	1.5 x 10^{12}	99%
snRNA U1	0.07 ng	8 x 10^8	90%
polyA+RNA	80 ng	5 x 10^{10} (if 2500 bases long)	
Ribosomal protein m-RNA	10 ng	2 x 10^{10}	-
Actin mRNA	~1 ng	5 x 10^8	-
Heat-shock 70m RNA	0.004 ng	10^6	-
Protein			
Yolk	250 µg	-	100%
Non-yolk	25 µg	5 x 10^{14} (30 K protein)	90%
Histones	140 ng	5 x 10^{12}	50%
Nucleoplasmin	250 ng	5 x 10^{12}	98%
RNA polymerase I and II		~ 10^5 x somatic cell	-
RNA polymerase III		5 x 10^5 x somatic cell	-
Precursors			
dTTP	10 pmol	-	-
rGTP	250 pmol	-	-
Methionine	40 pmol	-	-

This table is from 'Microinjection and Organelle Transplantation Techniques. Methods and Applications'. Edited by Celis J. E; Graessmann A; Loyter, A. (1986)

amount of ribosomal RNA, and approximately 2% of the ribosomal RNA was found to be engaged in protein synthesis during oogenesis [27]. An additional two fold increase is observed when maturation is induced in the oocyte [28]. Gurdon *et al*. have demonstrated that the stage VI oocytes have spare translational capacity, that is injected mRNAs are translated in addition to endogenous messages [29]. However, the latter studies have shown that the translational capacity of the oocyte is not uniform for different classes of messages. The injected messages that are translated on the free cytosolic polysomes were expressed, whereas the ones that are translated on the endoplasmic reticulum resulted in the accumulation of these injected mRNA [30]. This non-uniformity in the translation of mRNAs was apparently due to the limited availability of one of the translational machinery, the ribosomes on endoplasmic reticulum in the oocyte [31].

1.2.4 Gluconeogenic metabolism

In addition to the accumulation of yolk protein, the developing oocyte synthesizes a large amount of glycogen that is used as the source of energy during embryogenesis (from gastrulation stage onwards) [32]. Incorporation of microinjected ^{32}P-labelled glycolytic intermediates, such as ^{32}P-labeled phosphoenolpyruvate and glucose-6-phosphate into UDP-glucose and then presumably into glycogen in the stage VI oocytes, fertilized eggs, and cells of cleaving embryos has suggested that basic metabolism in these cells is gluconeogenic and glycogenic until the embryo reaches the late blastula stage [33]. Interestingly, rapid incorporation of ^{32}P-glucose-6-phosphate into ATP, inorganic phosphate and creatine phosphate in stage II oocytes and not in stage VI oocytes also indicated a metabolic transition from glycolytic to gluconeogenic state [33]. Since enolase is thought to out-compete pyruvate kinase for any phosphopyruvate, and the activity of the fructose

1, 6-bisphosphate is low in the stage II and VI oocytes [33], the inorganic ^{32}P is found in very low amounts compared to typical cells. This indicates that the oocyte metabolism is mainly gluconeogenic, and very little energy is derived from glycolysis. However, the (U-^{14}C)glucose microinjection into the oocytes Stage VI) of *Caudiverbera caudiverbera*, the Chilean frog, and *Xenopus laevis* (data not shown) has demonstrated glycogen synthesis by an indirect pathway involving glycolytic breakdown of glucose to lactate, which is then converted into glycogen via an apparently connected gluconeogenic pathway [34]. Therefore glycogen synthesis might be possible in both direct and indirect pathways in amphibian oocytes.

Since there is no glycogen breakdown until the gastrulation, the amino acids especially glutamine are used as the carbon source for cellular energetics and macromolecular synthesis in the fertilized egg and in the oocytes [33]. A similar type of metabolism where glutamate is a major energy source has also been observed in some tumor cells [35, 33] might explain some of the decreases in *O*-GlcNAc levels in these cells [36].

1.3 Introduction to *O*-linked-β-N-acetylglucosamine modification

The glycosidic linkage of the β-N-acetylglucosamine through the hydroxyl side chains of serine or threonine residues of proteins is termed as the *O*-linked-β-N-acetylglucosamine (*O*-GlcNAc) modification (Figure 1.3.1). The modification occurs in many nuclear and cytosolic proteins of metazoans [1, 37]. This novel post-translational modification was first discovered in murine lymphocytes by Torres and Hart in 1984. Since the first characterization, a myriad of proteins have been found to bear this modification [2] (Table1.2.1). Most of these *O*-GlcNAc modified proteins are also phosphoproteins. In an analogous manner to *O*-phosphorylation, the modification is regulated by a unique set of

proteins that add and remove the modification in response to cellular stimuli [7]. Given the dynamic nature of *O*-GlcNAc modification, and the fact that in at least in some cases it acts as an alternative to protein phosphorylation, this modification has increased the complexity of the regulatory processes in the cell [2, 9, 38-41].

The *O*-GlcNAc modification is added to protein by a ubiquitous enzyme, uridine diphospho-N-acetylglucosamine: polypeptide β-N-acetylglucosminyl transferase or *O*-GlcNAc transferase (OGT). The OGT gene that is present on the X chromosome was shown to be essential for cell viability [42]. OGT is a soluble protein found in the cytosol but more predominantly in nucleus was first characterized in rat liver extract by the Hart group [43]. The enzyme composed of three subunits in an $\alpha_2\beta$ conformation with two 110 kDa α-subunits and one 78 kDa β-subunit [44]. The UDP-GlcNAc level in the cell regulates the enzyme activity of the α-subunit with a low apparent K_m 545 nM for UDP-GlcNAc that can change with the concentration of UDP-GlcNAc and the other regulators [45]. OGT contains an N-terminal tetratricopeptide repeat (TPR) domain and C-terminal catalytic domain [46, 47]. The C-terminal domain that resembles glycogen phosphorylase superfamily of glycosyl transferase hypothesized to contain two Rossman type folds and UDP-GlcNAc binding site [47]. Whereas, the N-terminal TPR domain mediates protein-protein interaction that appears to be necessary for the enzyme self-association, as well as the substrate recognition [48-52]. The crystal structure of human OGT has shown that homodimeric TPR domain containing 11.5 TPR repeats form an elongated superhelix, and its concave surface is lined by a conserved array of asparagines. This asparagines array shows marked similarity to the array in armadillo (ARM) repeat proteins, importin α and β-catenin, and thus suggesting that the TPR domain of OGT uses a similar mecha-

Figure 1.3.1- *O*-linked β-N-acetylglucosamine (*O*-GlcNAc) modified protein. N-acetylglucosamine group in β-linkage at the hydroxyl group of the serine, Ser residue of the protein.

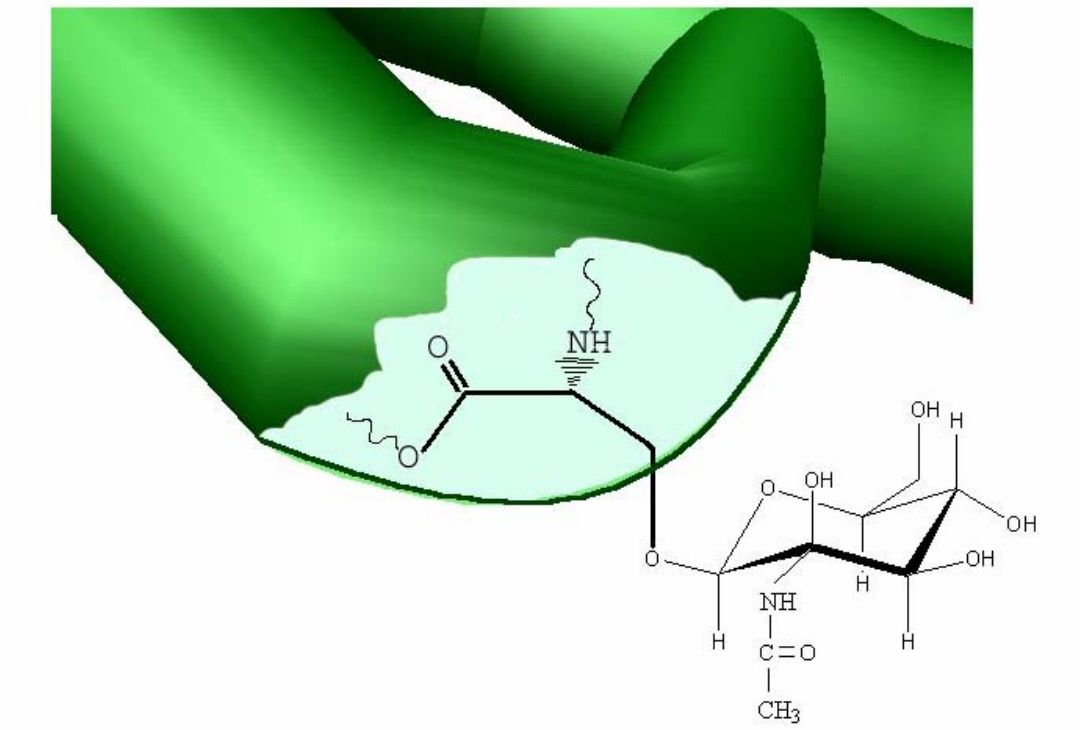

Table 1.3.1- List of the *O*-GlcNAc modified proteins classified based on their functions. Table from the review '**Proteomic Approaches to Analyze the Dynamic Relationships between Nucleocytoplasmic Protein Glycosylation and Phosphorylation'** by Whelan, Stephen A.; Hart, Gerald W. (Circulation research, (2003), 93, 1047-58).

Functional Subgroup	Protein	Reference from the above review paper
Chaperones	Heat shock protein 27 (HSP27)	90, 102
	Heat shock cognate 70 (HSC70)	96*
	Heat shock protein 70 (HSP70)	104
	Heat shock protein 90 (HSP90)	96*
Chromatin	Chromatin associated proteins	105
Cytoskeleton		
Actin-based	Ankyrin G	106
	Cofilin	96*
	E-cadherin	107*
	Myosin	108*
	Protein band 4.1	109
	Synapsin	110
	Talin	111
Intermediate Filaments	Keritins 8, 13, 18	112, 113
	Neurofilaments H, M, L	114, 115
Microtuble-based	α-tubulin	104*
	Dynein LC1	96*
	Microtubule associated proteins 2 & 4 (MAP 2 & 4)	116
	Tau	16
Other	Adenovirus type 2 & 5 fiber proteins	117, 118
	Assembly protein 3 & 180 (AP-3 & AP-180)	119, 120
	β-Amyloid precursor protein (β-APP)	23
	β-Synuclein	121
	Piccolo	96*
	Plakoglobin	122
Kinases and Adaptor Proteins	Casein Kinase II (CKII)	63
	Glycogen synthase kinase-3β (GSK-3β)	63
	Insulin receptor substrate 1 & 2 (IRS-1 & -2)	27, 28, 67
	PI3-kinase (p85)	28
Metabolic Enzymes	Enolase	96*
	Endothelial nitric oxide synthase (eNOS)	72
	Glyceraldehyde-3-phosphate dehydrogenase (GAPDH)	96*

	Glycogen synthase (GS)	70
	Phosphoglycerate kinase (PGK)	96*
	Pyruvate kinase (PK)	96*
	UDP-glucose pyrophosphrylase (UGP)	96*
Nuclear Hormone Receptors	Estrogen receptor-α & β (ER-α & -β)	17, 123, 124
	V-*erb*A	125*
Nuclear Pore Proteins (NUP)	Nup 62	126
	Nup 153, 214, 358	127
	Nup 180	128
	Nup 54, 155	96*
Phosphatases	Nuclear tyrosine phosphatase p65	129
	Phosphatase-2a inhibitor (i2pp2a)	96*
Polymerases	RNA Pol II	15
Prot*O*-oncogenes	c-Myc	14
RNA binding proteins	40S ribosomal protein S24 (40SrpS24)	96*
	Elongation factor 1-α (EF-1)	96*
	Eukaryotic initiation factor 4A1 (EIF 4A1)	96*
	Ewing-sarcoma RNA-binding protein (EWS)	96, 130
	RNA binding protein G (hnRNP G; La-antigen)	131
Transcription factors	AP-1 (c-fos and c-jun)	132*
	β-catenin	107
	CAAT box transcription factor (CTF, NF-1)	132*
	Cyclic AMP response element-binding protein (CREB)	95
	ELF-1 (Ets transcription factor)	26
	Enhancer factor 2D (EF-2D)	96*
	Hepatocyte Nuclear Factor 1 (HNF-1)	133
	KIAA0144, Oct1	96*
	NF-κB	134
	OGT interacting protein 106 (OIP-106)	38
	p53	135
	Pancreatic/duodenal homeobox-1 protein (PDX-1, IPF-1, STF-1)	136
	PAX-6	137
	Pancrease-specific transcription factor (PTF-1)	138*
	Human C1 transcription factor (HCF)	96*
	Serum Response Factor (SRF)	91
	Sp1	132
	Ying Yang 1 (YY1)	139
Tumor suppressors	Retinoblastoma protein (Rb)	unpublished
Viral Proteins	Baculovirus gp41 tegument protein	140
	HCMV UL32 (BPP) tegument protein	141
	NS26 Rotavirus Protein	142

	SV-40 large T-antigen	
	unpublished	
	Virion basic phosphoprotein	143
Other	Annexin 1	96*
	Collapsin response mediator protein-2 (CRMP-2)	121
	Elongation initiation factor-2 associated 67 kDa (EIF2α p67)	144
	Gaba-receptor interacting protein-1 (GRIF-1) & Splice variants	38
	Glut-1 & 4	145
	Nucleophosmin	96*
	Peptidyl prolylisomerase (PPI)	96*
	Proteosome component C2	96*
	O-GlcNAc transferase (OGT)	29
	Q04323, UCH homolog	96*
	Sec23, human homolog (hhSec23)	96*
	Ran	96*
	Rho GDP-dissociation inhibitor 1 (Rh*O*-GDI α)	96*
	Ubiquitin carboxy hydrolase (UCH)	121

*These identifications are still considered putative as supporting structural work has not been published.

nism of protein-protein interaction [52]. A group of proteins known as *O*-GlcNAc interacting proteins (OIP) exists that mediate the interactions between the tetratricopeptide repeats of enzyme and the substrates [53].

Even though, OGT is found in all tissues examined, the levels of expression differ among tissues. In addition, the levels of expression are not correlated to the activity, implying that the enzyme is regulated post-translationally [43, 46]. For example, OGT is modified by both tyrosine phosphorylation and *O*-GlcNAcylation [51], although the role of these modifications on the localization and the activity of enzyme are unknown. At the substrate level, both the K_m and V_{max} for a variety of substrates is altered by the UDP-GlcNAc levels. The enzyme has apparent K_m for UDP-GlcNAc ranges from 0.05 μM-4.8 mM in cell extracts. The UDP-GlcNAc levels are in turn depends on extracellular signals, the state of nutrition, development and differentiation [51, 54-59]. OGT remains active across the physiological range of UDP-GlcNAc in the absence of UDP, a potent inhibitor (K_i 200 nM) [45, 60].

The removal of *O*-GlcNAc group is accomplished by a specific enzyme, β-N-Acetylglucosaminidase (*O*-GlcNAcase) with a neutral pH optimum that is predominantly localized to the cytosol. The enzyme is characterized from both rat spleen and human brain. The ubiquitous enzyme is abundantly found in the brain, placenta and pancreas [61, 62]. *O*-GlcNAcase has molecular weight of 106 kDa, and exists as a αβ heterodimer with a 54 kDa α-subunit and 51 kDa β-subunit. The enzyme is found in both cytoplasm and nucleus. Unlike, the more general specificity of lysosomal hexoaminidases with acidic pH optima, the neutral enzyme is not inhibited by GalNAc or its analogs, and shows no other glycosidase activity. In addition, the enzyme does not cross-react with the antibodies against the lysosomal hexoaminidases [61,62]. However, similar to lysosomal hexoaminidases, *O*-GlcNAcase has a K_m = 1.1 mM for a general glycosidase substrate paranitrophenyl-GlcNAc [63]. In contrast, streptozotocin (STZ) a glucosamine nitrosourea specifically inhibits *O*-GlcNAcase and not other hexoaminidases [64]. Another strong inhibitor of *O*-GlcNAcase is *O*-(2-acetamido-2-deoxy-D-glucopyranosylidene) amino-N-phenylcarbamate (K_i =54 nM PUGNAc) [65, 66]. Interestingly, *O*-GlcNAcase retains the enzymatic activity upon cleavage by caspase-3 releasing the regulatory domain from the catalytic moiety, indicating that removal of *O*-GlcNAc may play a role in cell death process [63]. Many soluble nuclear and cytosolic proteins as shown in table 1.3.1 are the targets of OGT and *O*-GlcNAcase. Many of the proteins characterized so far, such as Estrogen Receptor β (ERβ), tau, SV-40 large T antigen, c-Myc oncogene, eNOS, RNA polymerase II and αβ-crystallin show that *O*-GlcNAc and *O*-phosphate groups compete for the same site [67-72]. However, in some proteins, there is a synergistic interplay of *O*-GlcNAc and *O*-phosphate [73], and in all likelihood an antagonist and/or even no connec-

Figure 1.3.2- Schematic diagram of the hexosamine biosynthetic pathway and the dynamic processing of *O*-GlcNAc modification by *O*-GlcNAc transferase and *O*-GlcNAcase. The diagram represents the substrates, enzymes and inhibitors of the hexosamine biosynthetic pathway (HBP) and during the regulation of *O*-GlcNAc modification.

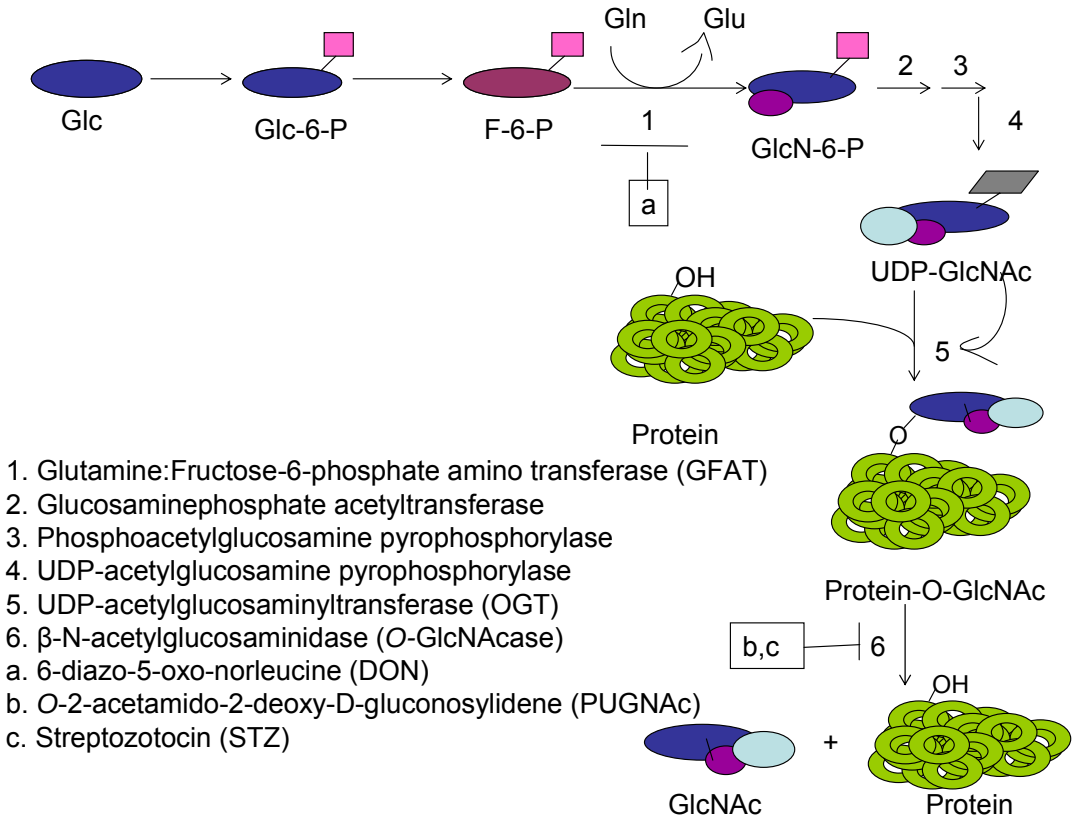

1. Glutamine:Fructose-6-phosphate amino transferase (GFAT)
2. Glucosaminephosphate acetyltransferase
3. Phosphoacetylglucosamine pyrophosphorylase
4. UDP-acetylglucosamine pyrophosphorylase
5. UDP-acetylglucosaminyltransferase (OGT)
6. β-N-acetylglucosaminidase (*O*-GlcNAcase)

a. 6-diazo-5-oxo-norleucine (DON)
b. *O*-2-acetamido-2-deoxy-D-gluconosylidene (PUGNAc)
c. Streptozotocin (STZ)

tive effect may well be formed as more proteins are analyzed.

The galactosyl capping studies using β-D-1-4-galactosyltransferase in *Xenopus* maturing oocyte have demonstrated the deleterious effect of the blocking the addition and removal of *O*-GlcNAc, thus suggesting this post-translational modification may play a significant role in cellular regulation [12, 74]. However, structural changes may also have played a role in these outcomes. In another study, the elevation of *O*-GlcNAc using PUGNAc has shown no effect on the cell growth rate [65]. The contradicting results might be due to the rapid turnover of the PUGNAc and the replacement of it every 48 hours. As mentioned earlier, the OGT deletion studies in ES cells, embryonic fibroblast or tissue using Cre-lox technology [75] is lethal, suggesting that OGT is essential for life at single cell level [42, 76]. Since the substrate specificity of OGT changes at different concentrations of UDP-GlcNAc, the *O*-GlcNAc levels on key regulatory proteins, including OGT can be modulated by altering the extracellular glucose levels through the hexosamine biosynthetic pathway (as shown in the Figure 1.3.3) [77-87]. The change in *O*-GlcNAc levels to different signals based on its nutritional state modulating the overall behavior of the cell suggests that *O*-GlcNAc is a nutritional sensor [41, 63, 82, 88, 89]. For instance, the glucose starvation and forskolin treatment led to decreased glycosylation and increased degradation of Sp1, transcription factor and synthetic peptide through the ATPases in 19S regulatory subunits [90]. Apart from being a nutritional sensor, *O*-GlcNAc is also a stress sensor [91]. In many other parallel studies, an increase in the *O*-GlcNAc levels due to increase in glucose flux into the cells is observed in response to the stress such as heat shock, UV, hypoxia, reductive, oxidative and osmotic stress [3]. Interestingly, the rapid induction of heat shock proteins (HSP) such as HSP70 and HSP40

with the increase in *O*-GlcNAc shows that *O*-GlcNAc mediates stress tolerance [3]. However, the studies on diabetes have associated hyperglycemia with the increased cell death in several systems that might be due to the down-regulation of AKT activation [92-94]. The paradox may be due to the differences in the sensitivities of tissues/ cells to insulin, the dependence on AKT signaling or the basal cell death rate to that of induced cell death rate [91].

1.4 Earlier findings of the studies on *O*-GlcNAc modification in oocytes of *Xenopus laevis*

Recent reports have demonstrated that changes of *O*-GlcNAc levels in oocytes are related to the oocyte growth and maturation [11, 95], the exact function of the modification and the role of the modified proteins are still unclear. Slawson *et. al*. demonstrated delayed progesterone stimulated maturation of the fully grown oocyte when incubated with compounds such as glucose, glucosamine and PUGNAc before progesterone stimulation [11]. Additionally, when the oocytes were incubated with the glutamine-fructose-6-phosphate amino trasferase (GFAT) inhibitor, DON (6-diazonorbenzene) that reduces UDP-GlcNAc synthesis, nullified the glucose effect on the maturation. While the total cellular *O*-GlcNAc content apparently does not change during progesterone stimulation [11], another study has showed an approximate 4.5-fold increase in the *O*-GlcNAc content, mainly on two cytoplasmic proteins, one of 97 kDa, identified as β-catenin and another unidentified 66 kDa protein [13]. Microinjection of GlcNAc has delayed progesterone-induced maturation in *Xenopus* oocytes without any change in *O*-GlcNAc content suggesting that the modification could regulate protein-protein interactions required for the cell cycle kinetic [13]. Like Sp1 transcription factor, β-catenin is also stabilized by *O*-

GlcNAcylation [83, 13]. In addition, the microinjection of galactosyl transferase (GalT) into the progesterone-stimulated oocyte was shown to be toxic [12]. This GalT toxicity was reported due to the galactosyl capping of the *O*-GlcNAc residues that appear to disrupt aster formation during the meiosis or causes any other cellular effects. Thus, the *O*-GlcNAc modification might be facilitating the protein–protein interactions necessary for the maturation process of the oocyte. Thus, showing one or more modified proteins might be critical for oocyte maturation.

In addition to the maturation of oocyte, the development of oocytes has also been associated with changes in *O*-GlcNAc levels [11]. A gradual decrease in the *O*-GlcNAc levels was observed as during the oocyte progression from the stage I to stage VI along with a concommitant increase in the activity of *O*-GlcNAcase. Analysis of the oocyte proteins of all the stages I-VI has clearly demonstrated the reduction of *O*-GlcNAc levels in the high molecular weight proteins (>36 kDa) and herein, this thesis [11]. This reduction in turn correlates with the metabolic transition of oocyte from glycolytic to gluconeogenic state [33]. In addition, no incorporation of ^{3}H-glucosamine into proteins in the stage VI suggested very low levels of new *O*-GlcNAc modification in this stage [96]. Interestingly, a similar phenomenon of change in *O*-GlcNAc levels was observed during the transition of cell to malignancy, indicating the fully grown oocyte (stage VI) may have more characteristics in common with a malignant cell where the regulation of *O*-GlcNAc modification is disrupted [36].

Chapter 2

Materials and Methods

2.1 Materials:

2.1.1 Reagents:

Reagents used in immunoprecipitation and polyacrylamide gel electrophoresis were obtained from Biorad (Richmond, CA), Fisher (Atlanta, GA), Pierce (Rockford, IL) and Sigma (St. Louis, MO). Anti-mouse RL-2 antibody was purchased from affinity Bio-reagents (Golden, CO), and CTD110.6 was a generous gift from Dr. Gerald Hart and laboratory at Johns Hopkins University, Baltimore MD. The Immobilized pH Gradient (IPG) strips and IPG buffer, both in the range of pH 3-10 and pH 6-11 were obtained from Amershams Biosciences (Piscataway, NJ). Collagenase, Anti-mouse IgM conjugated agarose beads, and streptozotocin were purchased from Sigma (St. Lousie, MO). Secondary antibodies anti-mouse and anti-rabbit IgG were obtained from Biorad (Hercules, CA). The affinity column material, agarose wheat germ agglutinin beads were obtained from Vector Laboratories (Burlingame, CA). Nanopure water is used in the preparation of the buffers. Spectra dialysis tubing of MW 10,000 cut-off and Amicon centricons of MW 3,000-30,000 cut-off was purchased from Fisher Scientific. The protein standards used were Biorad High range molecular weight and Invitrogen Benchmark prestained protein ladder. All the other reagents used were as per the ACS quality.

2.1.2 Equipment:

Mini-gel cassette and Genie Electroblotter were obtained from Idea Scientific (Minneapolis, MN). Conductivity meter and power supply for the electrotransfer were obtained from Biorad, while UV/ visible spectrophotometer from Pharmacia Biotech. Amershams Ettan^{TM} IPGphor^{TM} Isoelectric focusing system was borrowed from Bio-chemsitry Department, USF and 6.0 Dexon 3/8 Circle Reserve Cutting surgical needle along with absorbable suture or non-absorbable suture from Davis and Geck, Inc. (Pearl River, NY) and Ethicon (Somerville, NJ), were obtained. Optima^{TM} TL-100 Ultra-centrifuge obtained from Beckman Instruments, Inc., (Palo Alto, CA)

2.1.3 Animals:

Female *Xenopus laevis* frogs were purchased from Nasco (Fort Atkinson, WI) and maintained at room temperature (20-22 ^{o}C) and fed with Frog brittle from Nasco two to three times a week

2.1.4 Buffers and Solutions:

The *oocyte medium* called Oocyte Ringers solution 2 (OR-2) (Wallace *et al*., 1973) was composed of 82.5 mM NaCl, 2.5 mM KCl, 1.0 mM $MgCl_2$, 5 mM HEPES pH 7.8, 2 mM sodium pyruvate, 10,000 units penicillin, and 10 mg streptomycin. The *oocyte homogenization buffer* (Ten β) was comprised of 50 mM Tris–HCl (pH 7.4) containing 5 mM EDTA, the phosphatase inhibitors, 100 mM NaF and 25 mM β-glycerol phosphate; and in addition, the protease inhibitor 2 mM PMSF, and the *O*-GlcNAcase inhibitor 5 mM streptozotocin are added before use. Note: The stock solution of 200mM PMSF was prepared in isopropanol and stored.

For *immunoprecipitation with RL-2 antibody*, the immunocomplexed beads were washed with Wash Buffer 1 containing 150 mM NaCl, 10 mM HEPES pH 7.4, 1% Triton X-100, 0.1% SDS and Wash Buffer 2 with the same composition as Wash Buffer 1 without salt. For *immunoaffinity purification with CTD110.6 antibody* required the washing buffer, radioimmunoprecipitation assay (RIPA) buffer containing TBS (136.9 mM NaCl, 2.7 mM KCl, and 24.8 mMTris-HCl, pH 7.6) along with detergents such as 1% IGEPAL, 0.5% deoxycholate and 0.1% SDS was used to wash the immunoaffinity column before elution with 1M GlcNAc in TBS, pH 7.6.

In *affinity chromatography*, the binding buffer used for equilibrating the agarose wheat germ agglutinin beads contains 10 mM HEPES, pH 7.8. The used beads were stored in the storage buffer containing 10 mM HEPES, pH 7.5, 0.15 M NaCl, 20 mM GlcNAc and 0.08% sodium azide. The proteins of interest were eluted off the column using a buffer containing 10 mM HEPES, pH 7.8 with 0.3 M NaCl and 0.5 M GlcNAc. The column can be regenerated with 0.1% acetic acid buffer, pH 3.0 with 1 M NaCl.

In *one-dimensional (1D) gel electrophoresis*, the samples were diluted with protein solubilizing mixture (PSM) in the ratio 1:1. PSM is a 50 mM Tris-HCl buffered solution (pH 7.5) containing 2.5% (w/v) SDS, 25% (v/v) sucrose, 0.25 mg/ml pyronin Y, 25 mM Tris-HCl /2.5 mM EDTA and 1.5% β-mercaptoethanol. The resolving gel required 41.5% stock acrylamide solution (5.6 M acrylamide and 97mM bis-acrylamide), resolving buffer (2 M Tris pH 8.9), 20% SDS 10% ammonium persulfate and TEMED (N, N, N', N'-tetra-methyl-ethylenediamine). For the stacking gel, same materials except for 4% acrylamide and stacking buffer (0. 5 M Tris pH 6.7) was required. The SDS

electrophoresis buffer containing 25 mM Tris-base pH 8.3, 195 mM glycine and 0.1% (w/v) SDS was used to run the SDSPAGE.

In *two-dimensional (2D) gel electrophoresis*, the samples were solubilized in the IEF sample buffer containing 7 M urea, 2 M thiourea, 4% (w/v) CHAPS, 60 mM DTT, 0.2% (v/v) IPG buffer (pH 6-11 or pH 3-10), and 0.002%(w/v) bromophenol blue. The IPG strips were reswelled in rehydration solution containing 8 M urea, 2% (w/v) CHAPS, 0.2% (w/v) DTT, 0.5% (v/v) IPG buffer (pH 6-11 or pH 3-10) and 0.02% bromophenol blue. The 2^{nd} dimension equilibration buffer contained 2% (w/v) SDS, 50 mM Tris-HCl pH 8.8, 6 M urea, 30% (v/v) glycerol, 0.002% bromophenol blue and 100 mg of DTT or 250 mg iodoacetamide. The 0.5% agarose sealing solution containing 0.002% bromo-phenol blue was used to seal the IPG strip on SDS gel. All other solutions and buffers used were similar to that of 1D-gel electrophoresis.

The *molecular weight markers* used for molecular weight comparison were used in either the unstained form or prestained (dye modified) form. The prestaining (modification with dye) of these proteins alters the molecular weight and relative migration (M_r) through the gel, the relative molecular weights of both forms (normal/prestained) are presented. The protein standards included carbonic anhydrase (M_r 31 000/ 37 000), oval-bumin (M_r 45 00/50 000), serum albumin (M_r 66 200/ 75 000), phosphorylase b (M_r 97400/ 100 000), β-galactosidase (M_r 116 250/ 150 000) and myosin (M_r 200000/ 250000) respectively for unstained or stained.

The *gel staining solution*, Coomassie blue staining solution contains 80% stock solu-tion and 20% methanol (stock solution contains 1 g of Brilliant blue G250, 11.6 ml of 85% H_3PO_4 acid and 100 g $(NH_4)_2SO_4$ diluted to one liter).

For *electroblotting*, cold (4°C) transfer buffer containing 50 mM Tris, 192 mM glycine (pH 8.3) and 20% methanol was used. (Note: The pH of the solution is not measured)

For *CTD110.6 immunoblotting*, the buffers used were TBS-HT (136.9 mM NaCl, 2.7 mM KCl, and 24.8 mMTris-HCl pH 8.0/ 0.3% Tween-20) and TBSD (136.9 mM NaCl, 2.7 mM KCl, and 24.8 mMTris-HCl pH 8.0/ 0.25% deoxycholate/ 1% Triton X 100/ 0.1% SDS). The CTD110.6 antibody, monoclonal mouse IgM was stored at 0.2ug/ul in TBST (136.9 mM NaCl, 2.7 mM KCl, and 24.8 mMTris-HCl pH 8.0, with 0.05% Tween-20)/ 3% BSA in -70 °C freezer until needed. A stock dilution of antibody (1:500) was prepared in TBST/ 3% BSA/ 0.01% sodium azide stored at 4 °C and used for two weeks to one month.

The RL-2 immunoblot requires PBST (136.9 M NaCl, 2.7 mM KCl, 5 mM Na_2HPO_4, and 2 mM KH_2PO_4 pH 7.2/ 0.05% Tween-20) and high salt PBST (HSPBST) (479 mM NaCl, 3 mM KCl, 5 mM Na_2HPO_4, 2 mM KH_2PO_4 pH 7.2, 0.05% Tween-20). The RL-2 antibody, monoclonal mouse IgG1 was aliquoted in PBST (136.9 M NaCl, 2.7 mM KCl, 5 mM Na_2HPO_4, and 2 mM KH_2PO_4 pH 7.2, with 0.05% Tween-20) and 3% BSA and stored at -70 °C. A stock antibody dilution of 1: 500 in PBST/ 3% BSA/ 0.01% sodium azide stored at 4 °C lasts for a month.

The *membrane staining solutions* are 1% India ink in TBST (0.3% Tween) and 0.2% Ponceau S stain (stock solution contains 2% Ponceau S in 5% acetic acid) for nitrocellulose, and 0.1% (w/v) Coomassie blue R in 50% methanol and 10% acetic acid is used for PVDF membranes.

The *gel staining solution*, Coomassie blue staining solution contains 80% stock solution and 20% methanol (stock solution contains 1 g of Brilliant blue G250, 11.6 ml of 85% H_3PO_4 acid and 100 g $(NH_4)_2SO_4$ diluted to one liter).

2.2 Methods

2.2.1 Oocyte harvesting and isolation:

Mature *Xenopus* frogs were maintained in the tanks filled with dechlorinated tap water at room temperature. The animals were fed with Nasco vitamin fortified frog brittle two or three times per week. To obtain the oocytes, first a healthy frog without surgical scars or with clearly healed prior incisions was anesthetized by immersing in $NaHCO_3$ buffered solution of MS 222 (500 mg of MS222 and 10 mEq of $NaHCO_3$ in one liter deionized water) in a tank for 10-20 minutes. Later it was placed on its back on a bed of ice, and the ovarian tissue was surgically removed through incision on the ventral surface. The muscle incision was sutured with absorbable suture and the skin with non-absorbable suture. An injection of Xylazine hydrochloride (10 mg/kg) was given intracoelomically. The animal was transferred to an empty recovery tank and allowed to recover at room temperature. Once the frog flipped on its stomach, room temperature water was added until it covered the animal and monitored for 30 minutes. The frog was kept under observation for two–three days, and if apparently normal was transferred back to one of the common holding tanks until the ovarian sacs were regenerated [19].

The excised ovarian tissue was cut into small sections (~ 1 cm^2) and washed with OR-2 solution to remove all the debris. Then ovarian tissue in fresh OR-2 solution was incubated in collagenase (1 mg/ml) for approximately 4 hours to free the oocytes from collagen. Later the turbid supernatant of oocytes freed from ovarian tissue framework

was carefully decanted without disturbing the sedimented oocytes to remove the unreacted collagenase and fresh OR-2 containing Ca^{+2} was added. Being smaller in size and lighter than the other stages, the stage I and II oocytes do not sediment quickly. Therefore, these oocytes in the fresh OR-2 solution can be separated from the rest by a series of swirling followed by a quick decantation of the supernatant containing mostly stage I and II oocytes. Oocytes in this supernatant were sorted into stage I and II in a petridish under a microscope. Typically 1000-1500 stage I oocytes were isolated from a healthy frog.

2.2.2 Homogenization of the oocytes

The sorted oocytes were transferred to a test tube (200 µl) and the liquid carefully removed with a pipet. Oocytes were then washed twice with two volumes of ice cold Ten β that was removed by 20 µl pipette, and then followed by the addition of fresh ice cold Ten β, approximately 1ul per stage I oocyte, and 10 µl per stage VI oocyte was added. Oocytes were then homogenized on ice in Ten β by rapidly drawing and expelling them from the 200 µl pipette tip. For stage VI oocytes an equivalent volume (1:1) of ice cold Freon (1, 1, 2-trichloro-trifluoro-ethane) was added to remove yolk protein and lipid [97], and the solution mixed thoroughly. The solution is centrifuged at 12,000 x g at 4 °C for ten minutes to remove the yolk proteins and membrane materials. The aqueous supernatant was carefully collected without disturbing the pellet at the Freon/buffer interface and stored at -20 °C. Previous work has demonstrated that the Freon does not change the protein profile in stage VI oocyte [98]. Same procedure was used to homogenize the stage IV and V oocytes using 5 µl of Ten β per oocyte to lyse the oocytes, and followed by Freon extraction to remove the yolk. While, the stage II and III were homogenized in the same manner as the stage I, except the stage III requires 3 µl of Ten β per oocyte.

2.2.3 Protein Estimation:

The protein concentration of the homogenate was estimated using Bradford micro protein assay (Biorad). Pure bovine IgG (Biocompare, CA) (stored as 1 mg/ml in H_2O at -20 °C) was used to obtain the standard curve using protein concentrations from 2 ug to 20 ug. First, six dilutions of protein standard were prepared by thorough mixing with 200 ul of reagent and nanopure water. After incubation at room temperature for 5 minutes, the absorbance was read at 595 nm on a spectrophotometer. In the same way, the sample solution was prepared in triplicate and absorbances were recorded at 595 nm. The protein amount in the samples was calculated from the standard curve.

2.2.4 Immunoprecipitation with RL-2 antibody:

The *O*-GlcNAc modified proteins were immunoprecipitated using mouse monoclonal RL-2 antibody, monoclonal mouse IgG1 to form an immunocomplex with the Anti-rabbit IgG preabsorbed Protein A trisacryl beads [99]. All the steps of the procedure were performed at 4°C. Each experiment was performed with three samples. The immunoprecipitation was carried out using the homogenate of the stage I and a few stage II (<10%) oocytes, with the final concentration of protein 1-2 µg/ µl using Ten β.

The homogenate was incubated with RL-2 antibody (5 µg for every 1mg of protein) and protein A trisacryl beads (50 µl) that were preabsorbed by overnight incubation with Rabbit Anti-mouse IgG (50 µg) and left overnight on the rotating mixer. Later the immunocomplex with the beads was harvested by centrifugation at 10,000 x g for 10 minutes to collect the pellet. This procedure was repeated after each washing step using Wash Buffer 1 and Wash Buffer 2. Then the pellet was solubilized with PSM as mention-

ed in the above procedure. All the fractions, the supernatant, washes and pellet were analyzed by silver staining the gel and CTD110.6 antibody immunoblotting.

2.2.5 Immunoaffinity purification using CTD110.6 antibody

This method employed CTD110.6 antibody, mouse monoclonal IgM that specifically binds to the modified proteins to the Anti-mouse IgM conjugated agarose column [100]. All the steps of the procedure were performed at 4°C. Each experiment was performed with three separate samples. The immunoprecipitation was carried out using the homogenate of the stage I and a few stage II (<10%) oocytes, with the final concentration of protein 1-2 µg/µl using Ten β.

First to preclear so as to reduce non-specific binding, the homogenate was incubated with the Anti-mouse IgM conjugated agarose beads for one hour on the rotating mixer, and centrifuged at 10,000 x g for 10 minutes to collect the supernatant. The precleared homogenate was then incubated with CTD110.6 antibody (5 µg for every 1mg of protein) and Anti-mouse IgM conjugated Agarose beads (50 µl) for 3 hours on the rotating mixer. Next the slurry was transferred into the column (1.5 cm x 6.5 cm) and the flow through was collected. The column was then washed twice with five volumes of RIPA buffer and once with two volumes of TBS. After washing the column, the proteins were eluted three times, each with two volume of 1 M GlcNAc in TBS after 20 minutes incubation. The eluted fractions were precipitated by overnight incubation with ten volumes of cold methanol at -20 °C. Samples were centrifuged at 10,000 x g for 15 minutes and the pellets were solubilized in PSM by vortexing for 1-2 minutes and boiling for two

minutes. All fractions, the flow through, the washes and the elutions were analyzed by silver staining and RL-2 immunoblotting.

2.2.6 Affinity chromatography:

The affinity chromatography was based on agarose wheat germ agglutinin column that specifically binds to all the terminal N-acetyl glucosamine residues on proteins [101], and thus enriching the sample with proteins of interest. Initially, the affinity purification was performed using binding buffer containing 10 mM HEPES, pH 7.8 and 0.15 mM NaCl (as per the maufacturer's instructions). Later, the low salt conditions using the same binding buffer without NaCl were employed for affinity purification of the sample, in order to enhance binding to the wheat germ agglutinin [102]. Homogenate (typically 1 mg) with a final concentration of approximately 1-2 µg/µl was incubated with 100 µl of agarose wheat germ agglutinin (WGA) beads for two hours on the rotating mixer. Before incubation with the protein mixture, the beads were washed with binding buffer to remove salt and N-acetylglucosamine (GlcNAc) present in the storage medium and were resuspended in the binding buffer. The incubated mixture was poured into a column (1.5 cm x 6.5 cm). Next the affinity column was washed five times with five column volumes of binding buffer. Elutions were performed with two column volumes of the elution buffer containing 0.5 M GlcNAc. Then, the eluted beads were regenerated using regeneration buffer at pH 3.0. Once regenerated, the beads were stored in the storage buffer. The eluted fractions were concentrated and pooled using ultra-centrifugation device with10,000 MW cut-off. The concentrated samples were solubilized with 2x PSM.

2.2.7 Differential sedimentation for enrichment of *O*-GlcNAc modified proteins:

Stage I oocytes were first homogenized in ten β as mentioned in the previous sections, and centrifuged at 1,000 x g for 10 minutes to remove cell debris and unlysed cells. The collected supernatant was then centrifuged at 10,000 x g for 10 minutes and the pellet was stored at -70 ^{o}C for further analysis. Later, the supernatant at 10,000 x g was further centrifuged at 100,000 x g for one hour and the fractions were stored at -70 ^{o}C. All the above fractions were analyzed by 1D/ 2D gel electrophoresis.

2.2.8 One-dimensional gel electrophoresis:

Samples were further separated and analyzed on either 8-10% SDS-polyacryl-amide minigel (9.5 cm x 6.5 cm) (SDS-PAGE) that was made following the protocol of Laemmili [103]. The resolving gel was made from appropriate dilutions of 41.5% stock acrylamide solution (5.6 M acrylamide and 97mM Bis-acrylamide) with resolving buffer (2 M Tris pH 8.9), nanopure water, 20% SDS 10% ammonium persulfate and TEMED (N, N, N', N'-tetra-methyl-ethylenediamine). The mixture was degassed for a minute before adding ammonium persulfate and TEMED. The stacking gel was made in a same manner except the final percent acrylamide was 4%, and stacking buffer (0.5 M Tris pH 6.7) was used instead of resolving buffer. Gels were run at room temperature at 15 mamps for approximately 1-2 hours, usually 40-50 minutes after the dye has completely left the gel.

2.2.9 Two-Dimensional Gel Electrophoresis:

For higher resolution, the samples were subjected to two-dimensional (2D) Gel Electrophoresis. The method has two discrete steps. In the first step (first-dimension), the proteins were separated based on their isoelectric points using 7cm Immobilized pH gradient (IPG) strips of pH 6-11 or pH 3-10 NL from amershams. The proteins focused at their characteristic pI on the IPG strip were further analyzed based on their molecular weight in the second step (second-dimension) using SDS-PAGE.

IEF was performed in four main steps, the sample preparation, the rehydration of the IPG strips, the sample loading and the isoelectric focusing. First, the sample was prepared by dialyzing against low concentration Tris buffer, pH 7.4 (5 mM Tris, 0.1% IGEPAL and 1 mM DTT) using dialysis tubing with a 10,000 M.W. cut off to reduce the concentration of salts including Tris that interferes with IEF. The dialyzed sample was solubilized with IEF buffer in a ratio of 1:6. The pH range of IEF buffers depends on the pH range of the used strip. Note: If the samples are too diluted (<3 µg/µl) following dialysis, should be concentrated by ultra filtration or acetone precipitation [104]. The second step of IEF involved rehydration of IPG strip as per supplier's instructions. The dry IPG strip was soaked overnight with the gel-side down in rehydration solution containing the appropriate IPG buffer with the overlay of DryStrip Cover Fluid. A 7cm IPG strip requires 125 µl of rehydration solution [105].

Sample loading constitutes the third step in isoelectric focusing (IEF). For the IEF, the IPG strip was first positioned on the Ettan IPGphor Cup Loading Strip Holder as per the manufacturer's instructions. The sample was applied to the rehydrated strip by the

sample cup application method. For a basic IPG strip, the sample was applied at the anodic end and at the center for a whole pH range IPG strip to avoid significant extremes of pH that can lead to loss of O-GlcNAc modification and/or protein precipitation. The final step comprises of isoelectric focusing (IEF) of the samples by using Ettan IPGphor Isoelectric Focusing System (Amershams). According to the instructions given in the manual, '2D-Gel Electrophoresis using immobilized pH gradients, Principles and Methods', the IEF was performed on the rehydrated strip at constant amperage of 50 μA at 20^{o}C, and ramping the voltage initially in a gradient mode to 500 V for 1 m and 4000 V for 1h 30 m, and later in a step and hold mode to 5000 V for 45 m.

After the IEF, the IPG strip was transferred to 10ml screw capped tube and was either stored at -70 ^{o}C or analyzed by SDSPAGE in the second step. The second dimension consists of a 1 mm thick, 10% laemmili SDSPAGE polymerized in between two glass plates with one plate protruding out, to position the IPG strip; and 4% stacking gel with two small wells and a larger well. Prior to positioning the strip on gel, the strip was incubated in equilibration buffer for first 15 minutes with 100 mg of DTT. This was followed by 15 minutes incubation in equilibration buffer with 250 mg of Iodoacetamide. Subsequently, the equilibrated strip was briefly immersed in the SDS electrophoresis buffer to lubricate, and later the plastic ends of the strip were carefully trimmed to adjust its length according to the size of 2nd dimension. The lubricated strip was then loaded on to the prestacked second dimension gel with the plastic side against one of the glass plates and sealed into place using the agarose sealing solution described before. With the protein standards and sample loaded at left of the gel, the gel electrophoresis was

performed at amperage of 10 mA for 15 minutes and continued for 40 minutes after the dye runs off.

2.2.10 Gel Staining methods

The staining was performed usually to obtain overall protein profile of the sample resolved on SDS PAGE. Generally, the gel was first incubated in the fixing solution to enhance the staining. The method of staining completely depends on the requirement of the experiment.

2.2.10.1 Coomassie Blue staining

The gel was fixed in a solution containing 20% methanol, 10% Acetic acid with constant shaking for a total of 20 minutes changing solutions once after 10 minutes. The gel was rehydrated by soaking in nanopure water for 15 minutes with constant shaking. The rehydrated gel was then incubated overnight in the G-250 coomassie blue staining with 20% methanol with constant shaking. The stained gel was destained for two hours in deionized water to get rid of the background staining [106].

2.2.10.2 Silver Staining

The proteins separated by SDSPAGE were stained by using Biorad Silver stain kit (as per the instructions given by the manufacturer) The gel, after electrophoresis was incubated in fixing solution containing 40% methanol and 10% acetic acid for 30 minutes minimum. The fixed gel was immersed in oxidizing solution ($K_2Cr_20_7$) for five minutes. The gel was then washed with nanopure water for a maximum of 15 minutes, changing 6-7 times especially in the first 5 minutes. After washing the excess oxidizer, the gel was

immediately transferred to the Silver solution containing 8% silver reagent and incubated for 20 minutes. Next, the gel was quickly rinsed in nanopure water for a maximum of 30 seconds and immediately the developer (6.4 g/200 ml) was added to the gel. The developing solution is changed once brown or smoky precipitate appears. This step was repeated until a stain of desirable intensity was obtained. Then use 5% acetic acid to stop the staining for 15 minutes. All steps were performed on a shaker.

2.2.11 Gel Drying

Drying of the gel was done by various methods. In one of the method, the gel was dried using Idea scientific Gel drying frame. (as per the instructions of manufacturer). The gel was first incubated in 10% ethanol and 5% glycerol for 30 minutes. The gel was then sandwiched between the wet gel drying membranes, and left encased in the gel drying plastic frame to dry. In another method, the gel was thoroughly rinsed with nanopure water and placed on a wet filter paper covered with the wet cellophane paper. The gel was left in the heated gel dryer (Biorad) for one hour to dry.

2.2.12 Immunoblotting

The analysis of the samples on the SDSPAGE was followed by transfer of the proteins to nitrocellulose or PVDF membranes. [107] Both the hydrophobic membranes were first equilibrated in transfer buffer for 15 minutes. The PVDF membrane being highly hydrophobic was initially wetted by methanol (5 seconds) and followed immersions in nanopure water (5 minutes) with constant shaking. The Genie transfer apparatus (Idea Scientific) was used to transfer the proteins for 2-3 hours at a constant voltage of 12 volts at 4^{o}C in the cold (4^{o}C) transfer buffer.

2.2.12.1 CTD110.6 immunoblotting

The blot after the transfer was immediately incubated in the blocking solution, TBS-HT for 2-3 hours at room temperature with constant shaking. Typically all incubations were carried out in carefully cleaned parafilm boats containing 20-50 ml solution. Next the blot was transferred to the 1^{o} antibody (CTD110.6 antibody) in TBS-HT at a dilution of 1:5,000 and incubated overnight at 4 ^{o}C with constant shaking. The incubated blot was then washed 2 x 10 minutes with TBS-D and later 3 x 10 minutes each with TBS-HT. Next the blot was incubated in the 2^{o} antibody (Goat anti-mouse IgM) at a dilution 1: 15,000 in TBS-HT for 1 hour at room temperature with constant shaking. Followed by the washing step as mentioned above and then the dried blot was treated with the Super Signal chemiluminescent substrate (Pierce) for 5 minutes again following manufacturer directions. Immediately the blot was dried and transferred to the cassette and exposed to film for 30 seconds or longer. To demonstrate the specificity of the CTD110.6 antibody, a duplicate blot was produced using the same protocol as above, except the primary antibody solution contained 15 mM N-Acetylglucosamine as a competing sugar.

2.2.12.2 RL-2 immunoblotting

Nitrocellulose immunoblots using RL-2 antibody were allowed to dry after transfer to improve recovery of antigenic sites. The dried blot was first soaked in the PBS at 70 ^{o}C in water bath for one hour with constant shaking. The wet blot was then blocked using high salt PBST (HSPBST) with 3% BSA at room temperature for two hours with the constant shaking. Typically all incubations were carried out in carefully cleaned parafilm boats containing 30-50 ml solution. Following blocking the blot was transferred into

a solution containing the primary antibody, RL-2 in HSPSBT with 3% BSA at a dilution of 1: 5,000 and incubated with modest shaking for two hours. The incubated blot was then washed 5 x 10 minutes with HSPBST with 0.01% BSA. The washed blot was transferred to the secondary antibody, goat anti-mouse IgG in PBST with 3% BSA at a dilution of 1: 20,000 at room temperature for one hour. The blot was then washed 8 x 10 minutes with PBST and the dried membrane was treated with Super signal chemiluminescence for 5 minutes. The blot was quickly dried and placed in the cassette and exposed to the film for half a minute and longer [36].

2.2.13 Wheat germ agglutinin affinity blotting

The proteins resolved by the SDSPAGE were transferred to PVDF (Polyvinyl difluoride) membrane. The blot was blocked in a TBST (0.05% Tween 20) solution containing 5% BSA for two hours at room temperature with constant shaking. Once again, all incubations were carried out in carefully cleaned parafilm boats containing 30-50 ml solution. After blocking, the blot was rinsed with TBST, and incubated in HS-TBST (1 M NaCl) with the WGA-HRP at 1: 10, 000 dilution [108] for 2 h at room temperature. The blot was then washed 3 x 10 minutes with HS-TBST and then 5 x 10 minutes TBST. The washed blot was developed at room temperature using freshly prepared 3mM DAB (diaminobenzidine) and 3% peroxide in 50 mM Tris-HCl (pH 7.6). Typically developing times were from 10 minutes to 20 minutes. The developed membrane was then washed with PBS and dried.

2.2.14 Membrane staining methods

Once again, the staining method was used to visualize the overall protein profile of the sample transferred on to the membrane, and the method of staining was chosen based on the requirement of experiment.

2.2.14.1 India ink staining:

The nitrocellulose/PVDF membrane was first soaked in PBST with 0.05% tween 20 for 10 minutes. If the membrane is nitrocellulose, it was then treated with 1% KOH solution for 5 minutes to enhance India ink staining. The blot was incubated in PBS for 30 minutes with one change of solution after 15 minutes. Then the blot was incubated for one and half an hour at 37 ^{o}C and one hour at room temperature with PBST, 0.3% tween 20 with changes of the solution every 30 minutes. On completion of washing, the blot was incubated overnight in 1% India ink staining solution. The blot that was washed with PBST twice for a few seconds gives a permanently stained membrane [109]. Note: The membrane was first stripped with a glycine solution if it had been previously immuno-blotted. This staining method is more sensitive than other methods with high level of detection (100 ng).

2.2.14.2 Ponceau S staining

Ponceau S stain can be used for nitrocellulose membranes with a detection limit of 1ug protein. First, the membranes were incubated in 2% Ponceau S for 20-30 minutes until the stained bands appear. Then, the stained membrane was destained in nanopure water to remove the background. This stain is a reversible.

2.2.14.3 Coomassie staining

This method is used for staining PVDF membranes with detection limit of 1.5 µg of protein. The membrane is incubated in 0.1% Coamassie stain for 5-10 minutes. Once the stained bands appear, it is destained with a 50% methanol/10% acetic acid (v/v) solution to remove the background.

2.2.15 Membrane stripping methods

The immunoblot was incubated in 200mM glycine, pH 3.0 for 20 minutes at room temperature with constant shaking. The blot was then washed 3 x 10 minutes with PBST [110]. For affinity bolt, β-mercaptoethanol method was used. First the membrane was incubated in the stripping buffer containing 62.5 mM Tris pH 6.8, 2% (w/v) SDS, and 100 mM β-mercaptoethanol for 30 minutes at 60 ^{o}C. Next, the stripped blot was washed 3 x 10 minutes in TBST

2.2.16 Identification of the protein bands of interest

Once 2D-gels of oocyte (stage I) proteins were sufficiently stained with coomassie so that identification was possible, the protein bands of interest immediately were excised for protein sequencing. Being sure to wear gloves and taking care not to introduce any contaminants, protein material (ie. keratin). In order to identify these bands, the 2D-pattern of proteins in coomassie stain was compared to the 2D-pattern of *O*-GlcNAc modified proteins in the CTD110.6 immunoblot. The bands that matched the ones in the immunoblot by the distances traveled in both the dimensions were selected to be sequenced. The selected protein bands were cut as close to the stained portions to get rid of

extra gel using a razor. Each of these gel pieces containing the protein was then placed separately into a 1.5 ml eppendroff tube that was previously washed with acetonitrile to remove dust and keratin, and stored at -20^{o}C.

2.2.17 Mass Spectrometric peptide sequencing and identification of proteins

The protein bands that were identified as *O*-GlcNAc modified by using the CTD110.6 immunoblot All the protein bands of interest were excised from the coomassie stained gel and sent to John Hopkins The peptide sequencing and identification was performed by the Dr. Stephen A Whelan at John Hopkins University using the MS/MS peptide sequencing coupled with database search as described in the following three steps.

1. In gel digest:

The excised protein bands of the G-250 commassie stained 2D-gel were first chopped into small pieces. Then the gel pieces were destained by washing three times with 100 mM NH_4HCO_3 for 10 minutes each and dehydrating with acetonitrile for another 10 minutes. The dehydrated gel pieces were vacuum dried and rehydrated in 20 µl of 10 ng/µl trypsin (Promega, mass spectrometry grade) in 50 mM NH_4HCO_3 on ice for 45 minutes. Once the gel pieces were hydrated, excess trypsin was removed and gel pieces covered with 50 mM NH_4HCO_3, pH 8.0 were left overnight at 37 ^{o}C for digestion. Once digested, the peptides were extracted with 50 µl of 50 mM NH_4HCO_3 and then, followed by three washes with 50 µl of 5% formic acid/ 50% acetonitrile solution for 20 minutes each. The extractions were pooled and vacuum dried. The extracted peptides were suspended in 0.1% Trifluoro acetic acid (TFA) and passed through Vydac C18 silica Micro-

spin columns (The Nest Group Inc.) and eluted with 75% acetonitrile and 0.09% TFA. The purified peptide mixture was once again vacuum dried.

2. LC-MS/MS Analysis:

The vacuum dried and purified peptides were resuspended in 1% acetic acid and loaded on a 10 cm x 0.075 mm column packed with 5 μm diameter C18 beads using N_2 pressure. The column was then washed with 1% acetic acid and then the peptides were separated by a 75 minute gradient of increasing methanol at a flow rate of 190 nl/minute directing effluent into the source (Finnigan LCQ). The LCQ was operated in an automatic mode collecting a MS scan (2 x 500 ms) of the peptide mixture, followed by two MS/MS scans (3 x 750 ms) of the two high intensity peptides with a dynamic exclusion set at 2 with a mass gate of 2.0 Da.

3. Mass data analysis:

In order to identify the proteins, the MS/MS data was interpreted using Bioworks software. The MS/MS spectra of the peptides were searched against several protein data-base including *Xenopus laevis database* (downloaded from NCl, National Institutes of Health at Frederick, MD) using the bioworks software. The MS/MS protein or peptides spectra were identified based on "Best hits" in the *Xenopus laevis database* search. The "Best hits" were those showing high degree of confidence that is the Xcorr > 2.5 and the dX-corr for the second entry > 0.1 [111]. At the same time, the data was also manually inspected for accuracy.

Chapter 3

Results and Discussion

3.1 Confirmation of the presence of high *O*-GlcNAc modified proteins in the stage I oocytes compared to the stage VI oocytes per unit mass:

Slawson et. al. [11] have shown the presence of high levels of *O*-GlcNAc in stage I oocytes, and a dramatic reduction in the levels during stage progression (I-VI) of oogenesis. As a first step in elucidating the possible role of *O*-GlcNAc modification in developing oocytes, the initial efforts were focused on isolation and identification of these modified proteins. Prior to beginning the purification process, a series of experiments were performed to confirm and reexamine the modified proteins of interest, and to examine the specificity of the proteins to CTD110.6 antibody (Figure 3.1.1 & 3.1.2 respectively). Every experiment was repeated three separate samples to confirm the results. Several immunostained bands above 30 kDa were reduced in the intensity while progressing from stage I to VI. Figure 3.1.1 shows that the protein bands # 1-14 at approximately 29, 48, 52, 63, 66, 70, 76, 84, 90, 101, 106, 116, 128, and140 kDa respectively were of initial interest. Competition for antigen binding with 15mM/30mM N-acetylglucosamine for CTD110.6 antibody demonstrated the specificity of all the above mentioned protein bands. (Figure 3.1.2) For comparison and as a control, the cytosolic fraction of a glioma cell line (contributed by Aaron Mathews) that is rich in the *O*-GlcNAc modified proteins also clearly demonstrated the specificity, but interestingly

Figure 3.1.1- CTD110.6 immunoblot of one-dimensional gel separation of proteins from oocytes at stages I, II, III and VI. Approximately 20 µg of proteins each of oocytes at stages I, II, III and VI were individually separated on the 8% gel and immuno-blotted with CTD110.6 antibody as described in Methods. The figure represents an auto-radiogram of the blot showing the pattern of ***O***-GlcNAc modified proteins in oocytes at different stages and the decreasing trend on ***O***-GlcNAc levels during stage progression of oogenesis. The arrows on the left-hand side show the protein bands of interest # 1-14 at approximately 29, 48, 52, 63, 66, 70, 76, 84, 90, 101, 106, 116, 128 and140 kDa respectively.

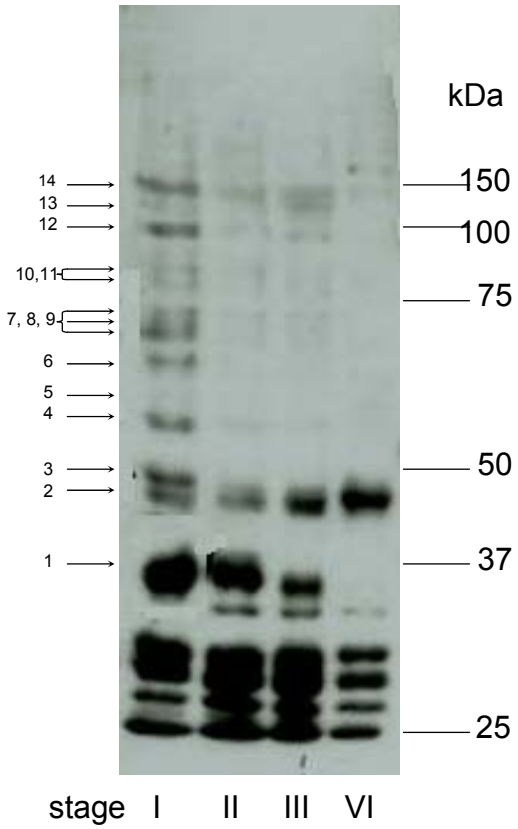

Figure 3.1.2- Competition with 15mM N-Acetylglucosamine to show specificity of *O*-GlcNAc modified to CTD110.6 antibody. Approximately 20 µg each of proteins from the cytosolic fractions from glioma cell line treated with 8 mM GlcNAc for 3 hours and 9 hours and the oocytes at stage I were individually separated, and immunoblotted with CTD110.6 antibody in absence and presence of 15mM/ 30mM GlcNAc. The figures represent the autoradiograms of the blots (a) without GlcNAc, (b) with 15 mM GlcNAc, and (c) with 30 mM GlcNAc while incubating the membrane with CTD110.6 antibody. The complete or partial disappearance of the bands in (b) and (c) indicates the specificity of the O-GlcNAc modified protein bands to CTD110.6 antibody.

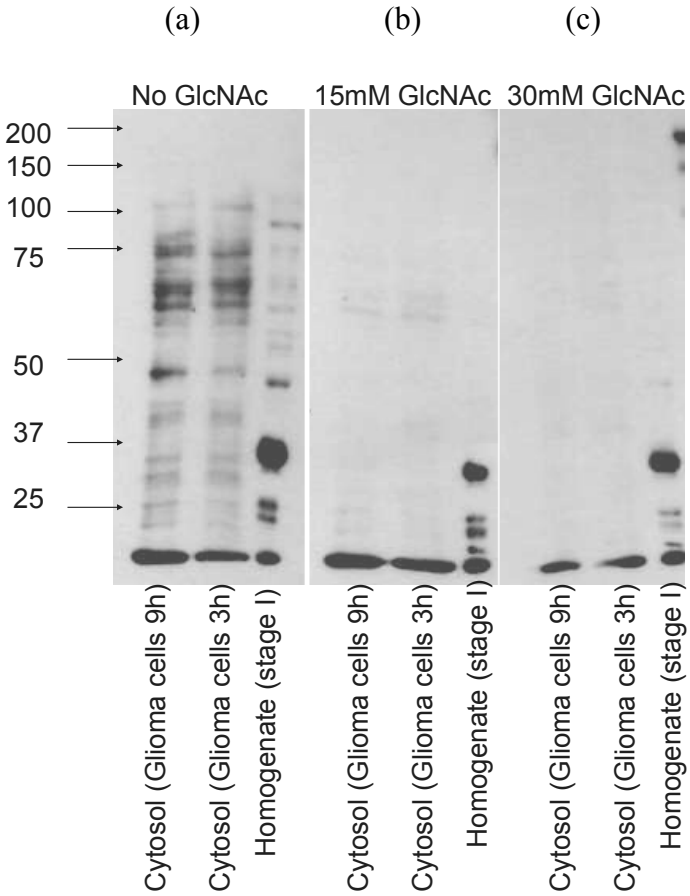

Figure 3.1.3- RL-2 immunoblot of one-dimensional gel electrophoretic separation of proteins from oocytes at stage I. Approximately 20 µg of protein was separated on the 10% gel and immunoblotted with RL-2 as described in Methods. The figure represents an autoradiogram of the blot showing a pattern of *O*-GlcNAc modified proteins in stage I oocytes similar to that shown by CTD110.6 antibody. The difference is in the intensity of specific bands especially the bands around 50 kDa. The positions of molecular weight marker are shown with arrows on left.

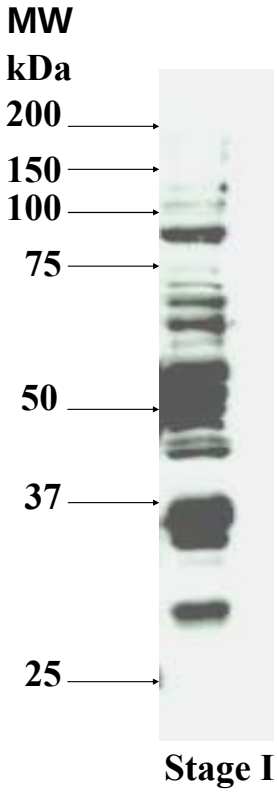

shows quite a different pattern of modified proteins. A similar pattern of oocyte modified proteins was observed using RL-2, another antibody recognizing with slightly different affinity but overlapping specificity to CTD110.6 antibody. Since stage I oocytes contained the largest amounts of these proteins per unit mass, these oocytes were used to isolate the *O*-GlcNAc modified proteins of interest. A few stage II oocytes (15% by number) that show a highly similar pattern of the modification were included to increase the amount of starting material so as to improve yields. Even though, the stage I oocytes are relatively abundant in the *O*-GlcNAc modified proteins, the total amount of these pro-teins in an oocyte is still small. Therefore, the strategy was to use a minimum number of purification steps to enhance overall recovery of proteins.

First step of the scheme was to examine the two-dimensional (2D) gel electrophoresis ability to directly separate the proteins of interest in quantities sufficient for sequencing. In addition, the level of detection of coomassie that used to stain the protein bands to be sequenced is low (1 ug). Depending on the success of this approach, the next step was to partially purify or enrich using various affinity technologies coupled with 2D-gel electrophoresis. The enrichment techniques attempted were immunoaffinity methods using the *O*-GlcNAc specific antibodies such as CTD110.6 and RL-2, affinity chromatography using the lectin, wheat germ agglutinin that specifically binds to the terminal N-acetylglucosamine residues; and differential sedimentation based on association of this protein with complex high molecular weight aggregates in the cell.

3.2 Two-dimensional gel analysis of the stage I and VI oocytes:

To examine and compare the 2D-pattern of the total proteins in stage I and VI oocytes, the whole cell homogenates were individually analyzed by 2D-gel electropho-

resis and immunoblotted with CTD110.6 antibody. Both samples were separately resolved by using two IPG strips with different pH ranges while performing IEF. In order to view all the oocyte modified proteins an IPG strip of full pH range 3-10 (Non-linear) was used. The non-linear range was initially selected since it gives a better resolution of the proteins within the range of pH 5-8, the range where generally the majority of cellular proteins are focused. Surprisingly, the majority of the modified proteins seen on one-dimensional SDS PAGE were not present on the final blot. The 2D analysis of stage I at this pH range 3-10 showed only three faint modified protein bands # 1-3 at approximately 29, 65 and 69 kDa respectively across an approximate pH range 5-8 on probing with CTD110.6 antibody. (Figure 3.2.1 a) However, the India ink total protein stain of same blot stripped using the glycine method showed the presence of several other proteins bands on the membrane. (Figure 3.2.1 b) Similar results were obtained with three separate samples. This suggests that the absence of the other bands of interests might be due to the unlikely hydrolysis and loss of the modification at the moderately low pH range. Alternately, and more likely the proteins might have focused off strip due to the steep rise in the pH near the end of non-linear pH strip, and as we all see later the very basic nature of the majority of proteins of interest. In addition to above reasons, the proteins get focused slightly at different regions due to the changes in the pH of the IPG buffer used during the IEF that might also explain the absence of the proteins that focus in pH range 8-10 in the later 2D-gel electrophoresis [112].

In the same manner, the proteins of stage VI oocytes were analyzed by 2D-gel electrophoresis and compared to the 2D-patterns of total proteins and *O*-GlcNAc modified proteins of the stage I oocytes. Similar results were obtained with three separate

Figure 3.2.1- Two-dimensional gel electrophoresis of oocyte proteins (stage I) using isoelectric focusing with pH range 3-10 in the horizontal dimension and SDS-PAGE (10%) in the vertical dimension. Approximately 100 µg of protein from oocytes at stage I was separated and immunoblotted with CTD110.6 and later the blot was glycine stripped and stained with India ink as described in Methods. Figures (a) Autoradiogram showing three faint bands at 29, 65 and 69 kDa respectively, and (b) India ink stain showing the overall 2D-pattern of the proteins of oocyte stage I. On the left hand side of the gel, 20 ug of the stage I was separated on one-dimension acts as reference.

(a)

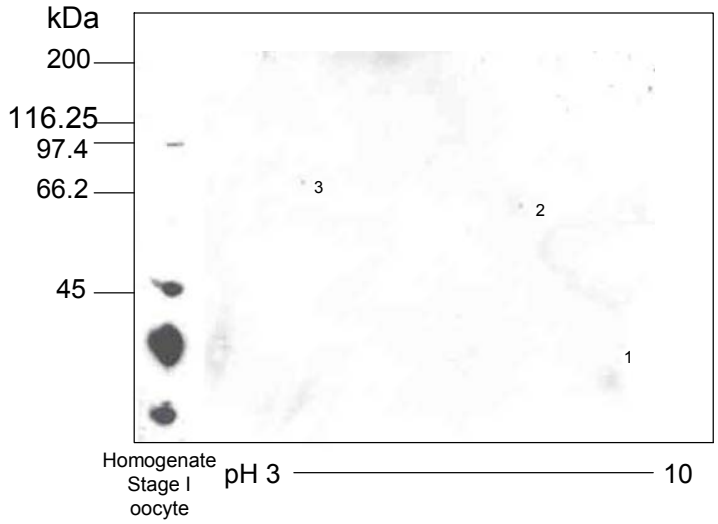

(b)

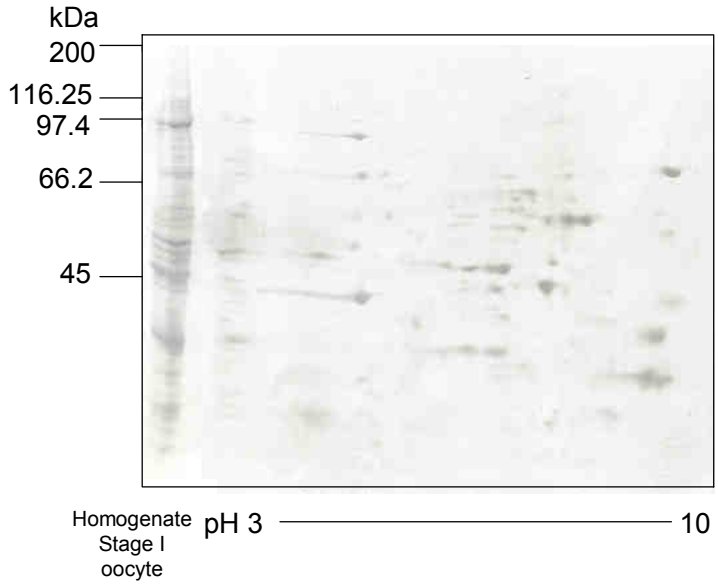

Figure 3.2.2- Two dimensional gel electrophoresis of oocyte proteins (stage VI) by isoelectric focusing with pH range 3-10 in the horizontal dimension and SDS-PAGE (10%) in the vertical dimension. Approximately 100 µg of protein from oocytes at stage VI was separated and immunoblotted with CTD110.6 and later the blot was glycine stripped and stained with India ink as described in Methods. Figures (a) Autoradiogram showing four bands # 1-4 at approx. 32, 35, 45 and 66 kDa respectively, and (b) India ink stain showing the overall 2D-pattern of the proteins of oocyte stage VI. On the left hand side of the gel, 20 ug of the stage VI was separated on one-dimension acts as reference.

(a)

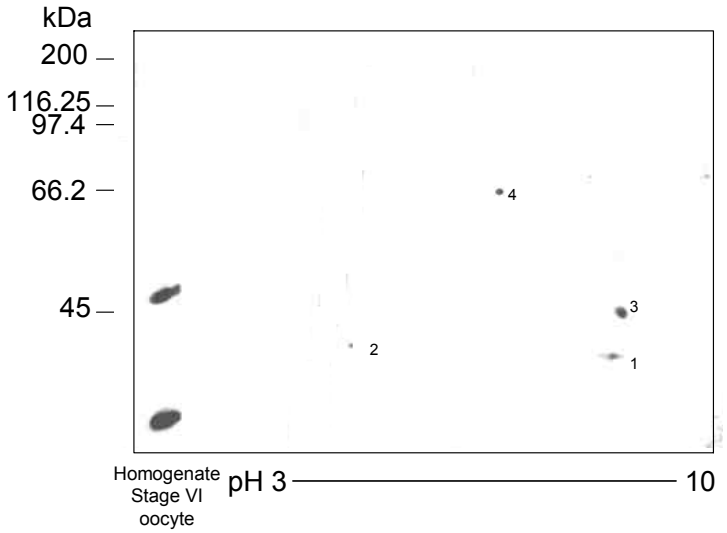

(b)

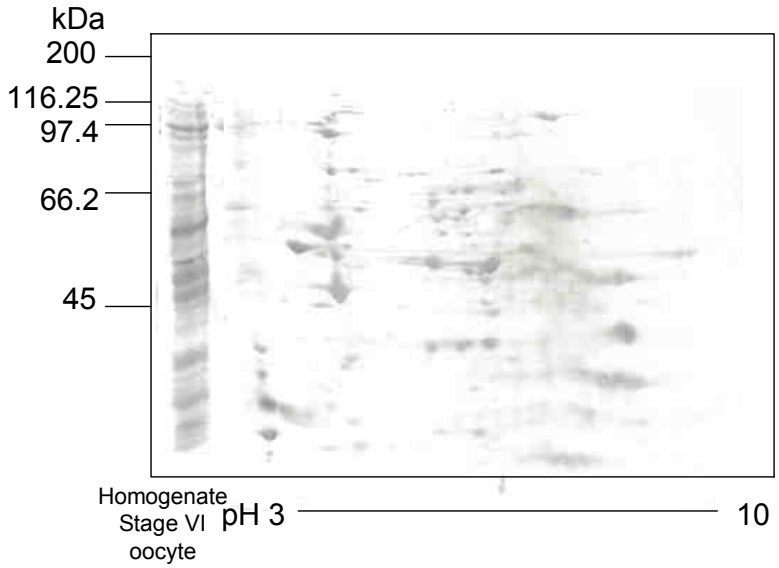

samples. Once again, the CTD110.6 immunoblot of stage VI oocyte proteins on the 2D-gel with pH range of 3-10 showed four small bands at approximately 32, 35, 45 and 66 kDa across an approximate pH range 5-8. (Figure 3.2.2 a) While the India ink stain of the stripped membrane gave the overall 2D-picture of the stage VI oocyte proteins. (Figure 3.2.2 b) In comparison to 2D-pattern of stage I oocyte proteins, the 2D-pattern of stage VI was once again quite different as clearly shown in India ink stain (Fig 3.2.2 b). Particularly, the protein bands of stage I oocytes that are focused at the extreme right of the membrane (around pH 10) were completely absent in stage VI oocytes. Careful examination of the India ink stains of the glycine stripped blots of stage I and stage VI oocytes have showed a large fraction of the stage I oocyte proteins, unlike that of stage VI were focused mainly at cathodic end of the IPG strip indicating that majority of stage I oocyte proteins are basic in nature.

Assuming that most of the *O*-GlcNAc modified proteins of interest in stage I were basic in nature and thus, suggesting that the proteins were focused off the IPG strip, the more basic range of pH 6-11 was selected for IEF. The stage I analyzed within this pH range showed the majority of the modified proteins resolved into 12 discrete protein bands within the pH range of 8-10. (Figure 3.2.3 a) These protein bands were numbered as 1-2, 3a, 3b, 7, 8a, 8b, 8c, 9a, 9b, and 10 as indicated in figure were approximately at 28, 35, 37, 49, 55, 58, 62, 67, 91 and 98 kDa respectively. Among these bands, the bands # 1-3 are clustered together (as seen in Figure 3.2.3 b) originated from the big band # 1 at 29 kDa in 1D-gel, and the bands # 4-10 corresponds to bands # 2-6 and 9-11 respectively in the 1D-gel. However, the high molecular weight bands (> 100 kDa) do not appear due to proteolytic degradation or precipitation of these proteins during IEF. This is

Figure 3.2.3- Two-dimensional gel electrophoresis of oocyte proteins (stage I) by isoelectric focusing with pH range 6-11 in the horizontal dimension and SDS-PAGE (10%) in the vertical dimension. Approximately 100 µg of protein from oocytes at stage I was separated and immunoblotted with CTD110.6 and later the blot was glycine stripped and stained with India ink as described in Methods. Figures **(a)** Autoradiogram showed the modified proteins mainly focused at approx. pH 8-10, and 12 distinct bands # 1-2, 3a, 3b, 7, 8a, 8b, 8c, 9a, 9b and 10 were identified at 28, 35, 37, 49, 55, 58, 62, 67, 91 and 98 kDa respectively, and **(b)** India ink stain showing the overall 2D-pattern of the proteins from stage I oocyte. On the left-hand side of gel, 20 µg of protein of stage I was separated on one-dimension acts as reference.

(a)

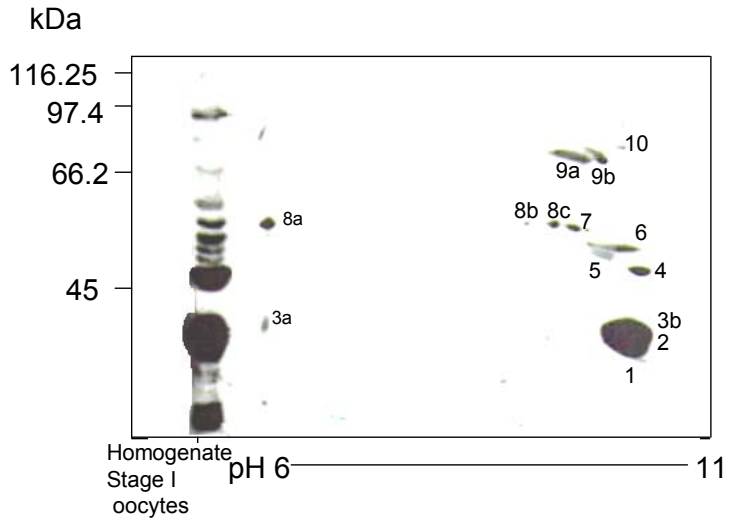

(b)

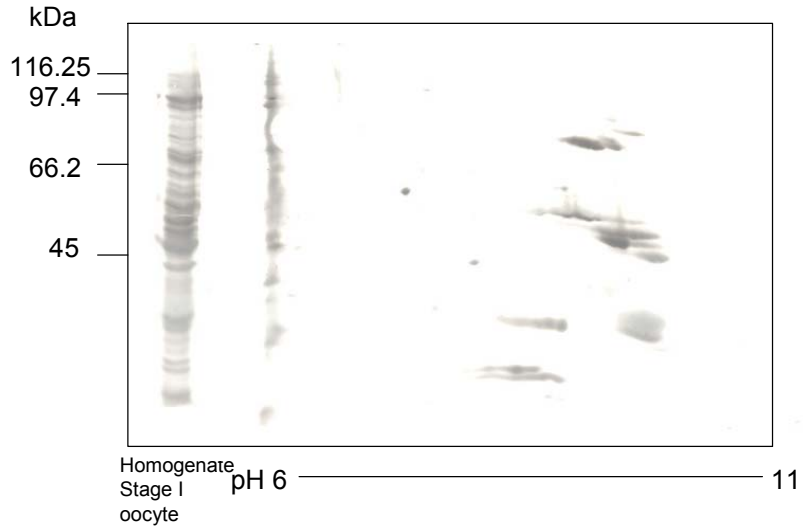

Figure 3.2.4- Two-dimensional gel electrophoresis of oocyte proteins (stage VI) by isoelectric focusing with pH range 6-11 in the horizontal dimension and SDS-PAGE (10%) in the vertical dimension. Approximately 100 µg of protein from oocytes at stage VI was separated on 10% two-dimensional gel and analyzed by CTD110.6 immunoblotting and later the blot was glycine stripped and stained with India ink as described in Methods. Figures **(a)** Autoradiogram showed the modified proteins mainly focused at approx. pH 7-10, and showing band # 1, 2, 3a. 3b. 4a-c, 5, and 6 at around 22, 25, 26, 43, 49, 63 and 65 kDa respectively with pI 7.8, 8.8, 8.2, 8.4, 7.1, 7.9, 8.5, 9.1, 6.9 and 10 resp.; and **(b)** India ink stain showing the overall 2D-pattern of the proteins of oocyte stage I. On the left-hand side of the gel 20 µg of protein of stage VI was separated on one-dimension acts as reference.

(a)

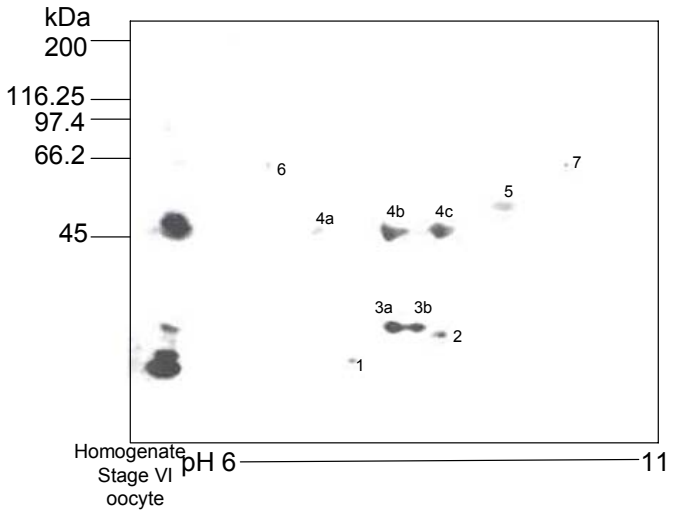

(b)

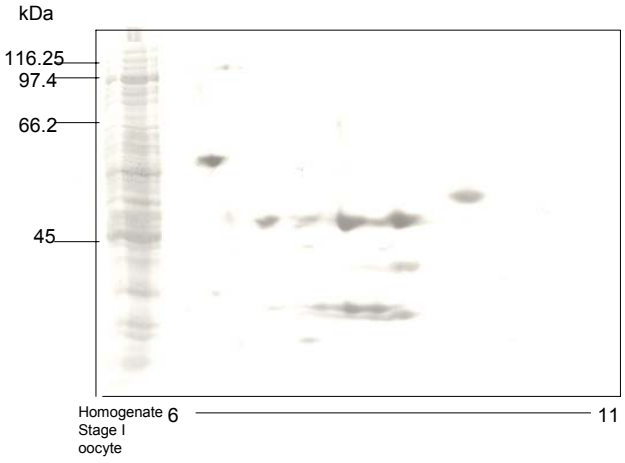

the limitation of the 2D-technique that was used. The India ink stain of the stage I have shown that most of the basic proteins were *O*-GlcNAc modified proteins. (Figure 3.2.3 b) Thus, the results of the 2D separation with pH range 6-11 substantiated the earlier findings, and indicated the majority of the oocyte proteins from a stage I oocyte were basic in nature, like most of the ribosomal proteins [113].

While the stage VI oocyte proteins in pH range 6-11 were resolved into a very different pattern to that of stage I. In stage VI, the majority of proteins focused within pH range of 7-10, with bands that were numbered as 1, 2, 3a, 3b, 4a-c, 5, 6 and 7 at approximately 22, 25, 26, 43, 49 63 and 65 kDa respectively with approximate pI 7.8, 8.8, 8.2, 8.4, 7.1, 7.9, 8.5, 9.1, 6.9 and 10 respectively. (Figure 3.2.4 a) Once again, the India ink stain of the stage VI oocytes have showed quite a different 2D-patterns of whole oocyte proteins from that of the stage I oocytes. (Figure 3.2.4 b) In addition to the differences in isoelectric points (pIs) of the proteins, there were fewer *O*-GlcNAc modified proteins of stage VI oocytes were apparent.

3.3 Immunoprecipitation with RL-2 antibody

Since, the proteins separated from the whole homogenate were not enough and sufficient to see by the coomassie staining, we felt the need to enrich the samples with *O*-GlcNAc modified proteins. Initially, the enrichment of *O*-GlcNAc modified proteins was attempted by the immunoprecipitation with *O*-GlcNAc specific antibodies such as RL-2 antibody. The immunoprecipitations with RL-2 antibody was successful in enriching at least some of O-GlcNAc modified proteins of interest as shown by results in the CTD110.6 immunoblot (Figures 3.3.1 a). Approximately 20 µg of protein from oocytes at stage I in lane 1, one tenth of the total immunoprecipitate in lane 2, and approximately 20

µg of supernatant in lane 3 (this amount was estimated taking into account the dilution and the concentration of original sample) were separated on 8% SDS PAGE and immunoblotted with CTD110.6 antibody. The second lane containing immunoprecipitate showed a few of the protein bands of interest namely those at 37, 54 and 62 kDa. The high intensity bands at 50 and 75 kDa in the same lane were of denatured antibodies. The RL-2 immunoprecipitation performed without the sample (the negative control) clearly showed the presence of these bands (Figure 3.3.1 c). Thus, the presence of foreign proteins such as heavy chains of the denatured antibodies, which get resolved at nearly the same regions as proteins of interest in one-dimensional gel electrophoresis interfered with the detection of the *O*-GlcNAc modified proteins.

In addition, huge difference in the band intensities of immunoprecipitate and supernatant lanes in the silver stain clearly indicated large portions of *O*-GlcNAc modified proteins remained in the supernatant. (Figure 3.3.1 b) The huge protein band at around 60 kDa in supernatant of the silver stain (shown by an arrow in Figure 3.3.1.b) appeared to be 'Protein A' conjugated to trisacryl beads used in RL-2 immunoprecipition. This band appears as a large non-illuminated area in the same region of supernatant lane on immunoblotting with CTD110.6 antibody (Figure 3.3.1.a). Since all the protein bands of interest in that region were completely concealed by this large Protein A band, it becomes difficult to estimate the *O*-GlcNAc modified proteins remaining in supernatant. In order to reduce the contamination with the Protein A, immunopurification by column method was attempted. But also gave poor results (Data not shown). Increasing the RL-2 concentrations in immunoprecipitation also did not significantly improve the yields, but increased the level of interference with immunoblot detection. (Data not shown) Thus,

Figure 3.3.1- One-dimensional gel electrophoresis of the RL-2 immunoprecipitate of stage I oocytes. Approximately 20 µg of protein from oocytes at stage I in lane 1, one tenth of the total immunoprecipitate in lane 2, and approximately 20 µg of supernatant in lane 3 (this amount is estimated taking into account the dilution and the concentration of original sample) were separated on 8% SDS PAGE and immunoblotted with CTD110.6 antibody and stained with silver as described in Methods.**(a)** Autoradiogram of CTD110.6 immunoblot and **(b)** silver stain showing few protein bands of interest approximately at 37, 59 and 62 kDa in the RL-2 immunocomplex; and (**c)** Autoradiogram of CTD110.6 immunoblot with RL-2 immunocomplex and RL-2 immunocomplex without oocyte proteins (representing a negative control) were loaded in lane 1 and 2 respectively, showing the bands at 50, 75 and 100 kDa might be the bands of antibody.

a. CTD110.6 immunoblot **b. Silver stain** **c. Negative control**

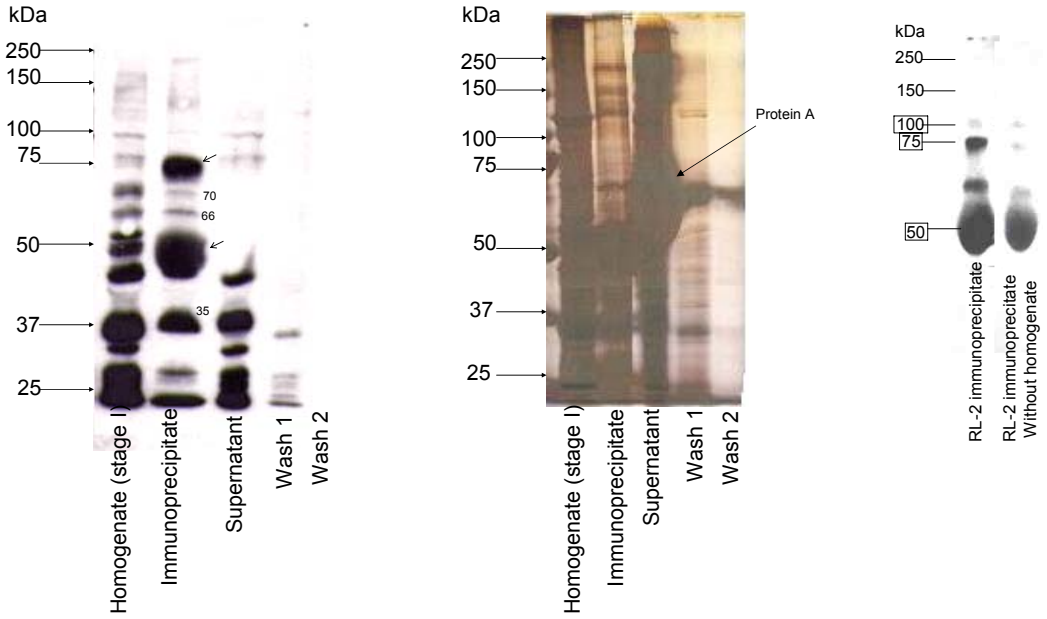

another approach was investigated.

3.4 Immunoaffinity purification using CTD110.6 antibody

To reduce the contamination of the samples with the foreign proteins (antibodies), the separation was performed using an anti-mouse IgM-agarose immunoaffinity column, where the antibody is covalently linked to the agarose bead while retaining its ability to specifically bind to CTD110.6 antibody (IgM sub-type). The proteins were eluted with a solution of TBS buffer containing 1 M N-acetylglucosamine and concentrated by methanol precipitation that also removes the majority of N-acetylglucosamine. All the collected column fractions and the precipitated elutions were analyzed by RL-2 immunoblotting and silver staining (Figure 3.2.2 a and b). Approximately 20 ug of stage I oocyte proteins (original sample) in lane 1, one half of the eluted proteins in lanes 2, 3 and 4, and approximately 20 ug of flow through (this amount was estimated taking into account the dilution and the concentration of original sample) in lane 5, one tenth of RIPA washes in lane 6 and 7, were separated on 8% SDS PAGE and analyzed by RL-2 immunoblotting. The analysis showed most of the *O*-GlcNAc modified proteins were in the flow through and washes (Figure 3.4.1.a). Thus, indicating poor binding of *O*-GlcNAc modified proteins to the column. Once again, the band at 60 kDa in both the flow through and washes that concealed the protein bands of interest. While some of this appears to be due to leaching of antibody from the column, it also represents the presence of BSA. BSA used as stabilizer in the stock solution of the CTD110.6 antibody used in the immunoprecipitation. Since so much of the proteins of interest were found in the flow through, this material was incubated with a new set of beads to see if the yield could be improved. On the analyzing the collected fractions, once again the elutions of the immunoaffinity puri-

Figure 3.4.1- One-dimensional gel electrophoresis of the CTD110.6 immuno-affinity purified proteins of stage I oocytes. Approximately 20 ug of stage I oocyte proteins (original sample) in lane 1, one half of the eluted proteins in lanes 2, 3 and 4, and approximately 20 ug of flow through (this amount was estimated taking into account the dilution and the concentration of original sample) in lane 5, one tenth of RIPA washes in lane 6 and 7, were separated on 8% SDS PAGE and analyzed by RL-2 immunoblotting and silver stained as described in Methods. (**a**) Autoradiogram of RL-2 immunoblot (8% gel) showing few protein bands approximately between 50-60 kDa in the immunopurified sample and most of the modified proteins in the flow through and washes; (**b**) silver stain of 10% SDS Gel showing the presence of majority of proteins in the flow through. (c) Autoradiogram of RL-2 immunoblot (8% gel) whose lanes representing fractions of repeated immunoprecipitation of flow through. The faint bands around 50-60 kDa indicated no improvement in the yield using immunoaffinity purification of the flow through.

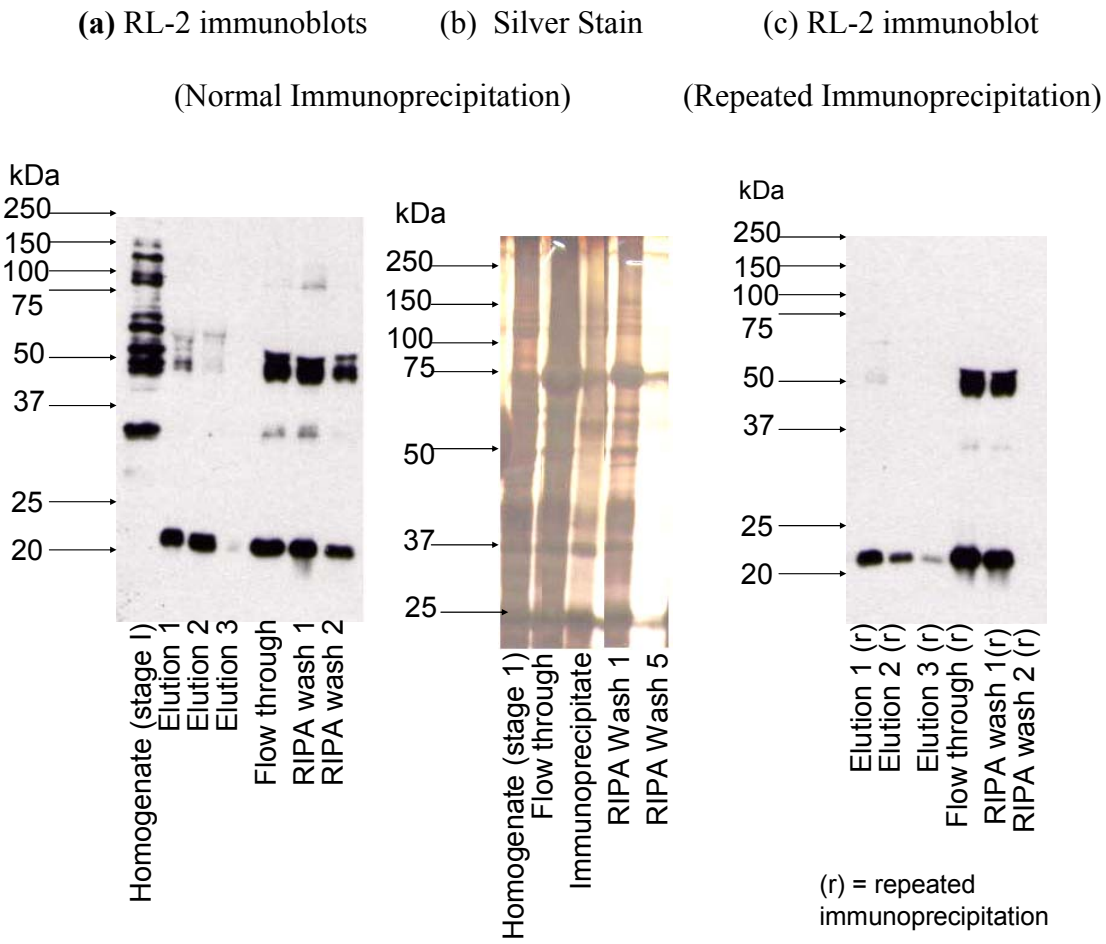

fication showed very weak bands at 50 kDa, and with majority of the proteins again in the flow through and washes. (Figure 3.4.1 c) The results was also confirmed with silver staining that demonstrated very low protein content in the elutions compared to the flow through. (Figure 3.4.1 b)

In an attempt to improve the yield, the batch-wise incubation method was adopted as a way of exposing more of the column material to the proteins for longer periods of time. Most of the protein bands of interest were detected on analyzing CTD110.6 immunoaffinity eluants following the same procedure of RL-2 immunoblotting. Again some of the bands were concealed by the heavy chains of antibodies at 60 and 100 kDa. These bands are confirmed as bands of the antibodies because similar bands at region of same molecular weight appeared when the anti-mouse IgM-agarose beads were resolved by SDS PAGE, and immunoblotted with RL-2 antibody (Figure 3.4.2 a). In addition, the presence of considerable amounts of *O*-GlcNAc modified proteins in the flow through indicated that significant amounts of proteins were still not being captured with this technique (Figure 3.4.2 a). Further purification of the immunopurified material by 2D-gel electrophoresis showed that the *O*-GlcNAc modified proteins were not in most cases sufficiently separated from contaminating immunoglobulin and BSA, which was clearly visible in the RL-2 immunoblot as shown in the Figure 3.4.2 b. Three protein bands on the extreme right of the membrane which are indicated by the arrows in the Figure 3.4.2 b appeared to be well separated in the immunoblot. However, the India ink stain of this blot after glycine stripping showed a huge smear in that region indicating the presence of additional protein and would thus, confound sequencing of the *O*-GlcNAc modified proteins (Data not shown). These streaking and smear that were also observed in the

Figure 3.4.2- One-dimensional and two-dimensional gel electrophoresis of CTD110.6 immunoprecipitate (Batch-wise incubation method) of stage I oocytes.
Approximately 20 µg of protein from oocytes at stage I, a quarter of the total immuno-precipitate collected, and a volume of supernatant representing 20 µg compared to Homo-genate (stage I) were loaded in the first three lanes of 10%1D-Gel; and nearly half of the immunocomplex was separated on 10% 2D-gel along with 20 ug of proteins of oocytes at stage I on left hand side of the gel as a reference and immunoblotted with RL-2 antibody as described in Methods. Autoradiograms of **(a)** 1D-gel showing most of the protein bands of interest in immunocomplex along with the bands of foreign proteins, and **(b)** 2D-gel showing vertical and horizontal streaking of the foreign proteins that overlaps the protein bands of interest pointed out using arrows.

(**a**)1D- Gel Electrophoresis (**b**) 2D- Gel Electrophoresis

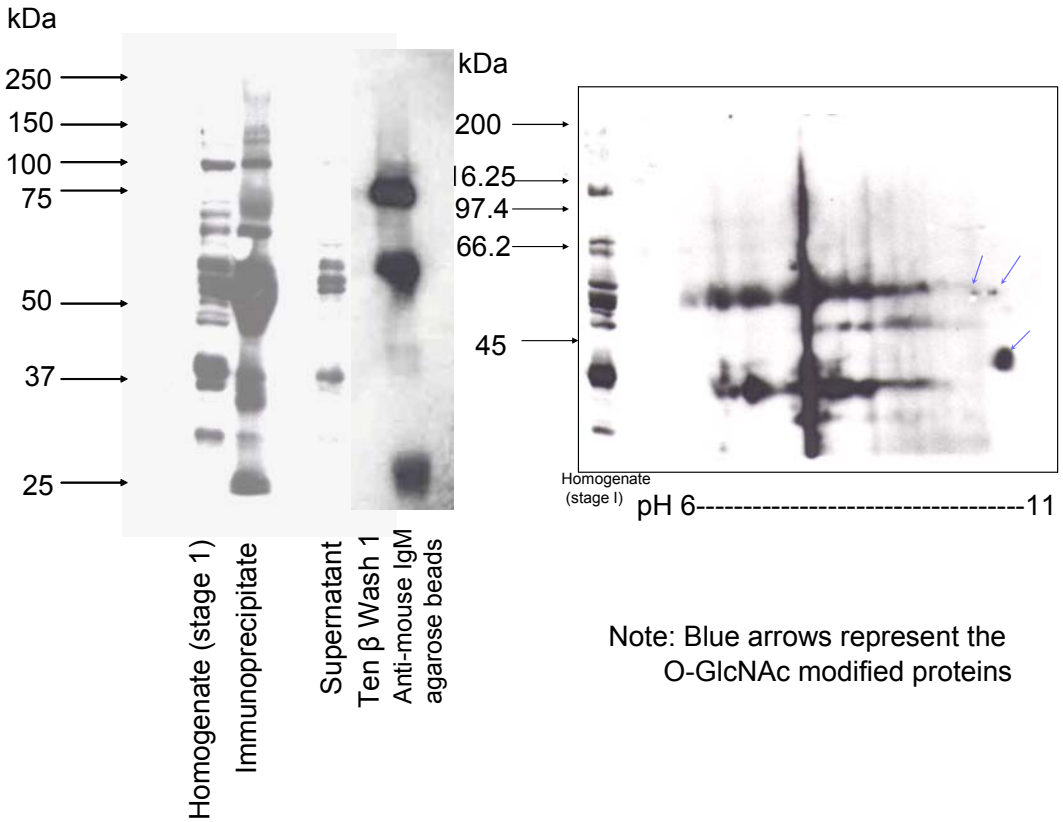

Note: Blue arrows represent the O-GlcNAc modified proteins

immunoblot might be due the presence of the agarose beads conjugated anti-mouse IgM in the immunoprecipitate. Even though, kits are available to remove some of the contaminating proteins, typically not all immunoglobulin and albumin were removed. Therefore, it was decided not to pursue the method, because of already low yields and potential loss of sample in additional steps.

3.5 Affinity chromatography

To overcome the problems of low yields and contamination with the foreign proteins mainly antibody, lectin affinity chromatography using agarose wheat germ agglutinin was used in an attempt to enrich the samples with *O*-GlcNAc modified proteins. This procedure has been used with some success in non-*Xenopus* somatic cell systems [114]. To first assess the potential effectiveness of this tool for our *Xenopus* system, oocytes stage I and stage VI were analyzed by the wheat germ agglutinin (WGA) affinity blotting. WGA binds to all glycoproteins with terminal N-Acetylglucosamine residues and thus, can bind to both *O*-GlcNAc modified proteins and glycoproteins with terminal GlcNAc on N-linked oligosaccharide chains. As expected the pattern of modified proteins from the affinity blot was similar but not identical to that observed in the immunoblots with CTD110.6 and RL-2 antibodies (Figure 3.1.1 and 3.1.3). For instance, the bands at 50 and 97 kDa of stage VI oocytes shown by arrows in Figure 3.5.1 appeared in the affinity blot, but did not show up in the previous shown immunoblots. While appearance was at a similar molecular weight on 1D-analysis, the proteins seen at 50 and 97 kDA in stage VI are likely not the same as those in stage I samples. This is likely due to the affinity of WGA for all the carbohydrate containing proteins, with terminal N-acetylglucosamine residues on some N-linked carbohydrate containing proteins.

Figure 3.5.1- WGA Affinity blot of the oocytes at stages I and VI. Approximately 20 µg of proteins from oocytes at stage I and stage VI were separated on the 10% SDS gel and probed with WGA-HRP. The blot showed all the bands that appeared on the immunoblots with CTD110.6 and RL-2 in comparatively lower intensities due to the low sensitivity of colorimetric detection. The bands of stage VI shown by arrows are absent in the CTD110.6 immunoblot of the same system.

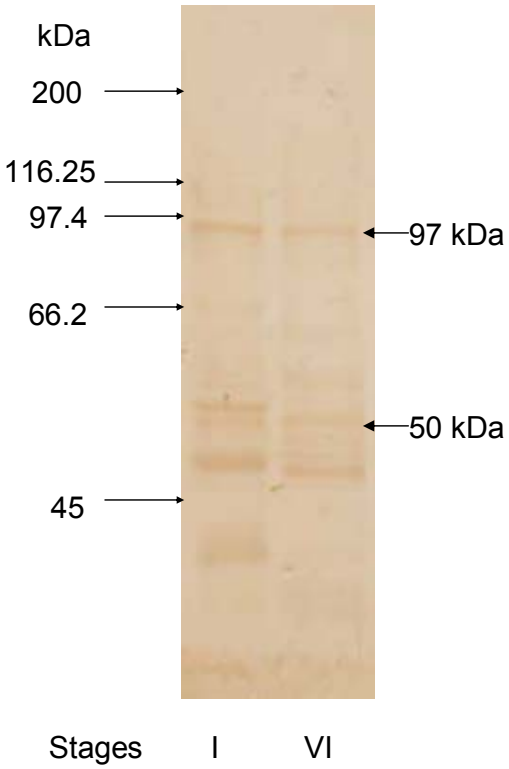

Moreover, only the most prominent bands were visible on the affinity blot due to lower sensitivity of the colorimetric detection method suggested for use by manufacturer. Attempts to use the chemiluminescent detection resulted in very high backgrounds that could not be sufficiently reduced with the standard blocking agents such as BSA, tween 20. (data not shown) Note non fat dry milk a popular blocking agent cannot be used with CTD110.6 and RL-2 antibodies, since one or more carbohydrates in the solution reduces the antibody signal and gives high background.

Once the affinity of WGA for the proteins of interest was verified, the affinity purification was initially performed at approximately 0.15 M NaCl as per the manufacturer's instructions, and later the concentration of salt was reduced to less than 0.1 M NaCl as suggested by a published study [102], in order to maintain the weak intermolecular interactions in protein complexes and improve yields. The results of both the experiments as shown in Figure 3.5.2 a & b demonstrated that low salt conditions improved yields of affinity purification. In both experiments, the proteins bound to the column were eluted using the binding buffer containing 0.15 M NaCl and 0.5 M GlcNAc. The collected fractions were pooled, desalted and concentrated by ultra-filtration using centricon-10 in order to proceed to 2D-gel electrophoresis, the next purification step. Once again, all the collected fractions were analyzed by CTD110.6 immunoblotting are shown in Figures 3.5.2 a and b represents the affinity purification at low salt (> 0.1 M NaCl) and high salt (0.15 M NaCl) conditions respectively. The second lane in the Figure 3.5.2 a shows the sample from the pooled elution contained all of the target bands, whereas the second lane in the figure 3.5.2 b did not show the bands at 54, 57 and 82 kDa. Thus, indicating that low salt binding conditions maximized both the yield and

Figure 3.5.2- One-dimensional gel electrophoresis of affinity purified proteins from oocytes at stage I. Approximately 20 µg of proteins from oocytes at stage I, a quarter of the pooled elution of the affinity purified proteins at two different conditions, 0.1 M NaCl and 0.15 M NaCl, estimated volume containing 20 µg calculated using the concentration of the homogenate (stage I) were separated in the first three lanes of the 10% gel and immunoblotted with CTD110.6 antibody as described in Methods. Autoradiograms of the affinity purification (a) at low salt conditions (< 0.1 M) showing almost all the protein bands of interest in elutions and (b) high salt conditions (0.15M) salt showing bands at 35, 59, 69 and 97 kDa only.

(a) Affinity purification in lower salt (< 0.1 M NaCl)

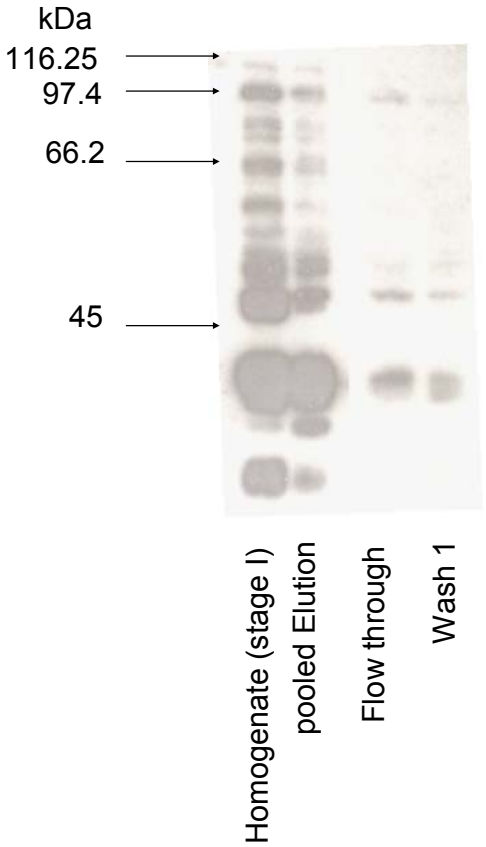

(b) Affinity purification in higher salt (0.15M NaCl)

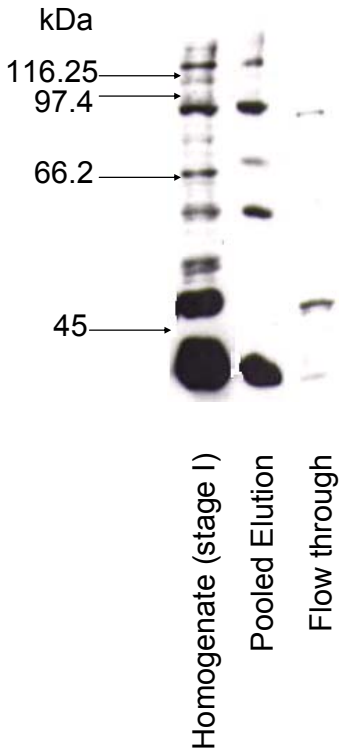

number of *O*-GlcNAc modified proteins. Therefore, the enrichment was qualitatively successful in concentrating all the modified proteins of interest. However, the yield was only 20% apparently due to the loss of proteins by aggregation and precipitation during the concentration process. Hence, in order to acquire sufficient amounts of protein for sequencing, with this technique we would need to start with a larger amount of the oocyte material which unfortunately is a limiting factor in our process of purification.

3.6 Differential Sedimentation

To overcome the problem of low initial proteins available from stage I oocytes, an another method was sought that minimized sample loss while still achieving enrichment of *O*-GlcNAc modified proteins. To this end, it was noted that the proteins of interest tended to precipitate in stored homogenates suggesting that the proteins tend to form high molecular weight complexes. Based on this hypothesis, the enrichment of the *O*-GlcNAc modified proteins was attempted by simple differential sedimentation. First, centrifugation of the lysed oocytes at 1,000 x g for 10 minutes was performed in order to sediment any unlysed cells and large cell debris. The supernatant-1 (that is collected after 1,000 x g) was then centrifuged at 10,000 x g for another 10 minutes, to further fractionate the homogenate (stage I oocyte) into supernatant-10 and pellet-10. The supernatant-10 was fractionated again by ultra-centrifugation at 100,000 x g for one hour into supernatant-100 and pellet-100. All the fractions were resolved on 10% SDS PAGE and analyzed by CTD110.6 immunoblotting (Figure 3.5.1 a). Later, this blot was stripped with glycine solution, and stained with India ink (Figure 3.5.1 b). All the lanes contained approximately 20 µg of oocyte proteins. The *O*-GlcNAc protein pattern in the supernatant-1 and supernatant-10 was similar to the earlier patterns of stage I. But the pellet-10 in the lane 2

Figure 3.6.1- One-dimensional gel electrophoresis of proteins from oocytes at stage I fractionated by Differential Sedimentation. The homogenate of the stage I oocytes (after 1,000 x g) was fractionated by the centrifugation at 10,000 x g and 100,000 x g, and 20ug each of the collected supernatants and pellets were separated on 10% ID-Gel electrophoresis and analyzed by CTD110.6 immunoblotting and later glycine stripped CTD110.6 blot was stained by India ink as described in Methods. (a) Autoradiogram showing few O-GlcNAc modified proteins in the pellet at 10,000 x g and the distribution of protein bands of interest in both the supernatant and the pellet collected at 100,000 x g where majority of O-GlcNAc modified proteins were found in pellet; (b) India ink stain of the glycine of the blot showing the concentration of the proteins bands of interest in the pellet at 100,000 x g.

a. CTD110.6 immunoblot

b. India ink stain of glycine stripped membrane

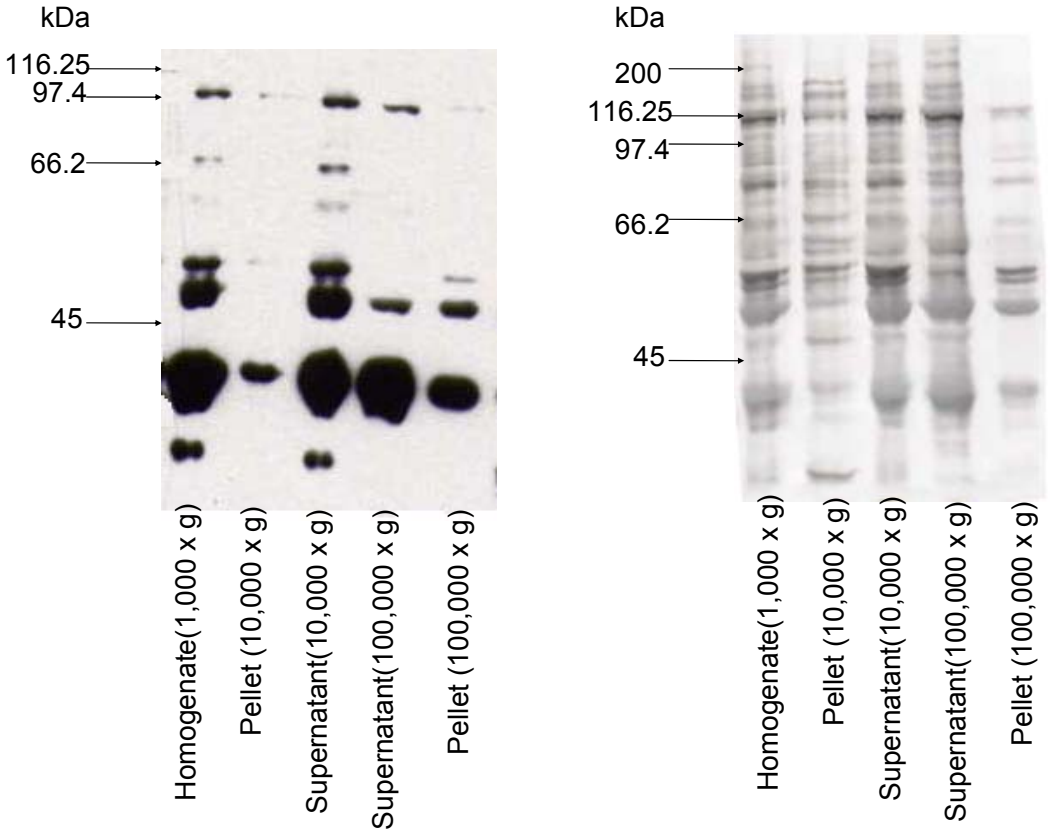

of India ink stain (Figure 3.5.1 b) showed the presence of large amounts of unmodified proteins indicating the centrifugation at 10,000 x g concentrated the proteins of interest in the supernatant-10. Thus, the centriguation of lysed oocytes at 10,000 x g can be performed to remove the unlysed oocytes and debris without significant loss of desired proteins. In contrast, the ultra-centrifugation of supernatant-10 at 100,000 x g for 1 hour had sedimented the majority of modified proteins as shown in the Figure 3.6.1 a. Interestingly, the India ink stain (Figure 3.6.1 b) revealed the fact that the majority of the oocyte's unmodified proteins remained in the supernatant-100. Therefore, this method not only enriched the target proteins, but also minimized the loss of these proteins.

The enriched samples analyzed by 2D-Gel Electrophoresis across the pH range 6-11, as expected showed the same 2D- pattern of the modified proteins as that of whole homogenate of stage I oocytes (Figures 3.6.2 a and 3.2.3 a). In addition, the majority of the proteins were basic in nature and were better resolved on the IPG strip, pH 6-11 as shown in Figure 3.6.2 a. Once again, the modified proteins were mainly focused in the pH range 8-10. Interestingly, these protein bands appeared at slightly lower molecular weight than that of the whole homogenate. The high electrophoretic mobility of the proteins might be due to the presence of few non-modified proteins in the sample. The estimated molecular weights of these protein bands # 1-7, 8a, 8b, 9a, 9b, 10, 11a and 11b in Figure 3.6.1a were 21, 23, 36, 46, 47, 53, 52, 54, 83, 87 and 108 respectively. In addition, the intensity of protein bands of the pellet-100 (figure 3.6.2 a) is higher than that of the homogenate (Figure 3.2.3) showing successful enrichment of *O*-GlcNAc modified proteins. Competition experiments with 15 mM GlcNAc demonstrated specificity through the reduction in the intensity of all the bands as seen in Figure 3.6.2 b, especially in

Figure 3.6.2- Two-dimensional gel electrophoresis of pellet at 100,000 x g from stage I oocytes by isoelectric focusing with pH 6-11 in the horizontal dimension and SDS-PAGE (10%) in the vertical dimension. Approximately 100 µg of protein from oocytes at stage I was separated and analyzed by CTD110.6 immunoblotting without and with 15 mM GlcNAc as described in Methods. (a) Autoradiogram of immunoblotting in the absence of GlcNAc showed the modified proteins mainly focused at approx. pH 8-10, and 10 distinct bands # 1-4, 5a, 5b, 6, 7, 8a, 8b, 9a, 9b,10, 11a and 11b were identified at 21, 23, 36, 46, 47, 53, 52, 54, 83, 87 and 108 kDa respectively. On the left-hand side of gel, 20 µg of protein of stage I was separated on one-dimension acts as reference. (b) Autoradiogram of immunoblotting in the presence of 15mM GlcNAc showed the modified proteins mainly focused at approx. pH 8-10, showing all bands nearly reduced in the intensity.

(a) Without GlcNAc

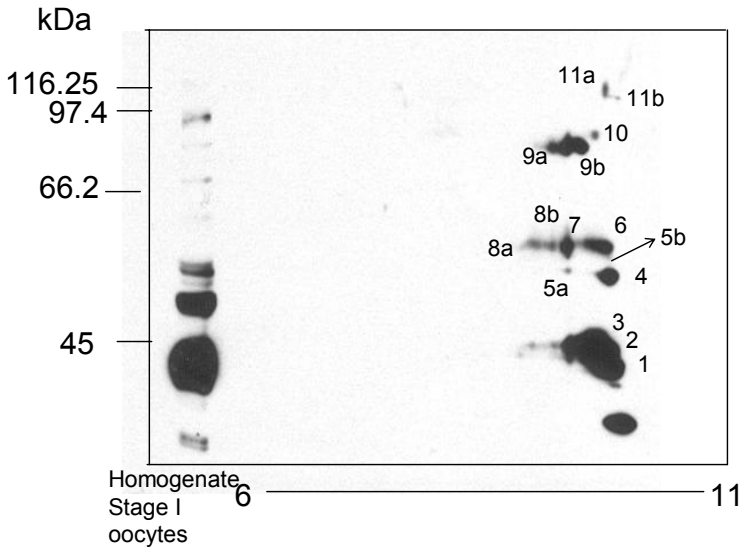

(b) With 15mM GlcNAc

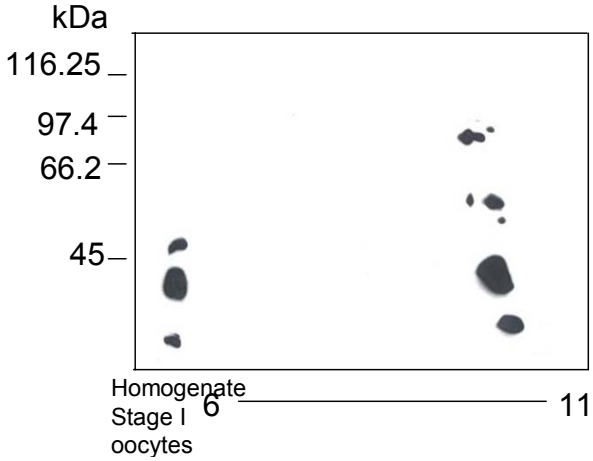

Figure 3.6.3- Two-dimensional gel electrophoresis of pellet at 100,000 x g from stage I oocytes by isoelectric focusing with pH 3-10(NL) in the horizontal dimension and SDS-PAGE (10%) in the vertical dimension. Approximately 100 µg of protein from oocytes at stage I was separated and analyzed by CTD110.6 immunoblotting as described in Methods. (a) Autoradiogram of immunoblot showed all the bands focused at the extreme right due to the non-linearity of the IPG strip. On the left-hand side of gel, 20 µg of protein of stage I was separated on one-dimension acts as reference.

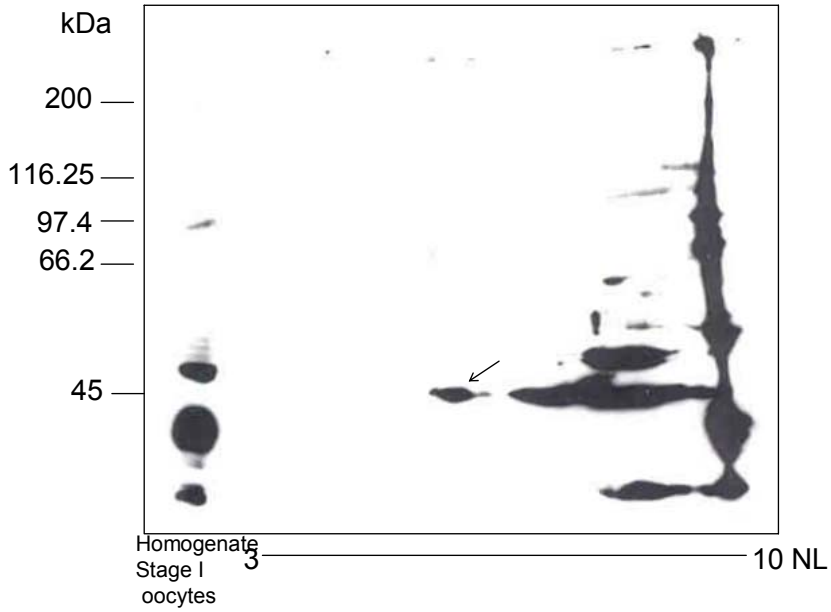

the case of bands # 5a, 5b, 11a, 11b and 4.

In addition, the 2D-Gel Electrophoresis using a full range IPG strip, pH 3-10 (non-linear) again showed the majority of the proteins bands of interest focused across the pH range 8-10 substantiating that most of the modified proteins are basic in nature. (Figure 3.6.3) However, the protein bands of interest are not well separated due to the sharp rise in the pH of the non-linear IPG strip (with an extended region across pH 5-8). Since the extended region on the IPG strip was pH 5-8, some of the neutral and weakly acidic proteins did separate (Highlighted by an arrow in the Figure 3.6.3). Especially the band 3a at pH 6-7 spotted in 2D-gel analysis of the homogenate (stage I) showed up once again in this 2D-gel (as shown with an arrow in Figure 3.2.3 a).

3.7 Identification and selection of the modified protein bands for sequencing

Once the scheme of purification was finalized as shown in the flow diagram, Figure 3.7.1, the proteins were isolated by differential sedimentation coupled with 2D-gel electrophoresis and coomassie stained for peptide sequencing by mass spectrometry. The 2D-separated proteins from stage I oocytes that are sufficiently stained with Coomassie nearly showed all the fifteen protein bands of interest. (Figure 3.7.2) Since the stained protein pattern was very much similar to the 2D-patterns observed earlier, the protein bands of interest could be easily identified by superimposing the CTD110.6 immunoblot of the stage I oocyte and by their positions on the gel. The identified protein bands shown in the Figure 3.7.2 by using arrows were carefully excised wearing gloves to avoid contamination.

Figure 3.7.1- Scheme for isolation and identification of the *O*-GlcNAc modified proteins

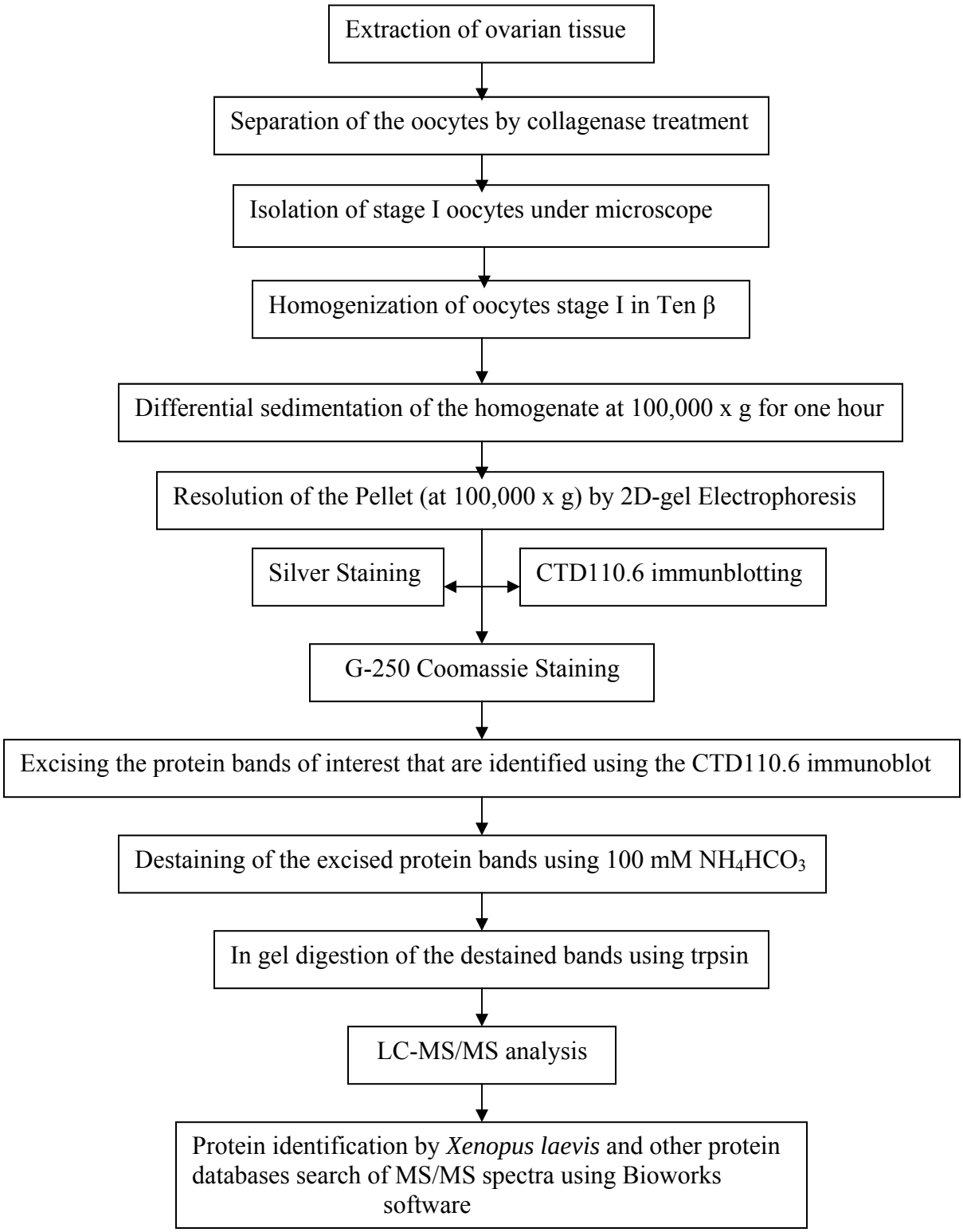

Figure 3.7.2- Two-dimensional gel electrophoresis of pellet at 100,000 x g from stage I oocytes by isoelectric focusing with pH 6-11 in the horizontal dimension and SDS-PAGE (10%) in the vertical dimension. Approximately 100 µg of protein from oocytes at stage I was separated on 10% two-dimensional gel, and stained by coomassie as described in Methods. The stain showed all the fifteen distinct bands # 1-4, 5a, 5b, 6, 7, 8a, 8b, 9a, 9b,10, 11a and 11b were identified at 21, 23, 36, 46, 47, 53, 52, 54, 83, 87 and 108 kDa respectively, mainly focused at approx. pH 8-10. On the left-hand side of gel, 20 µg of proteins of stage I was separated on one-dimension acts as reference.

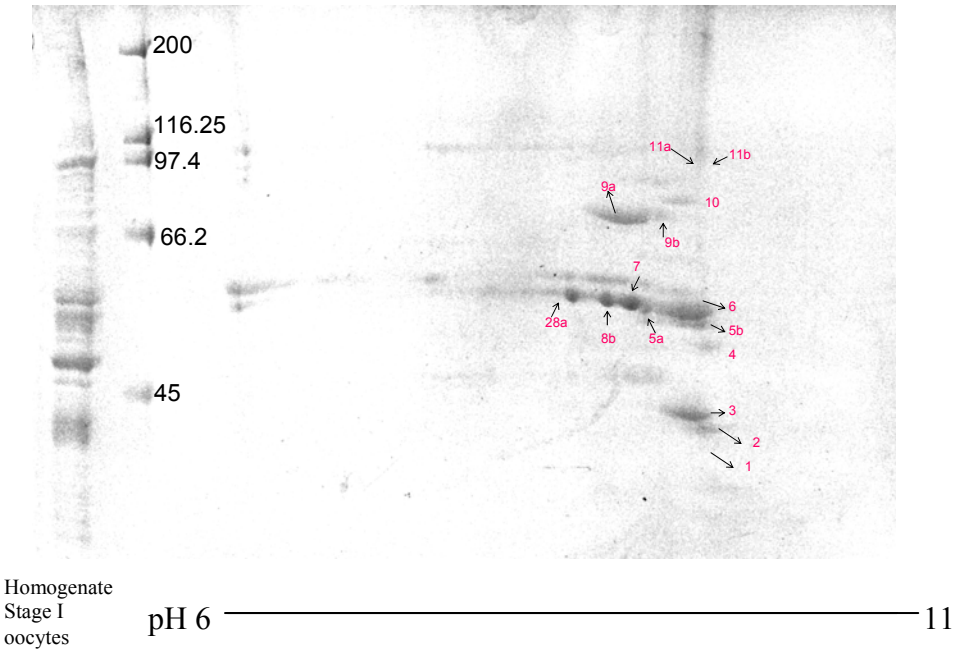

3.8 Mass Spectroscopy and database search

Gel containing proteins were treated with trypsin and extracted as described in the methods. The in-gel digested peptides of four protein bands were analyzed by LC-MS/MS and the MS/MS was interpreted using Bioworks software. All the MS/MS spectra identifying proteins or peptides reported in the appendix C were "best hits" or "best matches" in a *Xenopus* database search with an Xcorr > 2.5. The spectral data were also manually inspected for accuracy. First, the mass fingerprint of trypsin digested peptides was obtained, and then 5 to16 peptides that are easily ionizable were fragmented further. The fragmentation of peptides resulted in two types of peptide fragment ions, the N-terminal and the C-terminal ions. These fragment ions were labeled based on the type of bond cleavage as a, b and c for C-terminal ions and x, y and z for N-terminal ions as shown in the Figure 3.8.1. These peptide fragment ions were fed into the mass spectroscopy instrument to obtain a CID (Collision induced dissociation) spectrum of each peptide. The spectrum of each peptide revealed the peaks of all the fragments, from a molecular ion to a final product ion formed during fragmentation. Moreover, this dissociation into the peptide fragment ions helps to differentiate the isomers of amino acids or amino acids with nearly the same molecular masses, for example isoleucine from leucine and glutamine from lysine respectively.

In order to identify a protein, we need both the mass fingerprint of the protein (by MS scan) and the spectra of few peptide spectra for a given protein (by MS/MS scan). Figures 3.8.2 & 3.8.2, and Tables 3.8.1 & Table 3.8.2 provides an example of mass data analysis of one of the protein identified as Vg1 RNA binding protein variant A (Vg1RBP). The spectral data for rest of the identified proteins are given in Appendix C.

Figure 3.8.1- General fragmentation pattern of peptide and sequence nomenclature for mass ladder

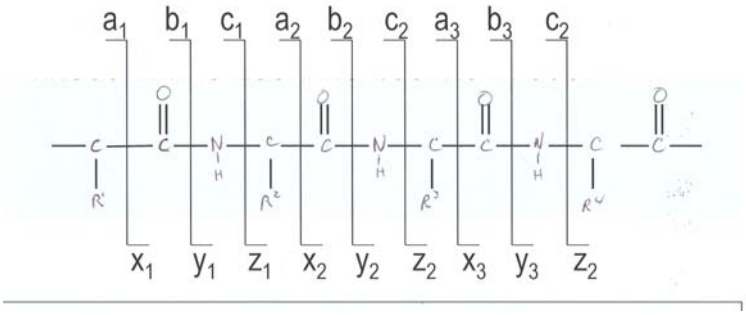

Figure 3.8.2- MS/MS spectrum of a protein band # 9a identified as Vg1 RNA binding protein variant A. CID spectrum/ product ion spectrum of a peptide **ITGHFYASQLAQR** of the Vg1 RBP showing the peaks of all the peptide fragment ion in the order of their molecular masses.

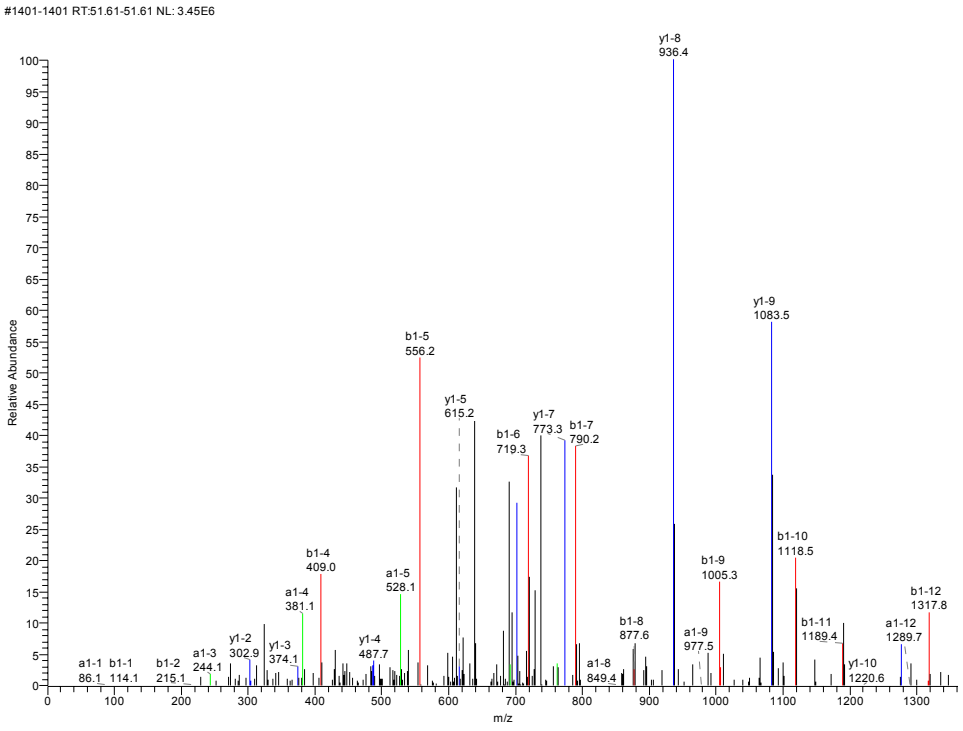

Table 3.8.1- Mass data of a peptide of Vg1 RBP variant A. Table lists out the masses of all the peptide fragment ions of the peptide **ITGHFYASQLAQR**

AA	M+nH	A	A*	Ao	B	B*	Bo	C	X	Y	Y*	Yo
I	115.10	86.10	69.07	68.09	114.09	97.07	96.08	131.12		1491.77	1474.74	1473.76
T	216.15	187.14	170.12	169.13	215.14	198.11	197.13	232.17	1404.67	1378.69	1361.66	1360.68
G	273.17	244.17	227.14	226.16	272.16	255.13	254.15	289.19	1303.62	1277.64	1260.61	1259.63
H	410.23	381.23	364.20	363.21	409.22	392.19	391.21	426.25	1246.60	1220.62	1203.59	1202.61
F	557.30	528.29	511.27	510.28	556.29	539.26	538.28	573.31	1109.54	1083.56	1066.53	1065.55
Y	720.36	691.36	674.33	673.35	719.35	702.33	701.34	736.38	962.47	936.49	919.46	918.48
A	791.40	762.39	745.37	744.38	790.39	773.36	772.38	807.42	799.41	773.43	756.40	755.42
S	878.43	849.43	832.40	831.42	877.42	860.39	859.41	894.45	728.37	702.39	685.36	684.38
Q	1006.49	977.48	960.46	959.47	1005.48	988.45	987.47	1022.51	641.34	615.36	598.33	597.35
L	1119.57	1090.57	1073.54	1072.56	1118.56	1101.54	1100.55	1135.59	513.28	487.30	470.27	469.29
A	1190.61	1161.61	1144.58	1143.60	1189.60	1172.57	1171.59	1206.63	400.19	374.22	357.19	356.20
Q	1318.67	1289.66	1272.64	1271.65	1317.66	1300.63	1299.65	1334.69	329.16	303.18	286.15	285.17
R	1474.77	1445.77	1428.74	1427.75	1473.76	1456.73	1455.75		201.10	175.12	158.09	157.11

Table 3.8.2- Peptide sequences of Vg1 RBP. Sequences of sixteen peptides of Vg1 RBP along with their ionic masses, positions, mass percentages and amino acids percentages were given. The total protein coverage of 20.62% by mass is a decent % to obtained the sequence of the protein.

Sequence	**MH+**	**%by Mass**	**Position**	**%byAA's**
ESKIPFTGQFLVK	1493.84	2.29	24 - 36	2.19
IPFTGQFLVK	1149.67	1.76	27 - 36	1.69
AIDTLSGK	804.45	1.23	53 - 60	1.35
VIEVEHSVPK	1136.63	1.74	67 - 76	1.69
PQSEVPLR	925.51	1.42	201 - 208	1.35
FTEEIPLK	976.54	1.49	282 - 289	1.35
ILAHNNFVGR	1140.63	1.75	290 - 299	1.69
FAGASIK	693.39	1.06	446 - 452	1.18
IAPAEGPDAK	968.51	1.48	453 - 462	1.69
MVIITGPPEAQFK	1430.77	2.19	465 - 477	2.19
LKEENFFGPK	1208.63	1.85	486 - 495	1.69
EENFFGPK	967.45	1.48	488 - 495	1.35
VPSYAAGR	820.43	1.26	506 - 513	1.35
DQTPDENDQVVVK	1486.70	2.28	538 - 550	2.19
ITGHFYASQLAQR	1491.77	2.28	551 - 563	2.19
IQEILAQVR	1069.64	1.64	565 - 573	1.52

Protein Coverage

By Mass 13475.2

% by Mass 20.62

By Position 122

% by AA's 20.57

Figure 3.8.3- Sequence of Vg1 RNA binding protein variant A Sequnce is downloaded from http://www.expasy.org/sprot/ and sequences in red are the ones analyzed by mass spectrometry to sequence the peptide and identify the protein band # 9a

Vg1 RNA binding protein variant A

gi|2801766|gb|AAB97457.1| KH domain-containing transcription factor B3 [Xenopus laevis]□gi|3172447|gb|AAC18597.1| Vg1 RNA binding protein variant A [Xenopus laevis]□gi|35505483|gb|AAH57700.1| MGC68429

MNKLYIGNLSENVSPPDLESLFKESK**IPFTGQFLVK**SGYAFVDCPDETWAMK
AIDTLSGKVELHGK**VIEVEHSVPK**RQRSRKLQIRNIPPHLQWEVLDSLLAQ
YGTVENCEQVNTDSETAVVNVTYANKEHARQGLEKLNGYQLENYSLKVTYIPD
EMATPQSPSQQLQQPQQQHPQGRRGFGQRGPARQGSPGAAARPKPQSEVPLRML
VPTQFVGAIIGKEGATIRNITKQTQSKIDIHRKENAGAAEKPITIHSTPEGCSAACKI
IMEIMQKEAQDTK**FTEEIPLKILAHNNFVGR**LIGKEGRNLKKIEQDTDTKIT
ISPLQDLTLYNPERTITVKGSIETCAKAEEEVMKKIRESYENDIAAMNLQAHLIPGL
NLNALGLFPPSSSGMPPPSAGVSSPTTSASYPPFGQQPESETVHLFIPALAVGAIIGK
QGQHIKQLSRFAGASIK**IAPAEGPDAK**LR**MVIITGPPEAQFK**AQGRIYGK
LKEENFFGPKEEVKLEAHIK**VPSYAAG**RVIGKGGKTVNELQNLTSAEVVVP
R**DQTPDENDQVVVKITGHFYASQLAQR**K**IQEILAQV**RRQQQQQQKT
AQSGQPQPRRK

Figure 3.8.2.showed all the peaks of the peptide fragment ions obtained from a peptide **ITGHFYASQLAQR** of Vg1RBP. The mass data given in the table 3.8.1 for the spectrum of peptide provides the sequence and molecular masses of the fragment ions. These overlapping fragment ions were aligned on the basis of their masses to identify the sequence of the peptide. All these operations were carried out by software programmed to operate mass spectroscopy instrument, Bioworks software was used for Finnigan LCQ in this study. Table 3.8.2 one of the outputs of this program that summarizes the number of peptides sequenced for one protein and protein coverage (by the portions of protein sequenced) percentages by mass and number of amino acids for protein identification. The sequenced peptides were then matched against one or more databases, and the protein with highest hits (matching the most peptides) in *Xenopus laevis* database with Xcorr > 2.5 was selected. The Xcorr >2.5 is the value used to determine efficacy of match [111]. The Figure 3.8.2 shows the sequence of the identified protein that was downloaded from http://www.expasy.org/sprot/. Figure 3.8.2 shows some portions of sequence highlighted in red were the sequenced peptides used in the protein identification.

The seven mass-analyzed protein bands were identified as following: Band # 3 as Zygote arrest 1 protein, Band # 4 as an oocyte specific form of elongation factor-1 alpha (42Sp50/thesaurin a), Bands # 7, 8a and 8b as Cytoplasmic mRNA binding protein p54 (y box factor homolog), Band # 9a as Vg1 RNA binding protein variant A, and Band # 10 as poly (A) binding protein. One peptide out of the protein bands around 50 kDa was identified as Xp54, RNA helicase with very high Xcorr. Most probably, the signals of other peptides of this protein might be lost or submerged among the strong signals of peptides from other proteins during mass analysis. The identified proteins are well characterized

proteins of *Xenopus laevis* oocytes. However, none of these proteins have previously been shown to be modified with *O*-GlcNAc. As oocyte specific proteins, they have been shown to play significant roles in the regulation of translation or intracellular mRNA translocation during the oogenesis. While, one of the proteins has been shown to play an important role in the oocyte-to-embryo transition.

Zygote arrest 1 (*Zar1*), protein band # 3 is an ovary-specific maternal factor that plays an important role during the transition of oocyte to embryo [115]. This 34 kDa protein is 295 amino acids long and found in multiple tissues including lung, muscle and ovary. Zar 1 mRNA is specifically synthesized in oocytes. Zar 1, localized predominantly in cytoplasm of oocytes, rapidly disappears at the two-cell stage of embryogenesis, suggesting a critical role in the oocyte-to-embryo transition [116]. Presence of an atypical eight cysteine Plant Homeo Domain (PHD) motif at C-terminus, suggests that the protein might act as a translational activator, repressor or cofactor, and/ or form complexes that modulate chromatin. In addition, Zar 1 is found to be essential for female fertility in mice [116]. The gradual disappearance of *O*-GlcNAc of protein or reduction in their levels suggests a role for *O*-GlcNAc in regulating the function of this protein.

Thesaurin a (42Sp50), the protein band # 4 was the first to be identified, and is homologous to eukaryotic EF-1 α and prokaryotic EF-Tu that recruits aminoacyl tRNA to the A-site of ribosome [117]. There are three forms of elongation factor-1 α in *Xenopus laevis*, two of them are oocyte specific forms, Thesaurin a and EF-1 α and third one is somatic form implying its absence in the oocyte, and present in embryo and adult cells only. Thesaurin a, consistent with our identification, is an early oocyte form, and unlike the other oocyte specific EF-1 α O, thesaurin a is exclusively and abundantly found in

previtellogenic oocytes (stage I, II and III) of *Xenopus laevis* [117]. In addition, thesaurin a is uniformly distributed throughout the cytoplasm with a one-order of magnitude lower activity than that of the EF-1 α O that is concentrated in the mitochondrial mass (Balbiani body) [117].

Thesaurin a is a major component of the 42S ribonucleoprotein (RNP) particle that in addition includes of thesaurin b (40 kDa protein), tRNA, and 5S RNA. [117] The main function of the 42S particle in oocytes is long-term storage of tRNA and 5S RNA. Thesaurin a show specific binding to tRNA, whereas thesaurin b specifically binds to 5S RNA. Even though, thesaurin a binds to tRNA, GTP and GDP like EF-1 α O, it has relatively low affinity for these ligands and low tRNA transfer activity. However, inspite of its low activity, the thesaurin a can presumably function as a substitute for EF-I α due to its high concentration in previtellogenic oocytes. Theusarin a differs from EF-1 α by its binding properties. Thesaurin a binds more strongly to GTP than GDP, and charged tRNA than uncharged tRNA, whereas the opposite is the case for EF-1 α. Since thesaurin a does not binds GDP weakly, the replacement of GDP can occur in the absence of the GDP/GTP exchange factor, EF-1 βγ. Thus, 42S particle containing thesaurin a can fully function as a substitute for both EF-1 α and EF-1 βγ in the previtellogenic oocytes, that is replaced by the EF-1 α O at the beginning of vitellogenesis, and which in turn is replaced by the somatic form of EF-1 α at the beginning of the embryogenesis [117] However, the presence of thesaurin a only in the earlier stages of oogenesis and its existence as a main component of the 42S particle with one order of magnitude low tRNA transfer activity also suggests the major function of thesaurin a is to store tRNA for later use during oogenesis and perhaps, early embryogenesis.

Even though, phosphorylation has not yet been demonstrated in thesaurin a, a genetically distant related form of EF-1 α from rabbit reticulocytes was reported to be phosphorylated [118]. Interestingly, this protein when phosphorylated dissociates from complexes of mono- and polyribosomes thus affecting the rate of polypeptide chain elongation, suggesting a regulatory role in translation for this post-translational modification. In another study, EF-1 α was immunoprecipitated with CTD110.6 antibody from rat liver extract suggesting that it might be *O*-GlcNAc modified or associated with proteins that are modified [119]. Now that thesaurin a has been identified as an *O*-GlcNAc containing protein, the role of this modification can be investigated. It is partially attractive to speculate that the disappearance of thesaurin a at the beginning of vitellogenesis, might be due to the removal of *O*-GlcNAc group from the protein, and thus, may lead to its proteasomal degradation as reported in the case of transcription factor, Sp1 [91].

While tRNA and 5SRNA stored along with thesaurin in complexes referred as thesaurisomes, oocyte maternal mRNA storage is also stored in a nontranslated ribonucleoprotein (RNP) complexes for the rapid translational recruitment during embryonic development, after mid-blastula stage [120]. The protein bands # 7, 8a and 8b were identified as *Cytoplasmic mRNA binding protein p54, y box factor homolog* is one of the non-ribosomal proteins associated with mRNAs in the RNP complexes. It can inhibit translation in vitro, and also has been considered as a putative translational regulator in vivo. This protein is found in two states in cells, a heterodimer form with p56 (another y-box factor) found free in cytoplasm or complex form with ribonucleoprotein particles. By stage II of oogenesis, the highest concentration of p54 is achieved and the levels of the

proteins were maintained throughout oogenesis and into early embryogenesis, but after gastrulation it is no longer found in soluble form.

This p54 is a basic protein with a high content of arginine residues (11%) with predicted to pI > 9 that is very near to our experimental value of pI 8.7. The protein's RNA binding site containing four arginine rich "basic/ aromatic islands" that are similar to the RNA-binding domain of bacteriophage mRNA antiterminator proteins and tat protein of human immunodeficiency virus [120]. In addition, the C terminal domain of the protein is homologous to the small E. coli cold-shock proteins These proteins are highly expressed at very low temperature and may protect the cells from damage due to freezing, by inhibiting translational initiation. By inference, from the cold shock proteins, the p54 may be involved in the partial blocking of translational initiation processes in an adaptive measure to store the untranslated mRNA for later use in early embryogenesis. In addition, the in-vitro studies have demonstrated that phosphorylation activates RNA binding [120]. The maintenance of p54 levels thoroughout the oogenesis in contrast to our observations where *O*-GlcNAc modified p54 is reduced might be due to the deglycosylation of these proteins in the later stages. Alternately, since our observations are based on the changes per unit mass, if total amount of protein is fixed while the oocyte enlarges and accumulates other proteins its relative amount would be reduced. Since the protein bands # 8a and 8b were also identified as y-box factor homolog, p54 suggests that the protein has different pI. This pI difference might be due to the different levels of phosphorylation of this protein. Highly phosphorylated protein is more acidic than less phosphorylated forms. Thereby, indicating that *O*-phosphorylation might be alternating with *O*-GlcNAcylation in this proteins.

Similar to y-box proteins, *Xp54 (ATP dependent RNA helicase p54)* is abundant and an integral component of stored mRNP particles [121]. This protein belongs to the family of DEAD-box RNA helicases that regulate RNA secondary structure in translation initiation, splicing and ribosome biosynthesis. It possesses ATP-dependent RNA helicase activity [121] High levels of Xp54 are expressed during early oogenesis, and are totally missing in adult tissue. Earlier studies suggested that the Xp54 might represent expression of an oocyte specific gene. High levels of Xp54 transcripts in small oocytes correlates to maximum production of stored mRNP particles, the levels is later on reduced may reflect relatively its low net production of mRNP particles in later stages of oogenesis and embryogenesis. Xp54 has multiple potential Caesin kinase 2 phosphorylation sites, with four out of five of these sites located near the C-terminus. It has been suggested the helicase activity might be regulated in two possible ways. One is by the addition or removal of phosphate groups, and the other by the availability of cofactor at appropriate stages of development. Since levels of Xp54 maximal remains fairly constant throughout ogenesis up to blastula, the decrease *O*-GlcNAc form seen in the stages suggests deglycosylation of the protein during the oogenesis.

In addition to the above proteins involved in storage of the tRNA and mRNA, the band # 9a was identified as an *O*-GlcNAc modified protein, *Vg1 RNA binding protein (RBP) variant A.* This protein associates Vg1RNA to the microtubules in order to translocate the RNA to the vegetal cortex [122] is identified as the O-GlcNAc modified proteins. The translocation of Vg1RNA requires intact microtubules and a 3' untranslated region (UTR) cis-acting element (termed vegetal localization element, VLE). This Vg1RBP has five domains, four K homology (KH) and one RNA recognition motif

(RRM) domains. The KH domains of *Xenopus* Vg1RBP appeared to mediate cytoplasmic trafficking, RNA binding and self association to homodimer [122]. However, the RRM does not have any role in the above mentioned processes although the sequence suggests potential for RNA binding [123]. This protein specifically binds to the VLE and is homologous to the micro-filament-binding zipcode binding protein (ZBP-1) that is involved in β-actin mRNA localization. The Vg1RBP appears to bind independently at two distinct sites in the VLE, and these binding sites represent a cis-acting element required for localization via the microtubule dependent pathway that oocurs in late stage III-early IV oocytes. Interestingly, *O*-GlcNAc modified protein disappears during the stage progression, indicating the modification may have some role to play in activating the protein after previtellogenesis (at stage III), perhaps through modulation of protein-protein associations.

The protein band # 10 has been identified as *Poly (A) binding protein (PABP).* This cytoplasmic 71 kDa protein is 633 amino acid long, binds to Poly (A) tail of adenylated mRNA and acts as positive regulator of translation [124]. PABP contains four RNA recognition motif (RRM) domains, three of which can act independently of each other in RNA binding, whereas the fourth one in the N-terminal region shows no detectable RNA binding activity [125]. Even though, Western blot analyses did not detect the Poly (A) binding proteins in oocytes or early embryos, but whole mount immunocytochemistry of oocytes (unpublished data) and direct analysis of oocyte messenger ribonucleoprotein particles [126] reveal the presence of this protein. Overall, these Northern and Western analyses suggests that the expression of PABP is not constitutive, but is instead

modulated in oocytes and the developing embryos [124]. This protein is localized in the cell types and subcellular domains that are most active in protein synthesis [124].

In immature oocytes, the cytoplasmic polyadenylation element (CPE) in 3' untranslated region (UTR) of maternal mRNA is bound by CPEB, which in turn bound by Maskin, which in turn bound by eIF4E [127, 128]. The progesterone stimulation induces CPEB phosphorylation and polyadenylation. Polyadenylation, through PABP destabilizes the Maskin-eIF4E complex, and leads to the binding of eIF4G with eIF4E that stimulates translation. Interestingly, the cyclin B which associates with protein kinase cdk1 to form MPF in *Xenopus* oocytes was found to be translated by this polyadenylation binding (PAB)-mediated stimulation [128]. Thus, the protein involved in the regulation of cyclin B1 mRNA translation that is essential for the embryonic cell cycle [128].

Since these cytosolic proteins are found in association with RNA and/ or other proteins, the characteristics of the proteins in these high molecular weight particles likely explains all the difficulties encountered during the initial purification attempt. Immunoaffinity and affinity methods depend on the availability of *O*-GlcNAc binding sites on the proteins. These sites may not be accessible in the particles due to steric constraints in the native associated state. Thus, explaining the low yields from these technologies. However, the presence of these proteins in the high molecular weight complexes provided an opportunity to both enrich samples with *O*-GlcNAc modified proteins and achieve high yields using differential sedimentation centrifugation. The complex formation had no effect on the ability to detect the *O*-GlcNAc modification by immunoblotting. Since this technique involves SDS-PAGE analysis prior to blotting. The denaturation of the com-

plexes during this process makes the *O*-GlcNAc available for antibody interaction and thus detection.

Apart from the proteins isolated thus far, there are some neutral proteins that need to isolated and identified in order to get the overall picture of the oocyte proteins showing the changes in their levels or the *O*-GlcNAc levels during the stage progression. In addition to the proteins associated to high molecular weight particles, there are a few soluble proteins left behind in the supernatant-100. These proteins which also show changes in the *O*-GlcNAc levels during oocyte development might play an important role in regulating the cellular processes of the oocyte. Since these proteins constitute a small percentage of total oocyte proteins, they need to be enriched by WGA affinity chromatography at low salt conditions, and later resolved by 2D-gel electrophoresis for protein sequencing and identification.

Chapter Four

Conclusion

The proteins that are identified thus far are among the most abundant, *O*-GlcNAc modified cytosolic proteins of *Xenopus laevis* oocytes (stage I) and largely basic in nature. Thesaurin a, y-box factor homolog, and Xp 54 (ATP dependent RNA helicase p54) that store tRNA and mRNA respectively as the ribonucleoprotein (RNP) complexes are found in maximum levels at early oogenesis. In addition, thesaurin a is an oocyte specific EF-1 α form that is present only in previtellogenic oocytes. Earlier studies have characterized these oocytes proteins as regulators of protein translation or as masking (repressing translation) proteins for mRNA or as involved in RNA translocation during oogenesis. The regulation of translation is crucial during the oogenesis, since the oocytes store mRNA and tRNA for the post-fertilization series of cell divisions until mid-blastula, a period where transcription is severely limited. In the same manner, the intracellular mRNA localization that leads to asymmetric protein synthesis is necessary for the pattern formation during early embryogenesis.

Interestingly, the zygote arrest 1 that is ovary specific protein has been suggested to play a critical role during the oocyte-to-embryo transition. Additionally, the presence of PHD motif also indicate a possible role as transcriptional activator, repressor or cofac-tors that are essential during the developmental process. On the other hand, the Poly (A) binding protein has a role in initiating the protein translation. Importantly, the cyclin B1 mRNA of *Xenopus* oocytes was shown to be translated by this polyadenylation binding.

Thus, indicating a role in regulating the cell cycle. To summarize, all the identified proteins play crucial roles in the developmental process, and the changes in the *O*-GlcNAc levels might be modulating their activities like the *O*-phosphorylation.

Finally, the high content of arginine residues in these proteins explains their basic nature, and these arginine rich regions facilitate the possible interactions with RNA. The *O*-GlcNAc on the proteins involved in the packaging, translocation and translation of RNA suggest that *O*-GlcNAc may play a role in the modulating the interactions. In addition, the sudden disappearance of *O*-GlcNAc modified thesaurin a that is at the stage III of oogenesis might be due to the deglycosylation leading to proteosomal degradation. Therefore, in order to understand the putative role of *O*-GlcNAc modification on this oocyte specific proteins, these proteins need to further studied. In addition, there are some more modified oocyte proteins that needs to be identified in order understand the significance of these proteins and the potential function of *O*-GlcNAc in the developmental process of oocyte. The findings of this investigation could be a significant contribution to the biochemistry of oocyte development and more generally to *O*-GlcNAc mediated cellular processes. In addition, it adds several more proteins to the growing list of *O*-GlcNAc modified proteins.

References

1. Torres, Carmen-Rosa; Hart, Gerald W. Topography and polypeptide distribution of terminal N-acetylglucosamine residues on the surfaces of intact lymphocytes. Evidence for *O*-linked GlcNAc. Journal of Biological Chemistry (1984), 259(5), 3308-17.

2. Whelan, Stephen A.; Hart, Gerald W. Proteomic Approaches to Analyze the Dynamic Relationships Between Nucleocytoplasmic Protein Glycosylation and Phosphorylation. Circulation Research (2003), 93(11), 1047-1058.

3. Zachara, Natasha E.; O'Donnell, Niall; Cheung, Win D.; Mercer, Jessica J.; Marth, Jamey D.; Hart, Gerald W. *Dynamic O*-GlcNAc Modification of Nucleocytoplasmic Proteins in Response to Stress: A Survival Response of Mammalian Cells. Journal of Biological Chemistry (2004), 279(29), 30133-30142.

4. Vosseller, Keith; Wells, Lance; Lane, M. Daniel; Hart, Gerald W. Elevated nucleocytoplasmic glycosylation by *O*-GlcNAc results in insulin resistance associated with defects in Akt activation in 3T3-L1 adipocytes. Proceedings of the National Academy of Sciences of the United States of America (2002), 99(8), 5313-5318.

5. Liu, Fei; Iqbal, Khalid; Grundke-Iqbal, Inge; Hart, Gerald W.; Gong, Cheng-Xin. *O*-GlcNAcylation regulates phosphorylation of tau: A mechanism involved in Alzheimer's disease. Proceedings of the National Academy of Sciences of the United States of America (2004), 101(29), 10804-10809.

6. Marshall S; Garvey W T; Traxinger R R. New insights into the metabolic regulation of insulin action and insulin resistance: role of glucose and amino acids. FASEB journal :official publication of the Federation of American Societies for Experimental Biology (1991 Dec), 5(15), 3031-6.

7. Hart, Gerald W. Dynamic *O*-linked glycosylation of nuclear and cytoskeletal proteins. Annual Review of Biochemistry (1997), 66 315-335.

8. Parker, Glendon; Taylor, Rodrick; Jones, Deborah; McClain, Donald. Hyperglycemia and Inhibition of Glycogen Synthase in Streptozotocin-treated Mice. Role of *O*-linked N-acetylglucosamine. Journal of Biological Chemistry (2004), 279(20), 20636-20642.

9. Zachara Natasha E; Hart Gerald W The emerging significance of *O*-GlcNAc in cellular regulation. CHEMICAL REVIEWS (2002 Feb), 102(2), 431-8.

10. Ferrell J E Jr *Xenopus* oocyte maturation: new lessons from a good egg. BioEssays :news and reviews in molecular, cellular and developmental biology (1999 Oct), 21(10), 833-42.

11. Slawson, Chad; Shafii, Susan; Amburgey, James; Potter, Robert. Characterization of the O-GlcNAc protein modification in *Xenopus laevis* oocyte during oogenesis and progesterone-stimulated maturation. Biochimica et Biophysica Acta (2002), 1573(2), 121-129.

12. Fang, Bin; Miller, Mill W. Use of Galactosyltransferase to Assess the Biological Function of O-linked N-Acetyl-D-Glucosamine: A Potential Role for *O*-GlcNAc during Cell Division. Experimental Cell Research (2001), 263(2), 243-253.

13. Lefebvre, T; Baert, F; Bodart, J F; Flament, S; Michalski, J C; Vilain, J P. Modulation of *O*-GlcNAc glycosylation during *Xenopus* oocyte maturation. J Cell Biochem. (2004) Sep 9.

14. Murray A W. Cell cycle extracts. Methods in cell biology (1991), 36 581-605.

15. Maller, James L. Regulation of amphibian oocyte maturation. Cell Differentiation (1985), 16(4), 211-21.

16. Donald D. Brown, A Tribute to the *Xenopus laevis* Oocyte and Egg. Journal of Biological chemistry. (2004), 279(44), 45291-45299.

17. Smith, L. Dennis. The induction of oocyte maturation: transmembrane signaling events and regulation of the cell cycle. Development (Cambridge, United Kingdom) (1989), 107(4), 685-99, 1 plate.

18. Smith, D; Xu, W; Varnold, R L. Oogenesis and Oocyte Isolation. Methods in Cell Biology: *Xenopus laevis*: Practical uses in cell and molecular Biology. (1991), 36 (4), 45-60.

19. Dumont J N Oogenesis in *Xenopus laevis* (Daudin). I. Stages of oocyte development in laboratory maintained animals. Journal of morphology (1972 Feb), 136(2),153-79.

20. Celis, J. E; Graessmann, A; Loyter, A. Microinjection and Organelle Transplant Techniques, methods and applications.1986.

21. Anderson, D. M; Smith, L. D. Synthesis of heterogeneous nuclear RNA in full grown oocytes of *Xenopus laevis*. Cell (1977), 11, 663-671.

22. Anderson, D. M; Smith, L. D. Patterns of synthesis and accumulation of heterogeneous RNA in lampbrush stage oocytes of *Xenopus laevis*. Dev. Biol. (1978) 67, 274-285.

23. Dolecki, G. I; Smith, L. D. Poly (A)+ RNA metabolism during oogenesis in *Xenopus laevis*. Dev. Biol. (1979) 69, 217-236.

24. Colman, A. Expression of exogenous DNA in *Xenopus* oocytes. In "Transcription and Translation: A Practical Approach" (B. D. Hames and S. J. Higgins, Eds.) (1984) 49-68. IRL Press, Oxford.

25. Wallace, Robin A.; Dumont, J. N. Induced synthesis and transport of yolk proteins and their accumulation by the oocyte in *Xenopus laevis*. Journal of Cellular Physiology (1968), 72(2) (Pt. 2), 73-89.

26. Jared, Donald W.; Dumont, James N.; Wallace, Robin A. Distribution of incorporated and synthesized protein among cell fractions of *Xenopus* oocytes. Developmental Biology (Orlando, FL, United States) (1973), 35(1),19-28.

27. Taylor, M. A; Smith, L. D. Quantitative changes in protein synthesis during oogenesis in *Xenopus laevis*. Dev. Bio. (1985) 110, 230-237.

28. Wasserman, W. J; Richter, J. D; Smith, L. D. Protein synthesis during maturation promoting factor- and progesterone-induced maturation in *Xenopus* oocytes. Dev. Biol. (1982) 89, 152-158.

29. Gurdon, J. B; Lan, C. D; Woodland, H. R; Marbiax, G. Use of frog egss and oocytes for the study of messenger RNA and its translation in living cells. Nature (London). (1971) 233, 177-182.

30. Richter, J. D; Smith, L. D. Differential capacity for the translation and lack of competition between mRNAs that segregate to free and membrane-bound polysomes. Cell. (1981) 27, 183-191.

31. Richter, J. D; Anderson. D. M; Davidson, E. H; Smith, L. D. Interspersed poly(A) RNAs of amphibian oocytes are not translatable. J. Mol. Biol. (1984) 173, 227-241.

32. Dworkin, Mark B.; Dworkin-Rastl, Eva. Glycogen breakdown in cleaving *Xenopus* embryos is limited by ADP. Molecular Reproduction and Development (1992), 32(4), 354-62.

33. Dworkin, Mark B.; Dworkin-Rastl, Eva. Metabolic regulation during early frog development: glycogenic flux in *Xenopus* oocytes, eggs, and embryos. Developmental Biology (Orlando, FL, United States) (1989), 132(2), 512-23.

34. Kessi E; Guixe V; Preller A; Ureta T Glycogen synthesis in amphibian oocytes: evidence for an indirect pathway. Biochemical journal (1996 Apr 15), 315 (Pt 2) 455-60.

35. Laevtrup-Rein, H.; Nelson, L. Changes in energy metabolism during the early development of *Xenopus laevis*. Experimental Cell Biology (1982), 50(3), 162-8.

36. Slawson, C.; Pidala, J.; Potter, R. Increased N-acetyl-β-glucosaminidase activity in primary breast carcinomas corresponds to a decrease in N-acetylglucosamine containing proteins. Biochimica et Biophysica Acta (2001), 1537(2), 147-157.

37. Holt, Gordon D.; Hart, Gerald W. The subcellular distribution of terminal N-acetylglucosamine moieties. Localization of a novel protein-saccharide linkage, O-linked GlcNAc. Journal of Biological Chemistry (1986), 261(17), 8049-57.

38. Comer, Frank I.; Hart, Gerald W. *O*-glycosylation of nuclear and cytosolic proteins: dynamic interplay between *O*-GlcNAc and *O*-phosphate. Journal of Biological Chemistry (2000), 275(38), 29179-29182.

39. Hanover, John A. Glycan-dependent signaling: *O*-linked N-acetylglucosamine. FASEB Journal (2001), 15(11), 1865-1876.

40. Haltiwanger R S; Busby S; Grove K; Li S; Mason D; Medina L; Moloney D; Philipsberg G; Scartozzi R. *O*-glycosylation of nuclear and cytoplasmic proteins: regulation analogous to phosphorylation? BIOCHEMICAL AND BIOPHYSICAL RESEARCH COMMUNICATIONS (1997 Feb 13), 231(2), 237-42.

41. Wells, Lance; Vosseller, Keith; Hart, Gerald W. Glycosylation of nucleocytoplasmic proteins: Signal transduction and *O*-GlcNAc. Science (Washington, DC, United States) (2001), 291(5512), 2376-2378.

42. Shafi, Raheel; Iyer, Sai Prasad N.; Ellies, Lesley G.; O'Donnell, Niall; Marek, Kurt W.; Chui, Daniel; Hart, Gerald W.; Marth, Jamey D. The *O*-GlcNAc transferase gene resides on the X chromosome and is essential for embryonic stem cell viability and mouse ontogeny. Proceedings of the National Academy of Sciences of the United States of America (2000), 97(11), 5735-5739.

43. Kreppel, Lisa K.; Blomberg, Melissa A.; Hart, Gerald W. Dynamic glycosylation of nuclear and cytosolic proteins. Cloning and characterization of a unique *O*-GlcNAc transferase with multiple tetratricopeptide repeats. Journal of Biological Chemistry (1997), 272(14), 9308-9315.

44. Haltiwager, R S; Holt, G D; Hart G W. Enzymatic addition of *O*-GlcNAc to nuclear and cytoplasmic proteins. Identification of a uridine diphospho-N-acetylglucosamine: peptide beta-N-acetylglucosaminyltransferase. J Biol Chem. 1990 Feb 15; 265(5): 2563-8.

45. Haltiwager, Blomberg, M A; Hart G W Glycosylation of nuclear and cytoplasmic proteins. Purification and characterization of a uridine diphospho-N-acetylglucosamine: polypeptide beta-N-acetylglucosaminyltransferase. J Biol Chem. 1992 May 5; 267(13): 9005-13.

46. Lubas WA, Frank DW, Krause M, Hanover JA. *O*-Linked GlcNAc transferase is a conserved nucleocytoplasmic protein containing tetratricopeptide repeats. J Biol Chem. 1997 Apr 4; 272(14): 9316-24.

47. Wrabl, James O.; Grishin, Nick V. Homology between *O*-linked GlcNAc transferases and proteins of the glycogen phosphorylase superfamily. Journal of Molecular Biology (2001), 314(3), 365-374.

48. Blatch G L; Lassle M. The tetratricopeptide repeat: a structural motif mediating protein-protein interactions. BioEssays : news and reviews in molecular, cellular and developmental biology (1999 Nov), 21(11), 932-9.

49. Iyer, Sai Prasad N.; Hart, Gerald W. Roles of the Tetratricopeptide Repeat Domain in *O*-GlcNAc Transferase Targeting and Protein Substrate Specificity. Journal of Biological Chemistry (2003), 278(27), 24608-24616.

50. Kreppel, Lisa K.; Hart, Gerald W. Regulation of a cytosolic and nuclear *O*-GlcNAc transferase. Role of the tetratricopeptide repeats. Journal of Biological Chemistry (1999), 274(45), 32015-32022.

51. Lubas, William A.; Hanover, John A. Functional expression of *O*-linked GlcNAc transferase: domain structure and substrate specificity. Journal of Biological Chemistry (2000), 275(15), 10983-10988.

52. Jinek, Martin; Rehwinkel, Jan; Lazarus, Brooke D.; Izaurralde, Elisa; Hanover, John A.; Conti, Elena.The superhelical TPR-repeat domain of *O*-linked GlcNAc transferase exhibits structural similarities to importin. Nature Structural & Molecular Biology (2004), 1(10), 1001-1007.

53. Iyer SP, Akimoto Y, Hart GW. Identification and cloning of a novel family of coiled-coil domain proteins that interact with *O*-GlcNAc transferase. J Biol Chem. 2003 Feb 14; 278(7): 5399-409. Epub 2002 Nov 14.

54. McClain Donald A Hexosamines as mediators of nutrient sensing and regulation in diabetes. Journal of diabetes and its complications (2002 Jan-Feb), 16(1), 72-80.

55. Bley, Ruben L.; Okubo, Hideo; Chandler, Albert M. Regulation of glucosamine synthesis in injury and partial hepatectomy. Proceedings of the Society for Experimental Biology and Medicine (1973), 144(1), 134-40.

56. Okubo, Hideo; Chandler, Albert M. Endocrine status and the response of glucosamine-6-phosphate synthetase to trauma. Experimental and Molecular Pathology (1976), 24(1), 91-104.

57. Okubo, Hideo; Chandler, Albert M. Regulation of glucosamine synthesis during the first twenty-four hours following injury and partial hepatectomy. Proceedings of the Society for Experimental Biology and Medicine (1974), 146(4), 1159-62.

58. Okubo, Hideo; Shibata, Katsunori; Ishibashi, Hiromi; Yanase, Toshiyuki. Developmental studies on glucosamine metabolism. Proceedings of the Society for Experimental Biology and Medicine (1976), 152(4), 626-30.

59. Wice, Burton M.; Trugnan, Germain; Pinto, Moise; Rousset, Monique; Chevalier, Guillemette; Dussaulx, Elisabeth; Lacroix, Brigitte; Zweibaum, Alain. The intracellular accumulation of UDP-N-acetylhexosamines is concomitant with the inability of human colon cancer cells to differentiate. Journal of Biological Chemistry (1985), 260(1), 139-46.

60. Comer, Frank I.; Hart, Gerald W. Reciprocity between *O*-GlcNAc and *O*-Phosphate on the Carboxyl Terminal Domain of RNA Polymerase II. Biochemistry (2001), 40(26), 7845-7852.

61. Dong, Dennis L.-Y.; Hart, Gerald W. Purification and characterization of an *O*-GlcNAc selective N-acetyl-□-D-glucosaminidase from rat spleen cytosol. Journal of Biological Chemistry (1994), 269(30), 19321-30.

62. Gao, Yuan; Wells, Lance; Comer, Frank I.; Parker, Glendon J.; Hart, Gerald W. Dynamic *O*-glycosylation of nuclear and cytosolic proteins. Cloning and characterization of a neutral, cytosolic β-N-acetylglucosaminidase from human brain. Journal of Biological Chemistry (2001), 276(13), 9838-9845.

63. Wells Lance; Gao Yuan; Mahoney James A; Vosseller Keith; Chen Chen; Rosen Antony; Hart Gerald W. Dynamic *O*-glycosylation of nuclear and cytosolic proteins: further characterization of the nucleocytoplasmic beta-N-acetylglucosaminidase, *O*-GlcNAcase. Journal of biological chemistry (2002 Jan 18), 277(3), 1755-61.

64. Roos, Mark D.; Xie, Wen; Su, Kaihong; Clark, John A.; Yang, Xiaoyong; Chin, Edward; Paterson, Andrew J.; Kudlow, Jeffrey E. Streptozotocin, an analog of N-acetylglucosamine, blocks the removal of *O*-GlcNAc from intracellular proteins. Proceedings of the Association of American Physicians (1998), 110(5), 422-432.

65. Haltiwanger, Robert S.; Grove, Kathleen; Philipsberg, Glenn A. Modulation of O-linked N-acetylglucosamine levels on nuclear and cytoplasmic proteins in vivo using the peptide *O*-GlcNAc-β-N-acetylglucosaminidase inhibitor *O*-(2-acetamido-2-deoxy-D-glucopyranosylidene)amino-N-phenylcarbamate. Journal of Biological Chemistry (1998), 273(6), 3611-3617.

66. Mohan, Halasyam; Vasella, Andrea. An improved synthesis of 2-acetamido-2-deoxy-D-gluconohydroximolactone (PUGNAc), a strong inhibitor of β-N-acetylglucosaminidases. Helvetica Chimica Acta (2000), 83(1), 114-118.

67. Cheng, Xiaogang; Cole, Robert N.; Zaia, Joseph; Hart, Gerald W.Alternative *O*-Glycosylation/*O*-Phosphorylation of the Murine Estrogen Receptor β. Department of Biological Chemistry School of Medicine, Johns Hopkins University, Baltimore, MD, USA.Biochemistry (2000), 39(38), 11609-11620

.

68. Liu, Fei; Iqbal, Khalid; Grundke-Iqbal, Inge; Hart, Gerald W.; Gong, Cheng-Xin. O-GlcNAcylation regulates phosphorylation of tau: A mechanism involved in Alzheimer's disease. Proceedings of the National Academy of Sciences of the United States of America (2004), 101(29), 10804-10809.

69. Chou, Teh-Ying; Hart, Gerald W.; Dang, Chi V. c-Myc is glycosylated at threonine 58, a known phosphorylation site and a mutational hot spot in lymphomas. Journal of Biological Chemistry (1995), 270(32), 18961-5.

70. Federici, Massimo; Menghini, Rossella; Mauriello, Alessandro; Hribal, Marta Letizia; Ferrelli, Francesca; Lauro, Davide; Sbraccia, Paolo; Spagnoli, Luigi Giusto; Sesti, Giorgio; Lauro, Renato. Insulin-dependent activation of endothelial nitric oxide synthase is impaired by *O*-linked glycosylation modification of signaling proteins in human coronary endothelial cells. Circulation (2002), 106(4), 466-472.

71. Cheng, Xiaogang; Hart, Gerald W. Alternative *O*-glycosylation/*O*-phosphorylation of serine-16 in murine estrogen receptor β. Post-translational regulation of turnover and transactivation activity. Journal of Biological Chemistry (2001), 276(13),10570-10575.

72. Comer, Frank I.; Hart, Gerald W. Reciprocity between *O*-GlcNAc and *O*-Phosphate on the Carboxyl Terminal Domain of RNA Polymerase II. Biochemistry (2001), 40(26), 7845-7852.

73. Chou C F; Omary M B. Mitotic arrest-associated enhancement of *O*-linked glycosylation and phosphorylation of human keratins 8 and 18. Journal of biological chemistry (1993 Feb 25), 268(6), 4465-72.

74. C. M. Snow, J. H. Shaper, N. L. Shaper, G. W. Hart, Mol. Biol. Cell. 6 (1996) 357.

75. Zheng, Binhai; Sage, Marijke; Sheppeard, Elizabeth A.; Jurecic, Vesna; Bradley, Allan. Engineering mouse chromosomes with Cre-loxP: range, efficiency, and somatic applications. Molecular and Cellular Biology (2000), 20(2), 648-655.

76. O'Donnell, Niall; Zachara, Natasha E.; Hart, Gerald W.; Marth, Jamey D. Ogt-dependent X-chromosome-linked protein glycosylation is a requisite modification in somatic cell function and embryo viability. Molecular and Cellular Biology (2004), 24(4),1680-1690.

77. Walgren, Jennie L. E.; Vincent, Timothy S.; Schey, Kevin L.; Buse, Maria G. High glucose and insulin promote *O*-GlcNAc modification of proteins, including α-tubulin. American Journal of Physiology (2003), 284(2, Pt. 1), E424-E434.

78. Du, Xue Liang; Edelstein, Diane; Dimmeler, Stefanie; Ju, Qida; Sui, Chengyu; Brownlee, Michael. Hyperglycemia inhibits endothelial nitric oxide synthase activity by posttranslational modification at the Akt site. Journal of Clinical Investigation (2001), 108(9), 1341-1348.

79. Federici, Massimo; Menghini, Rossella; Mauriello, Alessandro; Hribal, Marta Letizia; Ferrelli, Francesca; Lauro, Davide; Sbraccia, Paolo; Spagnoli, Luigi Giusto; Sesti, Giorgio; Lauro, Renato. Insulin-dependent activation of endothelial nitric oxide synthase is impaired by *O*-linked glycosylation modification of signaling proteins in human coronary endothelial cells. Circulation (2002), 106(4), 466-472.

80. Parker, Glendon J.; Lund, Kelli C.; Taylor, Rodrick P.; McClain, Donald A. Insulin Resistance of Glycogen Synthase Mediated by *O*-Linked N-Acetylglucosamine. Journal of Biological Chemistry (2003), 278(12), 10022-10027.

81. Han, InnOc; Roos, Mark D.; Kudlow, Jeffrey E. Interaction of the transcription factor Sp1 with the nuclear pore protein p62 requires the C-terminal domain of p62. Journal of Cellular Biochemistry (1998), 68(1), 50-61.

82. Vosseller, Keith; Wells, Lance; Lane, M. Daniel; Hart, Gerald W. Elevated nucleocytoplasmic glycosylation by *O*-GlcNAc results in insulin resistance associated with defects in Akt activation in 3T3-L1 adipocytes. Proceedings of the National Academy of Sciences of the United States of America (2002), 99(8), 5313-5318.

83. Han, Innoc; Kudlow, Jeffrey E. Reduced *O*- glycosylation of Sp1 is associated with increased proteasome susceptibility. Molecular and Cellular Biology (1997), 17(5), 2550-2558.

84. Buse, Maria G.; Robinson, Katherine A.; Marshall, Bess A.; Hresko, Richard C.; Mueckler, Mike M. Enhanced *O*-GlcNAc protein modification is associated with insulin resistance in GLUT1-overexpressing muscles. American Journal of Physiology (2002), 283(2, Pt. 1), E241-E250.

85. Konrad R J; Janowski K M; Kudlow J E Glucose and streptozotocin stimulate p135 *O*-glycosylation in pancreatic islets. Biochemical and biophysical research communications (2000 Jan 7), 267(1), 26-32.

86. Han, Innoc; Oh, Eok-Soo; Kudlow, Jeffrey E. Responsiveness of the state of *O*-linked N-acetylglucosamine modification of nuclear pore protein p62 to the extracellular glucose concentration. Biochemical Journal (2000), 350(1), 109-11.

87. Yki-Jarvinen, Hannele; Virkamaki, Antti; Daniels, Marc C.; Mcclain, Don; Gottschalk, W. Kirby. Insulin and glucosamine infusions increase *O*-linked N-acetyl-glucosamine in skeletal muscle proteins in vivo. Metabolism, Clinical and Experimental (1998), 47(4), 449-455.

88. Wells, L.; Vosseller, K.; Hart, G. W. A role for N-acetylglucosamine as a nutrient sensor and mediator of insulin resistance. Cellular and Molecular Life Sciences (2003), 60(2), 222-228.

89. Wells, Lance; Whalen, Stephen A.; Hart, Gerald W. *O*-GlcNAc: a regulatory post-translational modification. Biochemical and Biophysical Research Communications (2003), 302(3), 435-441.

90. Zhang, Fengxue; Su, Kaihong; Yang, Xiaoyong; Bowe, Damon B.; Paterson, Andrew J.; Kudlow, Jeffrey E. *O*-GlcNAc modification is an endogenous inhibitor of the proteasome. Cell (Cambridge, MA, United States) (2003), 115(6), 715-725.

91. Zachara, Natasha E.; Hart, Gerald W. *O*-GlcNAc a sensor of cellular state: the role of nucleocytoplasmic glycosylation in modulating cellular function in response to nutrition and stress. Biochimica et Biophysica Acta (2004), 1673(1-2), 13-28.

92. Fiordaliso, Fabio; Leri, Annarosa; Cesselli, Daniela; Limana, Federica; Safai, Bijan; Nadal-Ginard, Bernardo; Anversa, Piero; Kajstura, Jan. Hyperglycemia activates p53 and p53-regulated genes leading to myocyte cell death. Diabetes (2001), 50(10), 2363-2375.

93. Ido, Yasuo; Carling, David; Ruderman, Neil. Hyperglycemia-induced apoptosis in human umbilical vein endothelial cells: inhibition by the AMP-activated protein kinase activation. Diabetes (2002), 51(1), 159-167.

94. Liu K; Paterson A J; Chin E; Kudlow J E Glucose stimulates protein modification by O-linked GlcNAc in pancreatic beta cells: linkage of *O*-linked GlcNAc to beta cell death. Proceedings of the National Academy of Sciences of the United States of America (2000 Mar 14), 97(6), 2820-5.

95. Fang, Bin; Miller, Mill W. Use of Galactosyltransferase to Assess the Biological Function of *O*-linked N-Acetyl-D-Glucosamine: A Potential Role for *O*-GlcNAc during Cell Division. Experimental Cell Research (2001), 263(2), 243-253.

96. Feldherr, C. M. Uptake of endogenous proteins by oocyte nuclei. Experimental Cell Research (1975), 93(2), 411-19.

97. R.A. Laskey, B. M. Honda, A. D. Mills, and J. T. Finch. Nucleosomes are assembled by an acidic protein which binds histones and transfers them to DNA. Anture 275 (1978) 416-420.

98. Evans, J.P., and Kay, B.K. Biochemical fractionation of oocytes. Methods Cell Biol. (1991), *36,* 133-148.

99. Konrad, Robert J.; Mikolaenko, Irina; Tolar, Joseph F.; Liu, Kan; Kudlow, Jeffrey E. The potential mechanism of the diabetogenic action of streptozotocin: inhibition of pancreatic β-cell *O*-GlcNAc-selective N-acetyl-β-D- glucosaminidase. Biochemical Journal (2001), 356(1), 31-41.

100. Comer, Frank I.; Vosseller, Keith; Wells, Lance; Accavitti, Mary Ann; Hart, Gerald W. Characterization of a mouse monoclonal antibody specific for O-linked N-acetylglucosamine. Analytical Biochemistry (2001), 293(2), 169-177.

101. Nagata, Yoshiho; Burger, Max M. Wheat germ agglutinin. Molecular characteristics and specificity for sugar binding. Journal of Biological Chemistry (1974), 249(10), 3116-22.

102. Kita, Konami; Omata, Saburo; Horigome, Tsuneyoshi. Purification and Characterization of a nuclear pore glycoprotein complex containing p62. Journal of Biochemistry (Tokyo, Japan) (1993), 113(3), 377-82

103. Lefebvre, Tony; Cieniewski, Caroline; Lemoine, Jerome; Guerardel, Yann; Leroy, Yves; Zanetta, Jean-Pierre; Michalski, Jean-Claude. Identification of N- acetyl-D-glucosamine-specific lectins from rat liver cytosolic and nuclear compartments as heat-shock proteins. Biochemical Journal (2001), 360(1), 179-188.

104. U. K. Laemmli. Cleavage of structural proteins during the assembly of the head of bacteriophage T4. Nature 227 (1970) 680-685.

105. Hager, Dayle A.; Burgess, Richard R. Elution of proteins from sodium dodecyl sulfate-polyacrylamide gels, removal of sodium dodecyl sulfate, and renaturation of enzymic activity: results with sigma subunit of Escherichia coli RNA polymerase, wheat germ DNA topoisomerase, and other enzymes. Analytical Biochemistry (1980), 109(1), 76-86.

106. 2D-Gel Electrophoresis using immobilized pH gradients, Principles and Methods. Amershams

107. Peisker, Klaus. Application of Neuhoff's optimized Coomassie Brilliant Blue G-250/ammonium sulfate/phosphoric acid protein staining to ultrathin polyacrylamide gels on polyester films. Electrophoresis (1988), 9(5), 236-8.

108. E. Harlow and D. Lane. Antibodies, a laboratory manual. New York: Cold Spring Harbor Press (1998).

109. Lefebvre, Tony; Alonso, Catherine; Mahboub, Said; Dupire, Marie-Joelle; Zanetta, Jean-Pierre; Caillet-Boudin, Marie-Laure; Michalski, Jean-Claude. Effect of okadaic acid on O-linked N-acetylglucosamine levels in a neuroblastoma cell line. Biochimica et Biophysica Acta (1999), 1472(1-2), 71-81.

110. Hoefer. Protein Electrophoresis, Application Guide 92-93.

111. De Fea, Kathryn; Roth, Richard A. Modulation of insulin receptor substrate-1 tyrosine phosphorylation and function by mitogen-activated protein kinase. Journal of Biological Chemistry (1997), 272(50), 31400-31406.

112. Haynes, Paul A.; Aebersold, Ruedi. Simultaneous Detection and Identification of O-GlcNAc-Modified Glycoproteins Using Liquid Chromatography-Tandem Mass Spectrometry. Analytical Chemistry (2000), 72(21), 5402-5410.

113. O'Farrell, Patricia Z.; Goodman, Howard M.; O'Farrell, Patrick H. High resolution two-dimensional electrophoresis of basic as well as acidic proteins. Cell (Cambridge, MA, United States) (1977), 12(4), 1133-41.

113. Lacey J C Jr; Pruitt K M Drug-biomolecule interactions: interactions of mononucleotides and polybasic amino acids. Journal of pharmaceutical sciences (1975 Mar), 64(3), 473-7.

114. Jackson S P; Tjian R Purification and analysis of RNA polymerase II transcription factors by using wheat germ agglutinin affinity chromatography. Proceedings of the National Academy of Sciences of the United States of America (1989 Mar), 86(6), 1781-5.

115. Wu, Xuemei; Wang, Pei; Brown, Christopher A.; Zilinski, Carolyn A.; Matzuk, Martin M. Zygote arrest 1 (Zar1) is an evolutionarily conserved gene expressed in vertebrate ovaries. Biology of Reproduction (2003), 69(3), 861-867.

116. Wu, Xuemei; Viveiros, Maria M.; Eppig, John J.; Bai, Yuchen; Fitzpatrick, Susan L.; Matzuk, Martin M. Zygote arrest 1 (Zar1) is a novel maternal-effect gene critical for the oocyte-to-embryo transition. Nature Genetics (2003), 33(2), 187-191.

117. Viel, Alain; Le Maire, Marc; Philippe, Herve; Morales, Julia; Mazabraud, Andre; Denis, Herman. Structural and functional properties of thesaurin a (42Sp50), the major protein of the 42 S particles present in *Xenopus laevis* previtellogenic oocytes. Journal of Biological Chemistry (1991), 266(16), 10392-9.

118. Davydova, E. K.; Sitikov, A. S.; Ovchinnikov, L. P. Phosphorylation of elongation factor 1 in polyribosome fraction of rabbit reticulocytes. FEBS Letters (1984), 176(2), 401-5.

119. Wells, Lance; Vosseller, Keith; Cole, Robert N.; Cronshaw, Janet M.; Matunis, Michael J.; Hart, Gerald W. Mapping sites of *O*-GlcNAc modification using affinity tags for serine and threonine post-translational modifications. Molecular and Cellular Proteomics (2002), 1(10), 791-804.

120. Murray M T; Schiller D L; Franke W W Sequence analysis of cytoplasmic mRNA-binding proteins of *Xenopus* oocytes identifies a family of RNA-binding proteins. Proceedings of the National Academy of Sciences of the United States of America (1992 Jan 1), 89(1), 11-5.

121. Ladomery, Michael; Wade, Eleanor; Sommerville, John. Xp54, the *Xenopus* homolog of human RNA helicase p54, is an integral component of stored mRNP particles in oocytes. Nucleic Acids Research (1997), 25(5), 965-973.

122. Havin, Leora; Git, Anna; Elisha, Zichrini; Oberman, Froma; Yaniv, Karina; Schwartz, Sigal Pressman; Standart, Nancy; Yisraeli, Joel K. RNA-binding protein conserved in both microtubule- and microfilament-based RNA localization. Genes & Development (1998), 12(11), 1593-1598.

123. Git, Anna; Standart, Nancy. The KH domains of *Xenopus* Vg1RBP mediate RNA binding and self-association. RNA (2002), 8(10), 1319-1333.

124. Zelus, Bruce D.; Giebelhaus, Dawn H.; Eib, Douglas W.; Kenner, Kimberly A.; Moon, Randall T. Expression of the poly(A)-binding protein during development of Xenopus laevis. Molecular and Cellular Biology (1989), 9(6), 2756-60.

125. Nietfeld, Wilfried; Mentzel, Helga; Pieler, Tomas. The Xenopus laevis poly(A) binding protein is composed of multiple functionally independent RNA binding domains. EMBO Journal (1990), 9(11), 3699-705.

126. Swiderski, Ruth E.; Richter, Joel D. Photocrosslinking of proteins to maternal mRNA in Xenopus oocytes. Developmental Biology (Orlando, FL, United States) (1988), 128(2), 349-58.

127. Groisman, Irina; Huang, Yi-Shuian; Mendez, Raul; Cao, Quiping; Theurkauf, William; Richter, Joel D. CPEB, maskin, and cyclin B1 mRNA at the mitotic apparatus: implications for local translational control of cell division. Cell (Cambridge, Massachusetts) (2000), 103(3), 435-447.

128. Groisman, Irina; Jung, Mi-Young; Sarkissian, Madathia; Cao, Quiping; Richter, Joel D. Translational control of the embryonic cell cycle. Cell (Cambridge, MA, United States) (2002), 109(4), 473-483.

Appendices

Appendix A: Abbreviations

O-GlcNAc	N-acetylglucosamine attached to a serine or threonine
GlcNAc	N-acetylglucosamine
O-GlcNAcase	N-acetyl-β-glucosaminidase
mRNA	Messenger RNA
DNA	Deoxy ribonucleic acid
GVBD	Germinal vesicle breakdown
tRNA	Transfer RNA
snRNA	Small nuclear RNA
rGTP	Guanosine triphosphate
dTTP	Deoxyribothymidine 5$^{'}$–triphosphate
UDP-glucose	Uridine Diphosphoglucose
HSP	Heat shock protein
OGT	*O*-GlcNAc Transferase
PUGNAc	*O*-2-acetamido-2-deoxy-D-glucopranosylidene
STZ	Streptozotocin
WGA	Wheat germ agglutinin
GFAT	Glutamine: Fructose-6-phosphate amidotranferase
DON	6-diazo-5-oxonorleucine
OR-2	Oocyte ringers buffer 2
HEPES	4-2-hydroxymethyl-1-piperazine ethanesulfonic acid
BSA	Bovine serum albumin
Tris	Tris-hydroxymethyl-aminomethane

IgG	Immunoglobulin type G
IgM	Immunoglobulin type M
UDP	Uridine diphosphate
SDS	Sodium dodecyl sulfate
PAGE	Polyacrylamide gel electrophoresis
TEMED	N, N, N', N'-tetra-methyl-ethylenediamine
PVDF	Polyvinyl difluoride
PBS	Phosphate buffer saline
RL-2	Monoclonal Antibody against O-GlcNAc
CDT110.6	Monoclonal Antibody against O-GlcNAc
PBST	Phosphate buffered saline with Tween 20
HSPBS	High salt phosphate buffered saline with Tween 20
CTD	C-terminal domain
TBST	Tris buffered saline with Tween 20
TBS-HT	Tris buffered saline with high Tween 20
TBS-D	Tris buffered saline with high detergent
DAB	Diaminobenzidine
ATP	Adenosine triphosphate
Glc	Glucose
Gal	Galaactose
PMSF	Phenylmethyl-sulfonyl fluoride
EDTA	Ethylene-diamine tetracetic acid
HRP	Horse radish peroxidase

1D-gel	One-dimensional gel
2D-gel	Two-dimensional gel
RIPA	Radioimmunoprecipitation assay
IPG	Immobilized pH gradient
IEF	Isoelectric focusing
NL	Non-linear
DTT	Dithiothretol
CHAPS	3-[(3-cholamidopropyl) dimethylammonio]-1-propanesulfonate
MS 222	Tricaine methyl sulfonate
PSM	Protein solubilizing mixture
RBP	RNA binding protein
Vg 1 RBP	Vegetal 1 RNA binding protein
VLE	Vetegal localization element
EF-1 α	Elongation factor-1 alpha
RNP	Ribonucleoparticle
EF-1 α O	Elongation factor alpha (oocyte specific form)
CK 2	Casein kinase 2
UTR	Untranslated region
KH	K Homolog
ZBP-1	Zipcode binding protein
HBP	Hexosamine biosynthetic pathway
Zar 1	Zygote arrest 1
Xp54	ATP dependent RNA helicase p54

PABP	Poly (A) binding protein
CPE	Cytoplasmic polyadenylation element
CPEB	Cytoplasmic polyadenylation element binding protein
eIF	Elongation initiation factor
pI	Isoelectric point

Appendix B: Structures of some of the discussed and used sugars and inhibitors

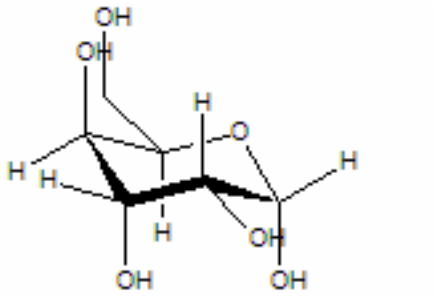

Glucose

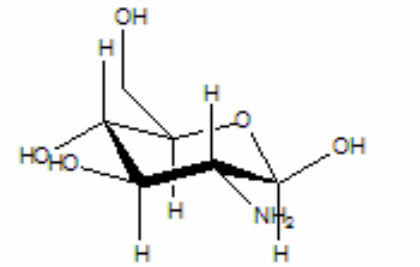

Glucosamine

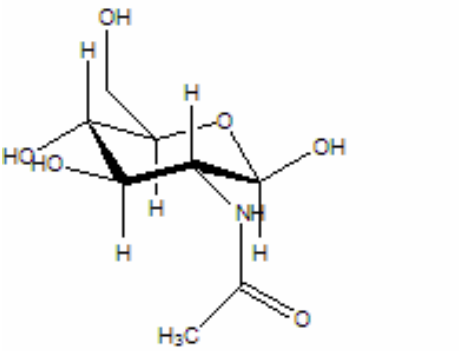

N-Acetylglucosamine

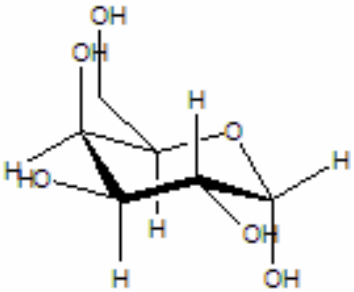

Galactose

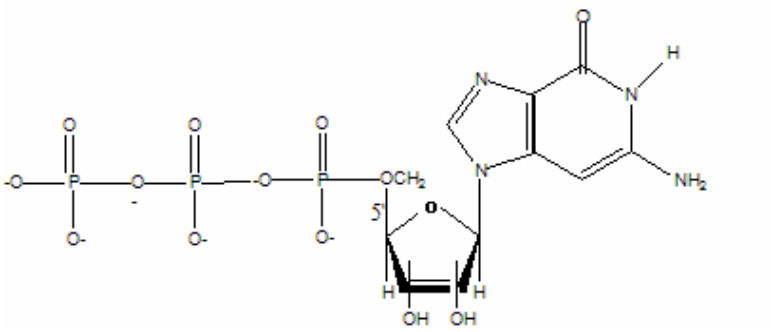

Guanosine 5’-triphosphate

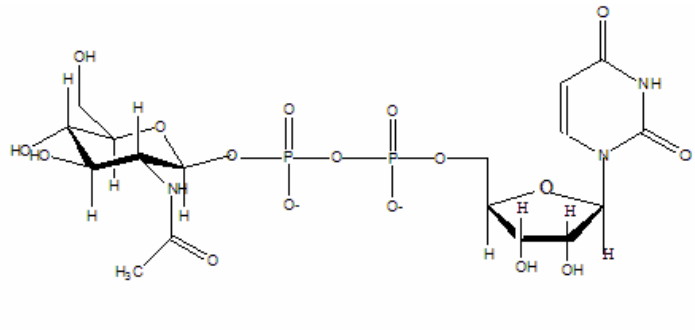

Uridine diphosphate-N-acetylglucosamine

Inhibitors

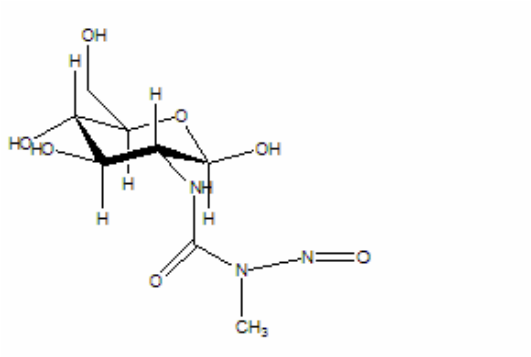

Streptozotocin

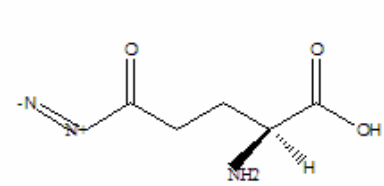

6-Diazo-oxonorleucine

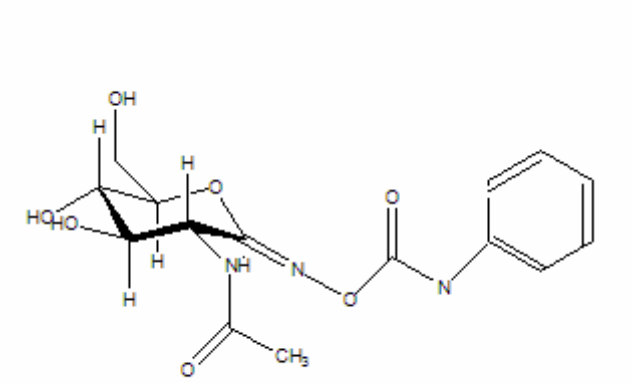

PUGNAc

Appendix C: Mass data analysis of Thesaurin a, p54 (y-box factor homolog), Xp54 RNA helicase, Zygote arrest 1 and Poly (A) binding protein

Figure 1-Mass spectrum of a peptide of Elongation factor (Thesaurin a)(42Sp50)

Elongation factor 1-alpha (EF-1-alpha) (42Sp50)

gi|416929|sp|P17506|EF11_XENLA Elongation factor 1-alpha (EF-1-alpha) (42Sp50) (Thesaurin A) gi|64489|emb|CAA79605.1| 42Sp50 [Xenopus laevis]

MTDKAPQKTHLNIVIIGHVDSGKSTTTGHLIYKCGGFDPRALEKVEAAAAQLGKSSFKFAWILDKLKAERERGITIDISLWKFQTNRFTITIIDAPGHRDFIKN
MITGTSQADVALLVVSAATGEFEAGVSRNGQTREHALLAYTMGVKQLIVCVNKMDLTDPPYSHKRFDEVVRNVMVYLKKIGYNPATIPFVPVSGWTGENISSPS
QKMGWFKGWKVKRKDGFTKGQSLLEVLDALVPPVRPANKPLRLPLQDVYKIGGIGTVPVGKIETGILKPGMTISFAPSGFSAEVKSIEMHHEPLQMAFPGFNIGFN
VKNIAVKSLKRGNVAGNSKSDPPTEASSFTAQVIILNHPGFIKAGYSPVIDCHTAHITCQFAELQEKIDRRTGKKLEDNPGLLKSGDAAIITLKPIKPFCVERFFDYPP
LGRFAARDLKQTVAVGVVKSVEHKAGAAARRQVQKPVLVK

Sequence	MH+	% by Mass	Position	% by AA's
VEAAAAQLGK	957.54	1.89	45 - 54	2.16
FTITIIDAPGHR	1340.73	2.65	88 - 99	2.59
RFDEVVR	920.50	1.82	169 - 175	1.51
FDEVVR	764.39	1.51	170 - 175	1.30
IGGIGTVPVGK	997.60	1.97	259 - 269	2.38
KLEDNPGLLK	1126.65	2.22	389 - 398	2.16
FFDYPPLGR	1111.56	2.19	418 - 426	1.94

Protein coverage Totals

By mass	6359.5
% by mass	12.56
By position	59
% by AA's	12.74

#934-934 RT:41.27-41.27 NL: 5.08E6

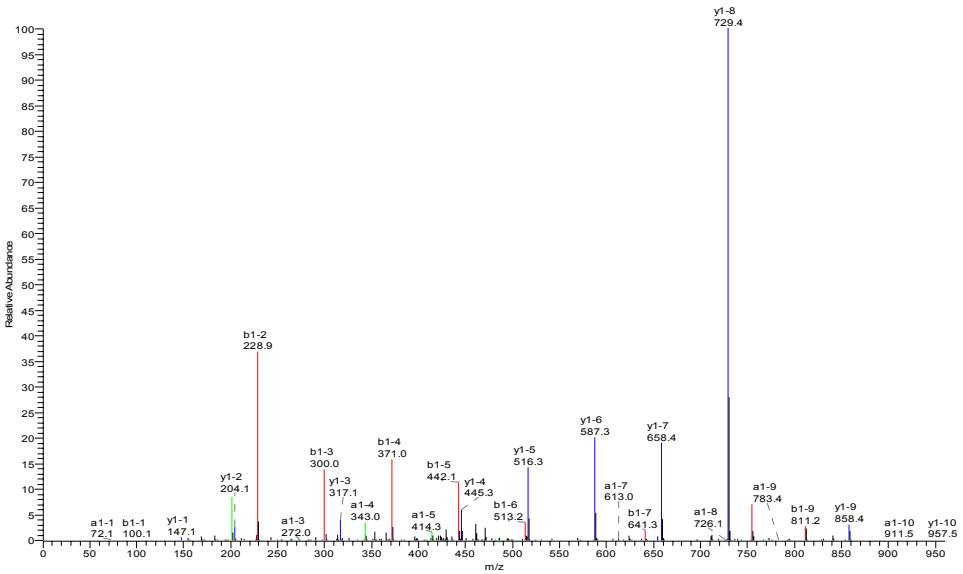

Figure 2- Mass data analysis of a peptide Xp54, RNA Helicase (only one peptide was found with High Xcorr).

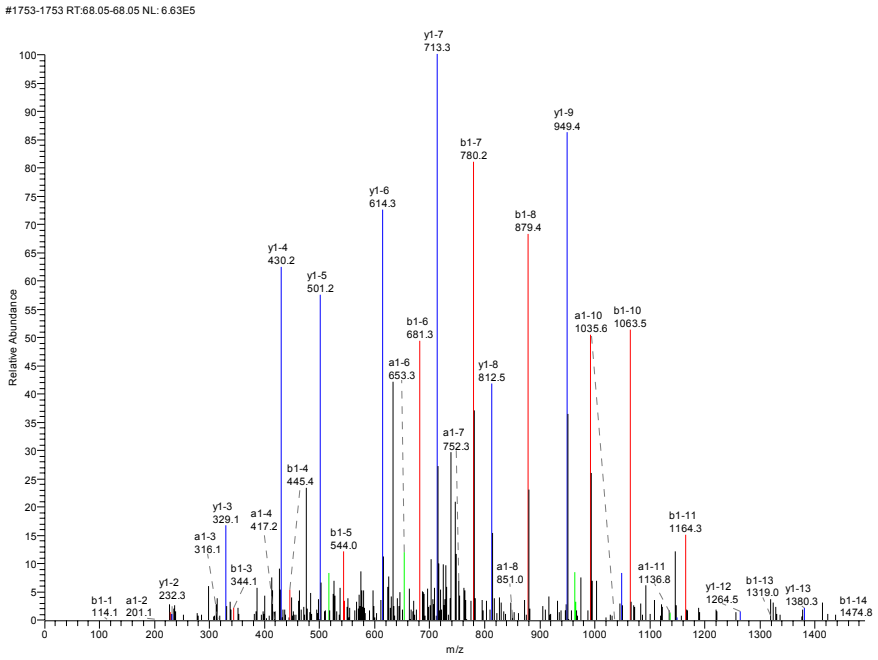

Figure 3- Mass data analysis of a peptide of p54, y-box factor homolog

MSSEVETQQQQPDALEGKAGQEPAATVGDKKVIATKVLGTVKWFNVRNGYGFINRNDTKEDVFVHQTAIKKNNPRKYLRSVGDGETVEFDVVEGEKGAEAANVT
GPEGVPVQGSKYAADRNHYRRYPRRRGPPRNYQQNYQNNESGEKAEENESAPEGDDSNQQRPYHRRRFPPYYTRRPYGRRPQYSNAPVQGEEAEGADSQGTDEQG
RPARQNMYRGFRPRFRRGPPRQRQPREEGNEEDKENQGDETQSQPPPQRRYRRNFNYRRRRPENPKSQDGKETKAAETSAENTSTPEAEQGGAE

Sequence	MH+	% by Mass	Position	% by AA's
MSSEVETQQQQPDALEGK	2004.92	5.79	1 - 18	5.94
EDVFVHQTAIK	1286.67	3.72	60 - 70	3.63
SVGDGETVEFDVVEGEK	1795.82	5.19	80 - 96	5.61
FPPYYTRRPYGR	1572.81	4.54	172 - 183	3.96

AA	M+nH	A	A*	Ao	B	B*	Bo	C	X	Y	Y*	Yo
S	89.05	60.04	43.02	42.03	88.04	71.01	70.03			1795.82	1778.80	1777.81
V	188.12	159.11	142.09	141.10	187.11	170.08	169.10			1708.79	1691.77	1690.78
G	245.14	216.13	199.11	198.12	244.13	227.10	226.12			1609.72	1592.70	1591.71
D	360.16	331.16	314.14	313.15	359.16	342.13	341.15			1552.70	1535.68	1534.69
G	417.19	388.18	371.16	370.17	416.18	399.15	398.17			1437.67	1420.65	1419.66
E	546.23	517.23	500.20	499.22	545.22	528.19	527.21			1380.65	1363.63	1362.64
T	647.28	618.27	601.25	600.26	646.27	629.24	628.26			1251.61	1234.58	1233.60
V	746.34	717.34	700.32	699.33	745.34	728.31	727.33			1150.56	1133.54	1132.55
E	875.39	846.38	829.36	828.37	874.38	857.35	856.37			1051.49	1034.47	1033.48
F	1022.46	993.45	976.43	975.44	1021.45	1004.42	1003.44			922.45	905.43	904.44
D	1137.48	1108.48	1091.45	1090.47	1136.47	1119.45	1118.46			775.38	758.36	757.37
V	1236.55	1207.55	1190.52	1189.54	1235.54	1218.52	1217.53			660.36	643.33	642.35
V	1335.62	1306.62	1289.59	1288.61	1334.61	1317.59	1316.60			561.29	544.26	543.28
E	1464.66	1435.66	1418.63	1417.65	1463.65	1446.63	1445.64			462.22	445.19	444.21
G	1521.68	1492.68	1475.65	1474.67	1520.68	1503.65	1502.67			333.18	316.15	315.17
E	1650.73	1621.72	1604.70	1603.71	1649.72	1632.69	1631.71			276.16	259.13	258.15
K	1778.82	1749.82	1732.79	1731.81	1777.81	1760.79	1759.80			147.11	130.09	129.10

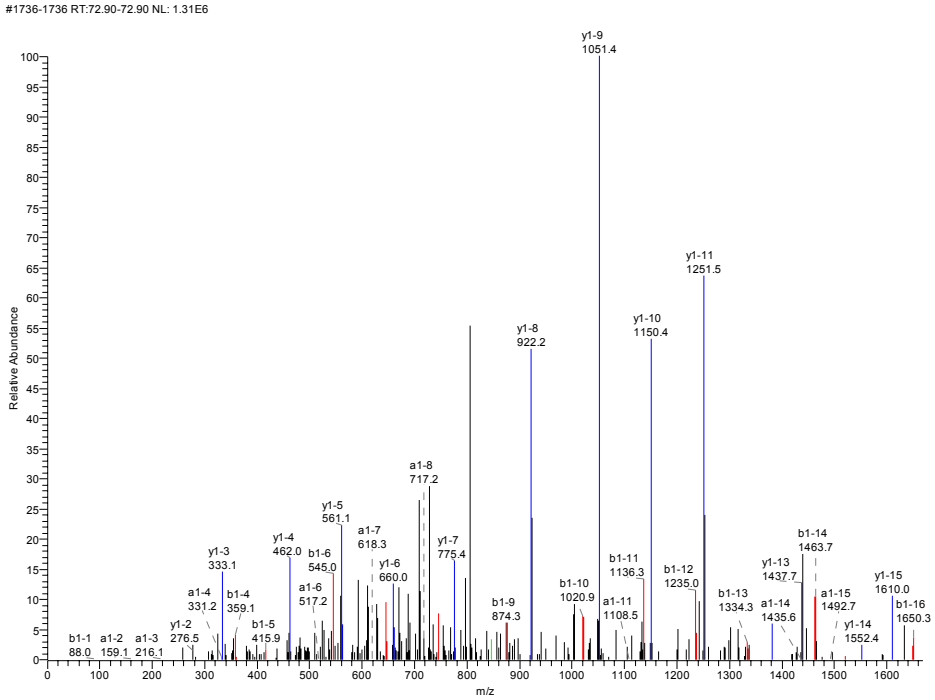

Figure 4- Mass data analysis of a peptide of Zygote arrest 1, Zar 1

Sequence of Zar 1

MYPAYNPYSYRYLNPRNKGMSWRQKNYLASYGDTGDYCDNYQRAQLKAILSQVNPNLTPR
LCRANTRDVGVQVNPRQDASVQCSLGPRTLLRRRPGALRKPPPEQGSPASPTKTVRFPRT
IAVYSPVAAGRLAPFQDEGVNLEEKGEAVRSEGSEGGRQEGKQGDGEIKEQMKMDKTDEE
EAAPAQTRPKFQFLEQKYGYYHCKDCNIRWESAYVWCVQETNKVYFKQFCRTCQKSYNPY
RVEDIMCQSCKQTRCACPVKLRHVDPKRPHRQDLCGRCKGKRLSCDSTFSFKYII

AA	M+nH	A	A*	Ao	B	B*	Bo	Y	Y*	Yo
A	73.05	44.05	27.02	26.04	72.04	55.02	54.03	1422.81	1405.78	1404.80
I	186.14	157.13	140.11	139.12	185.13	168.10	167.12	1351.77	1334.74	1333.76
L	299.22	270.22	253.19	252.21	298.21	281.19	280.20	1238.69	1221.66	1220.68
S	386.25	357.25	340.22	339.24	385.25	368.22	367.23	1125.60	1108.58	1107.59
Q	514.31	485.31	468.28	467.30	513.30	496.28	495.29	1038.57	1021.54	1020.56
V	613.38	584.38	567.35	566.37	612.37	595.35	594.36	910.51	893.48	892.50
N	727.42	698.42	681.39	680.41	726.42	709.39	708.40	811.44	794.42	793.43
P	824.48	795.47	778.45	777.46	823.47	806.44	805.46	697.40	680.37	679.39
N	938.52	909.52	892.49	891.51	937.51	920.48	919.50	600.35	583.32	582.34
L	1051.60	1022.60	1005.57	1004.59	1050.59	1033.57	1032.58	486.30	469.28	468.29
T	1152.65	1123.65	1106.62	1105.64	1151.64	1134.62	1133.63	373.22	356.19	355.21
P	1249.70	1220.70	1203.67	1202.69	1248.70	1231.67	1230.68	272.17	255.15	254.16
R	1405.80	1376.80	1359.77	1358.79	1404.80	1387.77	1386.79	175.12	158.09	157.11

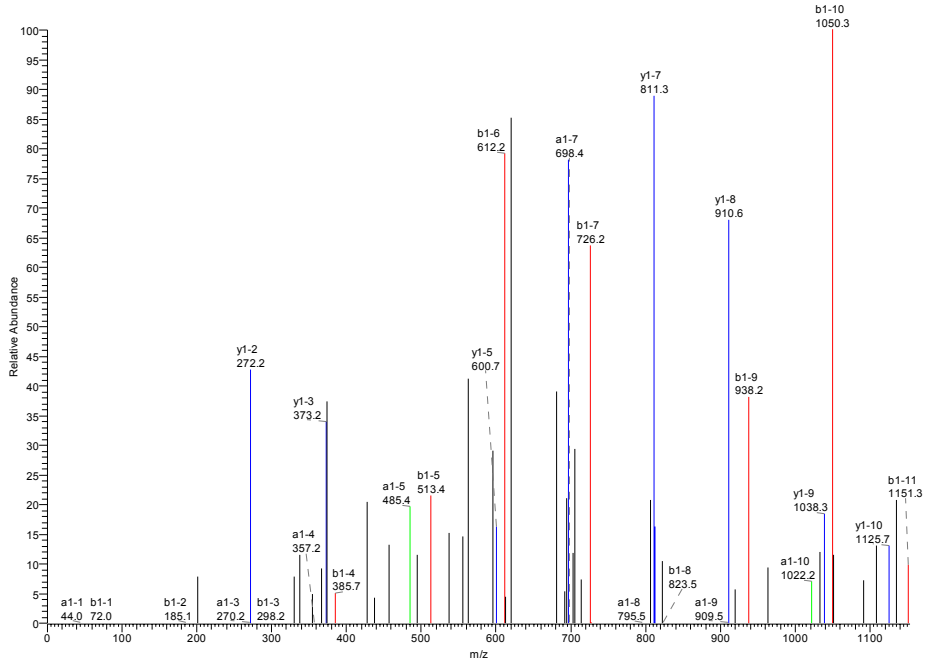

Figure 4- Mass data analysis of a peptide of Ploy (A) binding protein (PABP)

Sequence of PABP

QPADAERALDTMNFDVIKGRPVRIMWSQRDPSLRKSGVGNIFIKNLDKSIDNKALYDTFS
AFGNILSCKVVCDENGSKGYGFVHFETQEAAERAIDKMNGMLLNDRKVFVGRFKSRKERE
AELGARAKEFTNVYIKNFGDDMNDERLKEMFGKYGPALSVKVMTDDNGKSKGFGFVSFER
HEDAQKAVDEMYGKDMNGKSMFVGRAQKKVERQTELKRKFEQMNQDRITRYQGVNLYVKN
LDDGIDDERLRKEFLPFGTITSAKVMMEGGRSKGFGFVCFSSPEEATKAVTEMNGRIVAT
KPLYVALAQRKEERQAHLTNQYMQRMASVRVPNPVINPYQPPPSSYFMAAIPPAQNRAAY
YPPGQIAQLRPSPRWTAQGARPHPFQNMPGAIRPTAPRPPTFSTMRPASNQVPRVMSAQR
VANTSTQTMGPRPTTAAAAAASAVRAVPQYKYAAGVRNQQHLNTQPQVAMQQPAVHVQGQ
EPLTASMLAAAPPQEQKQMLGERLFPLIQAMHPTLAGKITGMLLEIDNSELLHMLESPES
LRLKVDEAVAVLQAHQAKEAAQKVVNATGV PTA

M+nH	A	A*	Ao	B	B*	Bo	Y	Y*	Yo
130.07	101.07	84.05	83.06	129.07	112.04	111.06	1389.67	1372.64	1371.66
201.11	172.11	155.08	154.10	200.10	183.08	182.09	1261.61	1244.58	1243.60
338.17	309.17	292.14	291.16	337.16	320.14	319.15	1190.57	1173.55	1172.56
451.25	422.25	405.23	404.24	450.25	433.22	432.24	1053.52	1036.49	1035.50
552.30	523.30	506.27	505.29	551.29	534.27	533.28	940.43	923.40	922.42
666.34	637.34	620.32	619.33	665.34	648.31	647.33	839.38	822.36	821.37
794.40	765.40	748.37	747.39	793.40	776.37	775.39	725.34	708.31	707.33
957.47	928.46	911.44	910.45	956.46	939.43	938.45	597.28	580.26	579.27
1088.51	1059.50	1042.48	1041.49	1087.50	1070.47	1069.49	434.22	417.19	416.21
1216.57	1187.56	1170.54	1169.55	1215.56	1198.53	1197.55	303.18	286.15	285.17
1372.67	1343.66	1326.64	1325.65	1371.66	1354.63	1353.65	175.12	158.09	157.11